

1985

Origins of the Lake Bonaparte wollastonite deposit, Remington Corners, Lewis County, New York /

Collins T. Awak
Lehigh University

Follow this and additional works at: <https://preserve.lehigh.edu/etd>

 Part of the [Geology Commons](#)

Recommended Citation

Awak, Collins T., "Origins of the Lake Bonaparte wollastonite deposit, Remington Corners, Lewis County, New York /" (1985). *Theses and Dissertations*. 4542.

<https://preserve.lehigh.edu/etd/4542>

This Thesis is brought to you for free and open access by Lehigh Preserve. It has been accepted for inclusion in Theses and Dissertations by an authorized administrator of Lehigh Preserve. For more information, please contact preserve@lehigh.edu.

ORIGIN OF THE LAKE BONAPARTE WOLLASTONITE
DEPOSIT, REMINGTON CORNERS,
LEWIS COUNTY, NEW YORK

by
Collins T. Awak

A Thesis
Presented to the Graduate Committee
of Lehigh University
in Candidacy for the Degree of
Master of Science
in
Geological Sciences

Lehigh University

1985

This thesis is accepted and approved in partial fulfillment
of the requirements for the degree of Masters of Science.

Sept. 18, 1985

(Date)

Charles B. Klar

Professor in Charge

Robert Canyon

Chairman of Department

ACKNOWLEDGMENTS

I wish to thank my thesis advisor, Dr. C. B. Sclar, who suggested this thesis topic and for his critical review, suggestions and guidance throughout the laboratory investigations and during the writing of this paper. I also acknowledge my great indebtedness to Mr. John Weakliem, a fellow graduate student, who was so helpful during the field work and laboratory studies, and to all my colleagues who made useful suggestions for the success of this work. The field work was funded by a Chevron (Standard Oil Company of California) grant in support of thesis and dissertation field work to the Department of Geological Sciences at Lehigh University. Finally my sincere appreciation is extended to the following for their technical assistance--Mr. D. Fluck, who prepared the thin sections, Mr. G. Yasko, who assisted with X-ray diffractometry and X-ray fluorescence spectroscopy, and Mr. James Kerner, who assisted with electron microprobe analyses.

This paper is dedicated to my late junior brother, Friday T. Awak, who passed away during my struggle to produce this work.

TABLE OF CONTENTS

	Page
ABSTRACT	1
INTRODUCTION	3
OBJECTIVES	6
GENERAL GEOLOGY	6
Introduction	6
Marble	7
Gneisses	8
Dike rocks	9
Granite and granite gneiss	9
Younger granites	10
Alaskite	10
Metamorphic rocks of complex and/or uncertain origin	11
Depositional event leading to the occurrence of the limestones (now marble)	11
Deformation and metamorphism	13
Introduction	13
Fold phases	14
Metamorphic event	15

GEOLOGICAL SETTING OF THE WOLLASTONITE DEPOSIT	18
PREVIOUS GEOLOGICAL WORK	23
METHODS OF STUDY	29
Field mapping	29
Petrographic methods	29
X-ray diffractometry	40
X-ray fluorescence analysis	40
Electron microprobe analysis	41
MINERALOGY AND TEXTURE	47
MINERAL CHEMISTRY	60
MINERAL EQUILIBRIA	69
Introduction	69
Stable reaction equilibria	70
Methods of equilibrium calculations	78
Introduction	78
Calculations of equilibria	79
Results of equilibrium calculations	85
GENERAL DISCUSSION	103
CONCLUSIONS	110
REFERENCES	114
VITA	124

LIST OF FIGURES

Figure		Page
1	Map of New York State showing the location of the wollastonite deposit.	4
2	Geological map of the area where the wollastonite deposit is located	5
3	Geological map of the wollastonite deposit, showing the contact with the syenite gneiss.	19
4	Geological map showing detailed features of the wollastonite deposit.	20
5	Vertical cross-section of the wollastonite deposit and the syenite gneiss.	22
6	Adirondack isotherms of Bohlen and others (1980) from magnetite, illmenite and K-feldspar-plagioclase thermometry.	26
7	Lake Bonaparte Wollastonite Deposit Sample Locality Map.	35
8	Distribution of mineral phases in the syenite gneiss and wollastonite deposit.	58
9	Mineral distribution and abundance in some representative samples in the wollastonite deposit and syenite gneiss.	59
10	Variation of Or, An against SiO_2 in the syenite gneiss.	62
11	Diagram showing the relationship between the analyzed wollastonite, diopside and epidote in the system SiO_2 -CaO-MgO in the wollastonite-bearing marble.	64
12	Variation of CaO, MgO, FeO, Al_2O_3 , K_2O , Na_2O against SiO_2 from XRF chemical analysis.	66

13	Diagram showing the relation between $\frac{1}{3} \text{SiO}_2 + \text{K}_2\text{O}-\text{MgO}-\text{CaO}-\text{FeO}$ and $\text{MgO}+\text{FeO}+\text{CaO}$, in the syenite gneiss.	67
14	ACF plot of the syenite gneiss showing the position of the rock composition.	68
15	Illustration of the phase rule, applied to the three-component system $\text{CaO}-\text{CO}_2-\text{SiO}_2$.	77
16	The formation of wollastonite from calcite and quartz as a function of temperature and pressure with CO_2 pressure (P_{CO_2}) = total pressure (P_{E}).	86
17	The formation of wollastonite from calcite + quartz at fixed $P_{\text{CO}_2} = 1 \text{ kb}$ and at 5 kb .	87
18	T-X diagrams for the reaction $\text{Cc}+\text{Qt} = \text{Wo}+\text{CO}_2$ showing experimental data of Greenwood, 1967b.	88
19	Stability relations of calcite, quartz, and wollastonite in supercritical mixtures of H_2O and CO_2 .	90
20	T-X diagrams calculated from log K expressions derived from experimental data at 2 kb .	91
21	The position of the Tr-Kspar (1) Di (2) An-Co (3) equilibrium in the system $\text{CaO}-\text{MgO}-\text{K}_2\text{O}-\text{Al}_2\text{O}_3-\text{SiO}_2-\text{CO}_2-\text{H}_2\text{O}$ in T-X (CO_2) space at 4 kb pressure.	92
22	T-X CO_2 diagrams at $P_{\text{t}} = 2 \text{ kb}$ showing total error limits ² in the location of various equilibria.	94
23	$\text{CO}_2-\text{H}_2\text{O}$ chemical potential diagram for reactions in the carbonate-quartz beds.	96
24	Summary of development of assemblages in the system $\text{CaO}-\text{MgO}-\text{KAlO}_2-\text{Al}_2\text{O}_3-\text{CO}_2-\text{H}_2\text{O}$ with excess quartz.	97

- 25 Phase relations in the system $\text{CaO-MgO-SiO}_2\text{-H}_2\text{O-CO}_2\text{-Al}_2\text{O}_3$ at 6 kb pressure for reactions that affect bulk composition with joint Qt-Do-CC. 101
- 26 Temperature plotted versus the mole fraction of H_2O and CO_2 . 102
- 27 Diagram showing predictable stages of growth of reactions in the wollastonite marble as observed in some selected samples. 103

LIST OF TABLES

Table		Page
1	Correlation of ages of major fold phases, metamorphism, and intrusive activity in the Adirondacks.	17
2	Summary of previous work.	28
3	Sample descriptions.	30-34
4	Mineral assemblages in the syenite gneiss and the wollastonite deposit.	36
5	Abbreviations and formulae of minerals in the text.	38
6	Modal analyses, (500 points per slide).	39
7	XRF analyses.	42
8	XRF analyses recalculated to 100%.	43
9	XRF norms, calculated weight %.	44 & 45
10	Electron microprobe analyses of feldspars, wollastonite, amphibole, diopside and carbonate.	48-56
11	Equilibrium reactions.	71
12	Thermodynamic data symbols.	80
13	Summary of results of equilibria calculations.	99
14	Stable reactions, equilibria, and equilibrium constants for phase relations in the system $\text{CaO-MgO-SiO}_2\text{-H}_2\text{O-CO}_2$.	100
15	Thermal constants.	107

ABSTRACT

A coarse-grained monomineralic lenticular mass of decussate wollastonite, containing prisms of wollastonite up to 10 cm in length, occurs at the contact between pink coarse-grained massive syenite and the Grenville marble near Remington Corners, New York. The wollastonite mass dips steeply to the east and has a maximum width of about 125 meters. It has been explored to a depth of about 270 meters. It is currently mined by the Gouverneur Talc Company. Interlayered with the wollastonite body are several lenses of very coarse-grained graphitic marble up to 10 meters thick composed of distinctly blue calcite. The adjoining leucocratic syenite is virtually free of quartz and is composed of sodic plagioclase, K-feldspar, brownish-green actinolitic hornblende, epidote, and accessory magnetite and apatite.

The lenses of blue graphitic marble and the wollastonite mass were probably derived from sedimentary beds of different bulk chemical composition in the Grenville limestone sequence. The close spatial association of the wollastonite body with the syenite contact suggests that the wollastonite is a product of thermal metamorphism of the Grenville marble by the intrusive syenite.

The wollastonite is associated with other minerals. These include diopside, tremolite, phlogopite, epidote, sphene, chlorite, K-feldspar, minor grossularite garnet and plagioclase, and accessory apatite. These phases can be related by the equilibria in the systems: $\text{CaO-MgO-SiO}_2\text{-H}_2\text{O-CO}_2$, and $\text{CaO-SiO}_2\text{-H}_2\text{O-CO}_2$. The metamorphic aureole developed at a peak temperature of 600°C to 650°C under total rock pressure of about 6.0 to 6.5 kb and variable $p\text{CO}_2$.

The mineral assemblages show that the original limestone was subjected to greenschist to middle amphibolite grade metamorphism. The discontinuous distribution of wollastonite along the syenite-marble contact suggests that the occurrence of wollastonite was controlled by those beds in the original limestone with favorable bulk chemical composition. The mineral distribution does not show well-defined thermal zonation. Besides the bulk composition, the observed non-zonal distribution of minerals may also be due to the non-uniformly distributed fluids derived from the syenite or to the non-uniform distribution of H_2O and CO_2 in the marble. It is probable that this thermal aureole was subsequently overprinted by the Grenville regional metamorphism.

INTRODUCTION

The wollastonite deposit is located in the Grenville marble that crops out near Remington Corners, Lewis County, New York, (Figure 1). This marble forms part of the southern extension of the Grenville province into the northwest Adirondack Lowlands, and constitutes part of the Gouverneur marble which is in direct contact with a portion of the Diana syenite gneiss complex. (See Figure 2.)

Most of the studies on the marbles in the Adirondack Lowlands have not given serious consideration to the contact mineral wollastonite. The petrogenetic aspects of the marbles have received thorough study, but neither chemical analysis nor the descriptive occurrence of the wollastonite in the marble have been published. Mention has been made of the association of the wollastonite with the contact between the marble and the intrusive igneous rocks.

Wollastonite is a key material for chemical industries which deal with ceramics, refractories, coatings, plastics, and fluxes. Its color, purity, chemistry and acceptable thermal properties should warrant thorough study of the mode and conditions of formation to serve as a guide to its exploration and exploitation. These reasons thereby provide the basis for defining temperature limits and fluid-composition parameters

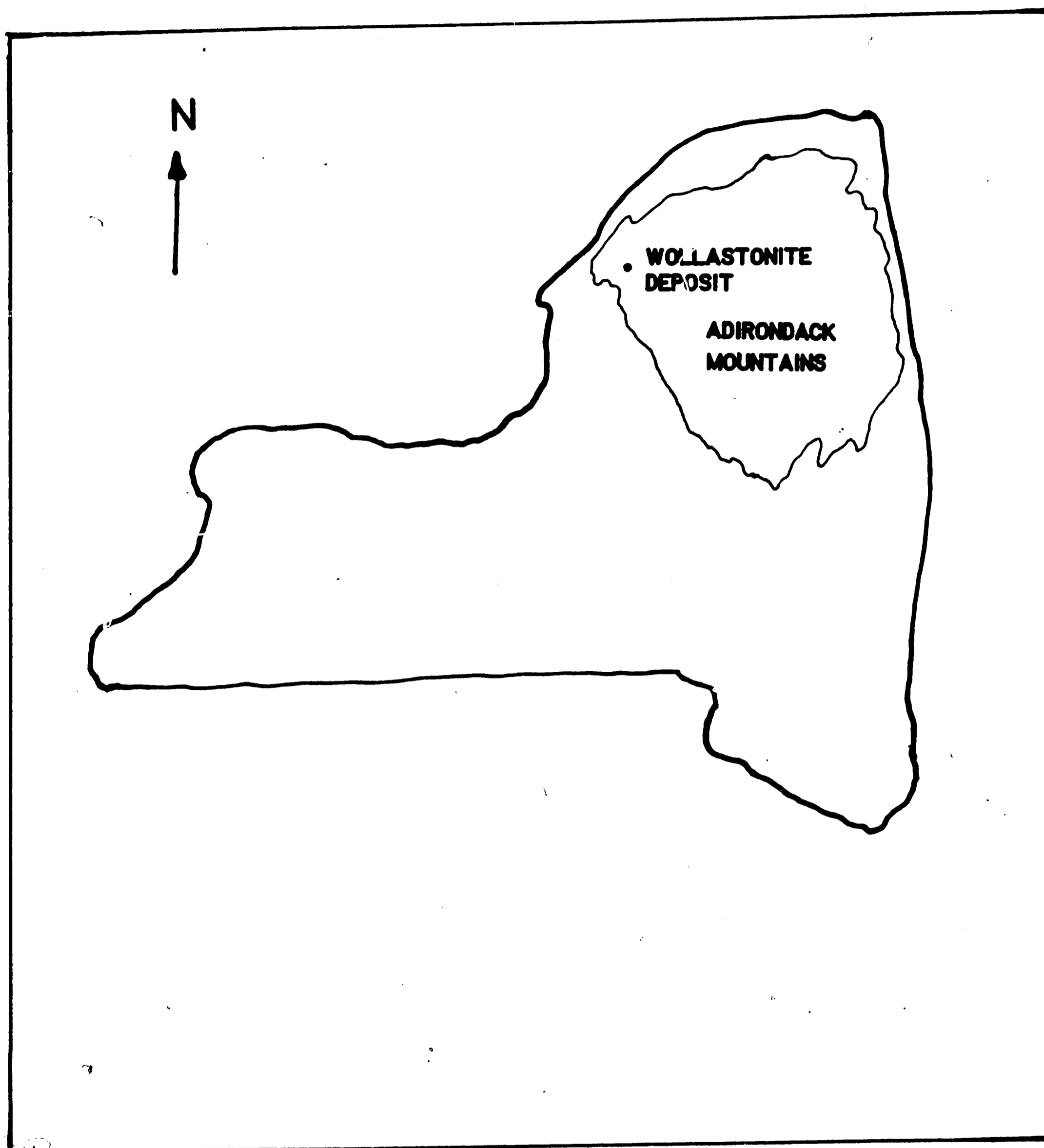
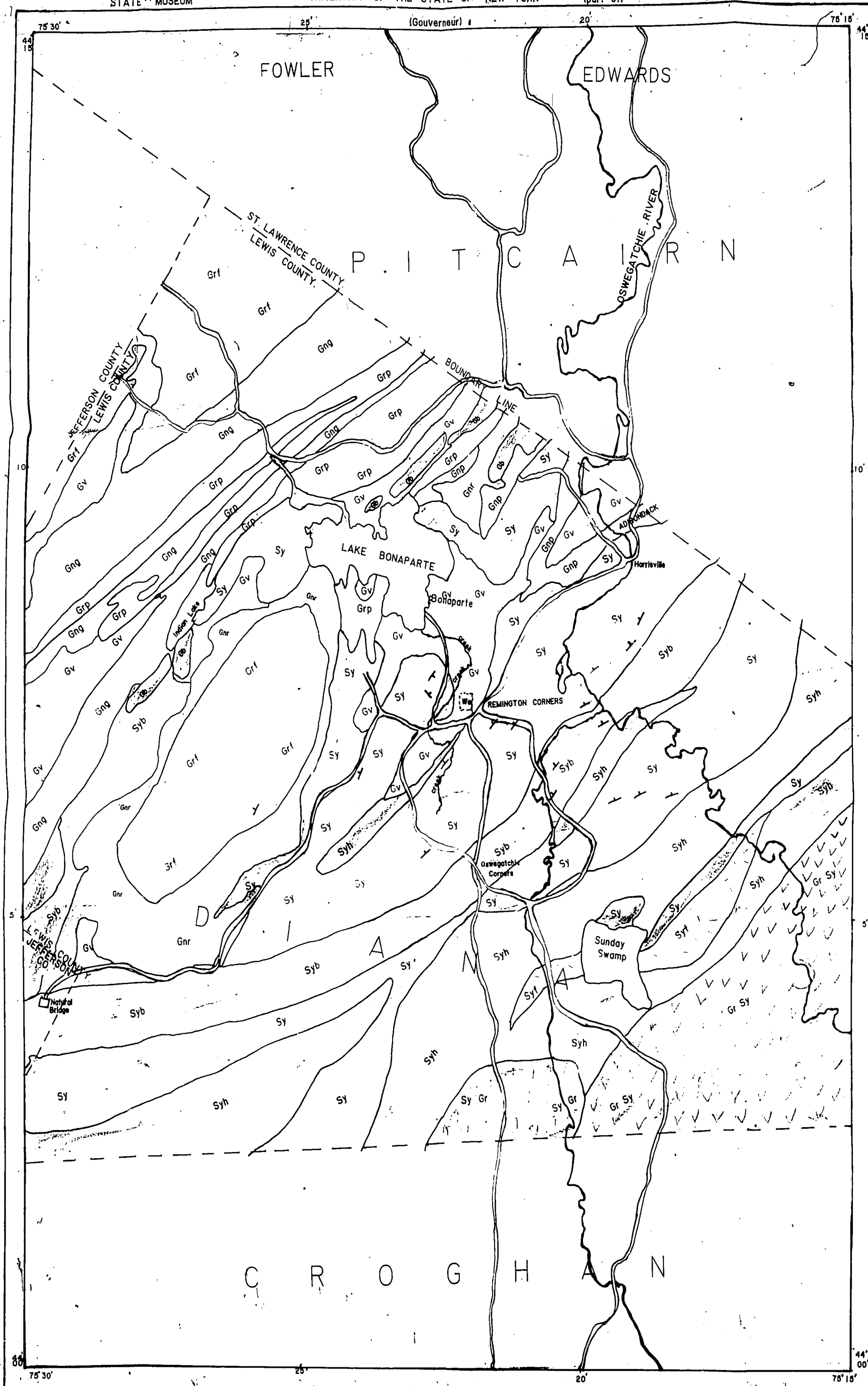


Figure 1. Map of New York State showing the location of the wollastonite deposit.

Figure 2

Figure 2. Geological map of the area where the wollastonite deposit is located.



LEGEND

SEDIMENTARY ROCKS

Gv. Crystalline Limestone (Grenville Series).

MIXED ROCKS

Gnp. Pyroxene gneiss (unmetamorphosed calcareous beds of Grenville formation, injected by pegmatite and syenite and intruded sheets of granite.)

Gnr. Undivided gneisses biotite, cordierite, garnet sillimanite, and pyritous gneiss members of Grenville formation injected by pegmatite and modified by granitic juices.

Gng. Biotite-garnet gneisses. Beds of Grenville formation in the last stages of disintegration by pegmatite vein and granitic juices.

IGNEOUS ROCKS

Grp. Granitic gneisses. Dominantly coarse porphyritic. may be medium grained near contacts.

Grf. Granite gneiss. fine grained gneissic structure, locally indistinct.

GrSy. Grano-syenite gneiss. fine grained equigranular.

GrSy. Hornblende biotite grano-syenite gneiss. medium grained equigranular.

Syh. Hornblende syenite gneiss. coarsely porphyritic red gneiss.

Syh. Augite syenite gneiss. coarsely porphyritic in main body. equigranular in masses intrusive into Grenville.

Syh. Basic augite syenite gneiss. coarsely porphyritic in main body, equigranular. south of Indian Pond, in part monzodiorite.

Syf. Augite-hypersthene syenite gneiss. coarsely porphyritic.

Gb. Gabbro amphibolite.

We. Wollastonite deposit.

P R E C A M B R I A N
MONZODIORITE-SYENITE GRANITE COMPLEX
YOUNGER GRANITES

Roads

Rivers

Outcrop boundaries

Strike and dip of foliation



APPROXIMATE MEAN DECLINATION 1912

Scale 1: 62500

Mapped by:

Buddington, A.F. and Smyth, C.H., 1926

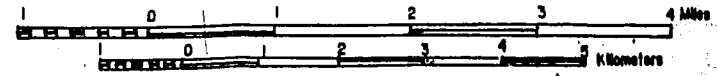


Figure 2

clearly, to be applied to geologically well characterized marbles, in order to define more precisely the environment of formation of wollastonite.

OBJECTIVES

The objectives of this study were as follows:

- (i) the study of geological occurrence and petrogenesis of the wollastonite body in the marble outcrop.
- (ii) to examine the contact relationships between the syenite gneiss and the marble.
- (iii) to deduce the conditions, such as temperature, pressure and the effect of fluid phase ($\text{CO}_2 + \text{H}_2\text{O}$), which prevailed during the formation of the wollastonite body and the associated calc-silicate minerals.

GENERAL GEOLOGY

Introduction

Virtually all the rocks associated with the marble in the Adirondack Lowlands are metamorphic. These rocks are probably the result of physical and chemical readjustment of pre-existing rocks to high temperature and pressure. Prominent among them are:

- (a) metamorphic rocks of sedimentary origin.

(b) metamorphic rocks of igneous origin.

(c) metamorphic rocks of complex and/or uncertain origin.

Marble

The early workers (Smyth, 1895; Buddington, 1934; Buddington and Smyth, 1926) mapped the distribution of the marble in the Lake Bonaparte quadrangle in St. Lawrence, Jefferson and Lewis Counties. The marble belt crops out from west of the Lowlands and extends eastward from the area of the village of Antwerp across Rossie and Gouverneur into Hermon. Another belt extends across Fowler into Edwards and contains extensive talc and tremolite deposits. Further south of the region, another belt extends discontinuously from the region of Natural Bridge in Jefferson County into Diana township in Lewis County and Pitcairn township in St. Lawrence.

Characteristically, the marbles are coarsely crystalline, siliceous, and usually light grey in color or white. Some contain lenses of coarsely crystalline blue calcite. Graphite occurs disseminated in some marbles. Phlogopite, diopside, epidote, pyrite, apatite, sphene, talc, tremolite, garnet, plagioclase, and K-feldspar have also been observed. Other associated metasedimentary rocks are quartzite and various paragneisses; the sedimentary precursors of these rocks include limestone, quartz sands, and shales.

Gneisses

Buddington and Smyth (1926) divided up the gneisses in this region. The gneisses are distributed as thick sheets and lenses interlayered with a variety of other rock types. Some gneisses, such as the Diana gneiss, are composed of layers which grade upwards from syenite through quartz syenite to granite. They are considered to represent the exposed parts of a single igneous sheet which differentiated during crystallization and later was folded and metamorphosed.

The rocks of the Diana mass are in general porphyroblastic. Most of the plagioclase grains are in microperthetic or cryptoperthetic intergrowth with potash feldspar. The potash feldspar contains a considerable amount of albite in solid solution. The rock analyses show that the series have affinity chemically with the monzonite family ranging from monzonite and quartz monzonite to granite, but the alkali content is higher than the typical monzonite of the western United States. The Diana gneisses contain microcline, orthoclase, albite, quartz, diopside, augite, hornblende, hypersthene and calcite. Accessory minerals include apatite, sphene, magnetite, ilmenite and pyrite. The variations of this igneous rock were mapped as augite-hypersthene syenite gneiss, basic augite syenite gneiss, augite syenite gneiss, hornblende syenite gneiss, hornblende

granosyenite gneiss, hornblende-biotite granosyenite gneiss and granite gneiss.

The Diana syenitic and the Croghan granosyenitic masses may represent portions of the two separate batholiths. The Croghan granosyenitic mass is more siliceous than the Diana mass and has an equigranular texture.

Dike Rocks

Dike rocks are common in all facies of the syenite and appear to be genetically allied with the syenite.

Granite and Granite Gneiss

The origin of the granite and granite gneiss in this region presents another problem. The granitic gneisses might have formed in any one or more of these ways: (a) intrusion of granitic magma from still deeper levels of the crust; (b) differential melting of pre-existing rocks approaching granite in composition (e.g. arkose, graywacke, and certain volcanic rocks) followed by movement of the melted before cooling and crystallization; (c) metamorphic recrystallization of rocks of granitic composition without notable addition or subtraction of material; and (d) partial replacement of pre-existing rocks by elements carried in fluids along grain boundaries. The mineralogy of granite gneiss consists of feldspars, quartz,

hornblende, biotite and/or pyroxene. Accessory minerals include opaques such as ilmenite and magnetite.

Younger Granites

The younger granites, based on their mode of occurrence and degree of metamorphism, are believed to be younger than the dominant facies of the syenitic rocks. The fine-to medium-grained younger granites constitute the California and the Clark Pond batholiths and other small and numerous stocks. The coarse porphyritic granite occurs principally as lenticular concordant bodies in the Grenville marbles. The dominant younger granitic rocks are medium grained, pink in color, and contain microperthite, quartz, light green to colorless augite and partially altered hornblende. Ilmenite, zircon, apatite and sphene are accessory minerals.

Alaskite

The alaskite in the NW Adirondack Lowlands, occurs as a thick series of leucocratic gneisses which are interlayered with amphibolite and biotite gneiss. The alaskite is thought to constitute a multiply folded rock unit (Foose, M. T. and Carl, J. D., 1977). Petrologic and chemical studies of alaskite by Carl and Van Diver (1975) suggest that this rock type represents a single vast felsic ash-flow tuff sequence with interbedded amphibolite layers that reflect compositional layering.

The alaskite rock unit has been important in working out the local lithologic succession (Foose, 1974; Lewis, 1969), and a variety of outcrop patterns. The alaskite outcrops are exposed around Hyde School, Dodds Creek and Payne Lake and in the Moss Ridge-Reservoir Hill areas.

Metamorphic Rocks of Complex and/or Uncertain Origin

The metamorphic rocks of complex and/or uncertain origin have had their original textures nearly or completely obliterated by metamorphism. Their present chemical composition can be matched by one or more types of both igneous and sedimentary rocks. Common among the rocks of this group are the amphibolites. The amphibolites are known to have recrystallized by one or more than one process. Some are recrystallized gabbro. Others are associated with marble and are believed to represent transformed limy shales or marls.

However, most amphibolites in the Adirondack Lowlands provide no obvious clue as to their exact parentage. Many might have originated by one of the above processes. Others probably represent metamorphosed lava flows and volcanic ash-falls (Buddington, 1939).

Depositional Event Leading to the Occurrence of the Limestones (now marble)

All the environments of deposition of the Grenville Series

appear to have been marine. The bulk of the carbonate-rich Grenville series seems to have been deposited in a large persistently negative, although not highly, negative basin. Precambrian rocks constitute the basement. Periodically, at least, waters in the basin appear to have been cut off from open oceans and to have become saline. This is shown by the great thickness of magnesian carbonate rocks and the interlayered anhydrite and halite in some areas of these Lowlands. The marked thinning of the carbonate units from northwest to southeast (Lewis, 1970), suggests that the basin was shallower eastward. The geochronological studies of some minerals in pegmatites and granites intrusive into the Grenville Series and ores (Holmes, 1937), show that the age of the intrusives ranges from 1.0 to 1.3 b.y. This age seems to reflect the age of the culmination of regional metamorphism in the NW Adirondack Lowlands.

Holmes, 1937, Shaub, 1940, Marble, 1943, and Hurley, 1951, found an average age of 1.10 b.y. for the culmination of the Grenville Orogeny. Also the inception of Grenville sedimentation might have been as early as 1.5 b.y. and probably exceeded 1.2 b.y. The deposition of the limestones (now marble) would have occurred synchronously with the Grenville sedimentation.

In the NW Adirondacks, the marbles are the common members of the exposed Grenville Series. Osborne, 1936a, estimated the

total thickness of the marble as 1.6 to 3.3 km. In the SE Adirondacks, Alling, 1927, described a sequence of the Grenville Series as some 0.5 km thick of which only about 10% is marble. A similar thin sequence is also observed in the south. Cushing, et al., 1925, estimated the thickness of marble in the NW Adirondack as 6.6 km. Buddington (1939) suggested a thickness of about 3.6 km of marble in the northwest. Engel and Engel (1939, 1958b) reported a thickness of about 5.3 km. Overall, the total thickness of marble is about 1.6 to 5 km in the NW Adirondack.

As a consequence of intense metamorphism, the limestones have been transformed to crystalline marble, the shales to schist and sillimanite-garnet gneiss and sandstones to quartzite. Fisher (1977) concluded that erosion proceeded in this region at the rate of about 4.3 cm/1000 years and that about 20 km thickness of over burden had been eroded between 470 to 485 m.y. ago, to expose the marble.

Deformation and Metamorphism

Introduction

About 75% of the rocks of the Grenville Lowlands of the NW Adirondacks are metasedimentary. The Highlands consist dominantly of orthogneisses. The boundary between the two regions is marked for most part of its length by intense shear zones, and extensive mylonitization. In some parts of these

shear zones, the primary texture of the igneous rocks is generally destroyed through deformation (Buddington, 1963). Most of the Grenville Series and the Grenville metasedimentary rocks in the Lowlands are highly folded, commonly along NE-trending axes. There is wide-spread chemical alteration and dynamothermal metamorphism largely related to intrusive emplacement. Flowage features are common in the carbonate zones.

Fold Phases

Four major phases of deformation affected the metamorphosed sedimentary rocks (deLorraine, 1979). The last three of the four fold phases affected the metamorphosed plutonic rocks. A fifth phase of deformation also occurred but is minor and local.

The first phase folds (F_1) are isoclinal and SE-directed nappes associated with peak Grenville metamorphism. The F_2 are also isoclinal and NW-directed nappes. Wide-spread intrusive activity, high-grade metamorphism, and mylonitization occurred along the Lowlands-Highland "boundary" (Wiener, 1977) accompanying the F_2 . Intrusion of gabbro, quartz syenite and related rocks of the Diana, Tupper, and Stark complexes, and hornblende granite occurred during this deformation. The F_3 are open to tight, upright to overturned folds with NE-trending axial surfaces.

The F_4 folds are mostly open and upright folds with NW-trending axial surfaces and steep dips. Locally, F_4 are tight and overturned. Where F_3 are overturned to the SE, F_4 axes plunge NW because both limbs of F_3 dip NW. But where F_3 folds are upright, F_4 axes plunge NW and SE on NW-SE dipping limbs of F_3 . Mineral lineation is locally developed parallel to the fold axes and axial plane slip cleavage or fracture cleavage is also present in places (Foose, 1974). The F_5 are only locally developed in the NW Adirondacks at Baimat NW of Clark Pond anticline and near Rossie. The F_2 and F_4 are believed to be associated with the deformation of the marble deposit in the NW Adirondack Lowlands.

Metamorphic Event

The foliation and bedding in the Grenville Formation are uniformly parallel. The NW Adirondack Lowlands is characterized by complex metamorphic and deformational events. An earlier dynamothermal metamorphism was accompanied by a later intrusion of igneous rocks. Thermal metamorphism on a regional scale has been superimposed upon an older metamorphism. Thermal metamorphism is not only confined to contacts but is in places distributed over large areas. It is possible that intrusion into a layered series under heavy load with consequent increase of both temperature and pressure would bring about a general

recrystallization (Daly, 1917). Metamorphic features are genetically related to the intrusion of magma into the Grenville metasedimentary series. Magmatic intrusion is believed to follow successively in this order of decreasing age: anorthosite, gabbro, diorite, syenite, and granite. The age of intrusion, from radiometric studies of Pb and U in granitic and pegmatite minerals ranges from 1.0 to 1.3 b.y., and the deformation and metamorphism occurred about the same time. This is essentially synchronous with the Grenville Orogeny. Metasomatic interaction between the intrusive magma and the carbonate host rock during metamorphism and deformation also contributed to the formation of new metamorphic minerals (Kemp, 1921; Agar, 1923). Table 1 shows the age correlation of fold phases, metamorphism, and intrusive activity in the Adirondacks.

Table 1. CORRELATION OF AGES OF MAJOR FOLD PHASES,
METAMORPHISM, AND INTRUSIVE ACTIVITY IN THE ADIRONDACKS

1. F_1 -earlier folds in NW (Wiener, 1981), South-Central isoclinal in Lake Durant Fm. Pre- F_1 , some foliation, Pre-Fowler syncline fold (deLorraine, 1981), Peak metamorphism 1.10-1.02 b.y. ago, partial melting of paragneisses, granitic melt.
2. F_2 -Major nappes directed to NW in the South; F_1 -Moss-Ridge, Gouverneur, Canton, early isoclinal folds, F_1 Fowler syncline, NW-directed fold thrust nappes. Major intrusive activity, mylonitization of charnockite, later intrusion and folding of hornblende granite which intruded 1.05 b.y. ago. Metamorphism of igneous rocks; gabbro 750°-850°C, 7-8 kb (McLelland and Whitney, 1980).
3. F_3 , major N70W-EW, N45E, open to tight folds. F_2 N45E trending, open to tight folds, upright, overturned to SE, Gouverneur anticline, Doming, Balmat Syncline.
4. F_4 NW-trending, open folds, domes, basins, interfere with F_3 NE trending folds in NW. But F_3 -open, discontinuous, NW trending folds, interfere with F_2 , intrusion and metamorphism of diabase dikes (Fisher et al, 1971), Retrograde metamorphism of sillimanite to muscovite (Foose, 1974) and diopside and forsterite to serpentine (Wiener, 1981).
5. F_5 -local slip on fracture cleavage (Highlands), Intrusion of muscovite pegmatite (Fisher et al, 1971). 930 ± 40 m.y. ago (Rb/Sr, Fisher et al., 1971), Retrograde metamorphism 600°-650°C, 3-5 kb (McLelland and Isachsen, 1980).

GEOLOGICAL SETTING OF THE WOLLASTONITE DEPOSIT

The wollastonite deposit (Figure 3) is about 200 m long along a N-S strike and dips eastward in the form of a wedge in the marble. A local dip of about 41° - 50° E and a strike of $N5^{\circ}$ W was measured on the outcrop. The wollastonite body is coarsely crystalline and generally massive. The color is grey-white to white and the deposit contains a layer of massive coarsely crystalline blue calcite marble about 10 meters thick. The eastern portion of this marble bed is thinly layered with alternating blue and white laminae ranging in thickness from 1 to 5 cm. Some of the white layers contain K-feldspar, calcite, tremolite, and diopside. The wollastonite in this area is medium to coarse grained. Some thin veins (e.g. specimen 31) in the wollastonite deposit can be traced for a few meters. These veins may have served as conduits for cation exchange during metamorphism, metasomatism, and mineral formation.

The marble is generally siliceous. Within the blue calcite bed, disseminated graphite flakes, about 0.5 to 1 cm in diameter, occur. The south to south-western portion of the wollastonite deposit is in direct contact with pink porphyroblastic syenite gneiss. A thin film of reddish white clay about 5 cm thick, consisting of a mixture of minerals derived from both the syenite gneiss and the marble, occurs at the contact (Figure 4).

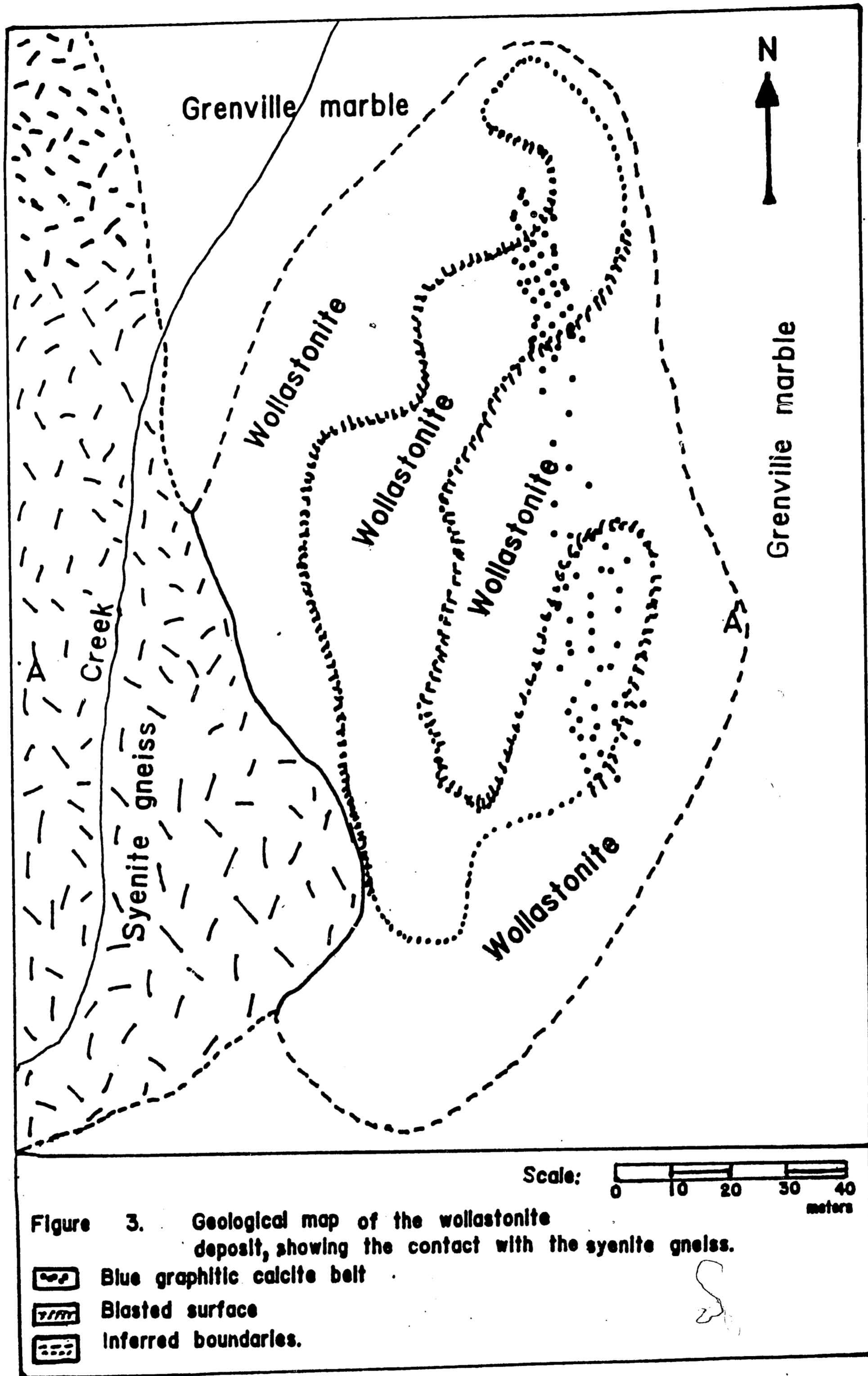


Figure 3. Geological map of the wollastonite deposit, showing the contact with the syenite gneiss.

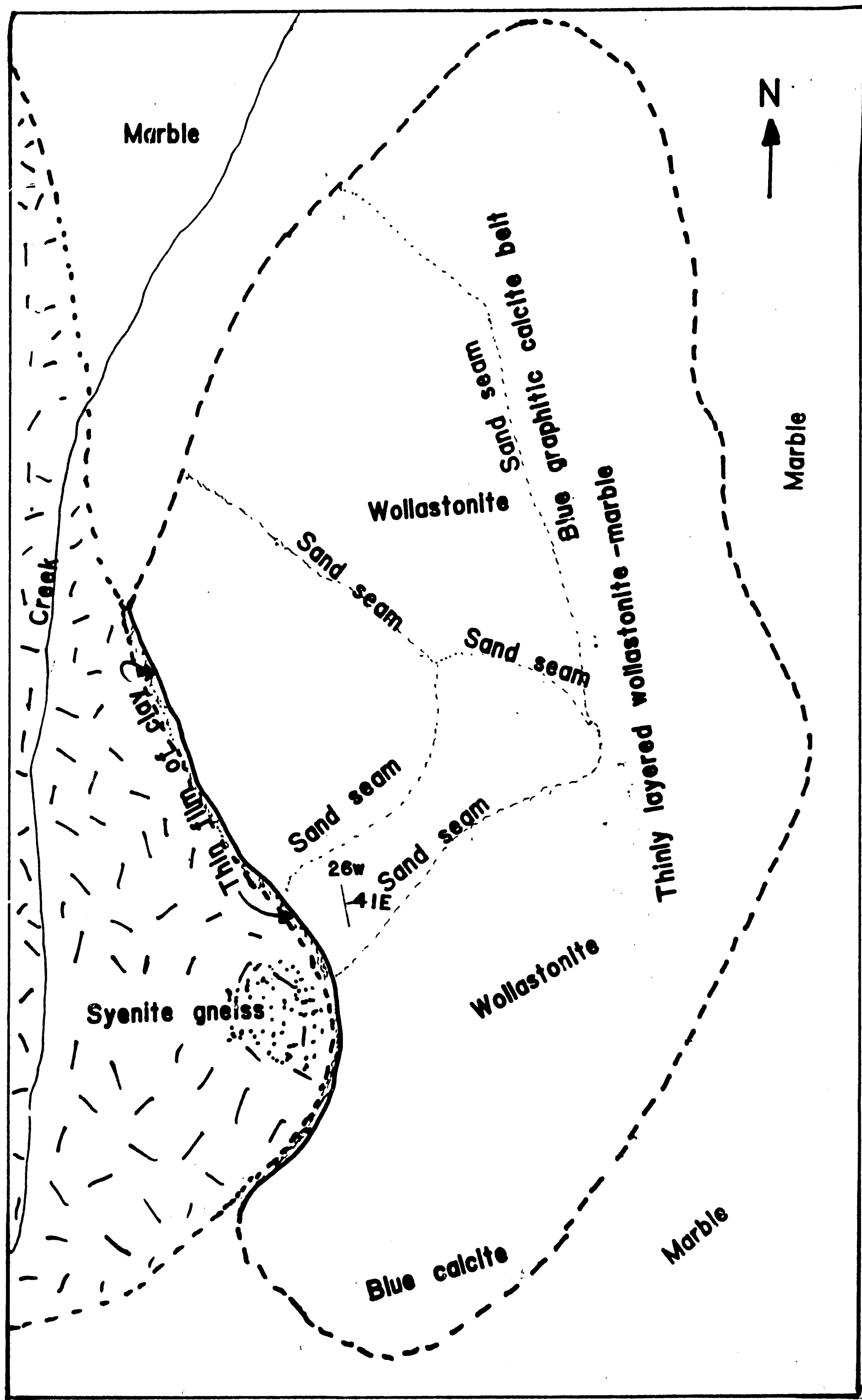


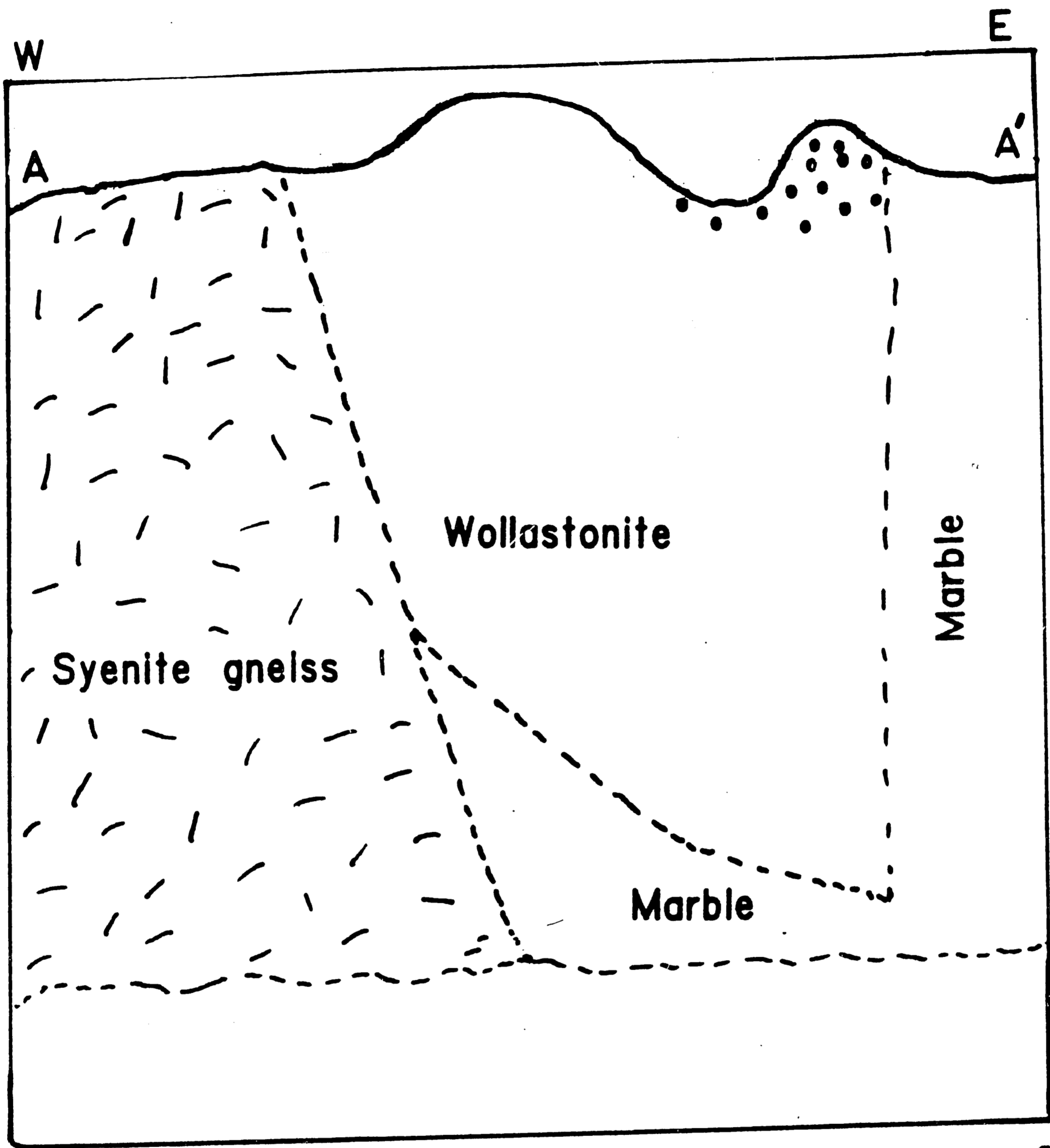
Figure 4.

0 10 20 30 40 meters

Geological map showing detailed features of the wollastonite deposit. Dotted area is grey-white syenite gneiss.

The syenite gneiss is composed dominantly of K-feldspar, which contains small amounts of albite and minor plagioclase. Dark patches of amphibole, pyroxene, epidote and magnetite were observed on the outcrop. The syenite outcrop strikes almost parallel to the western contact and is believed to have been roofed by the marble (Totten, geologist, Gouverneur Talc Co., personal communication).

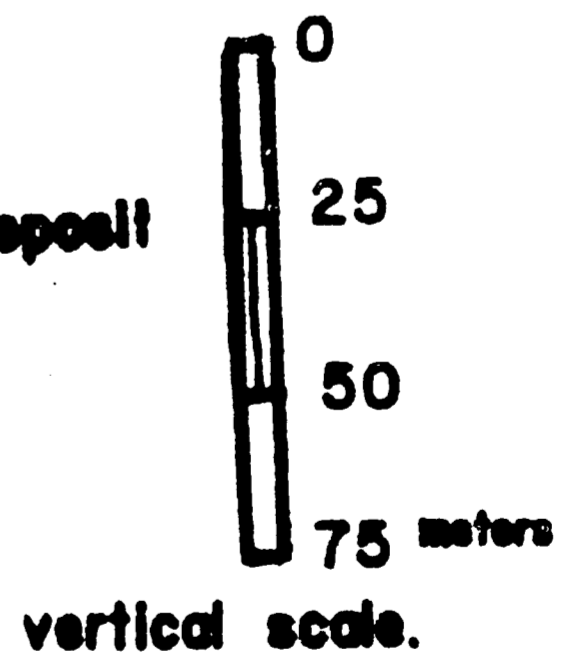
The Wollastonite occurs in several discontinuous masses distributed through the marble. This occurrence suggests the uneven distribution of beds of favorable bulk chemical composition in the original limestone sequence. It may also reflect an inadequate supply of wollastonite-forming materials (SiO_2) from the intrusive magma or may be due to external control by the fluid phase in the marble. The total depth of workable wollastonite in the marble is about 270 meters (Figure 5). Graphite is restricted to the blue calcite marble layer. The origin of the graphite is not fully understood. The source might have been carbonaceous shaley beds. Some other occurrences of graphite in the marble of this region is considered to be genetically linked with the intrusive magma of the contact. In this locality, graphite is not related to the contact but is restricted to the blue calcite and this supports the hypothesis that the carbon is of sedimentary origin.



(Drilling data, courtesy, Beauverneur Talc CO.)

Figure 5. Vertical cross section of the wollastonite deposit and the syenite gneiss.

(Section A-A' of geological map).



Previous Geological Work

Geological mapping and investigations of the Grenville marble and the associated rock types in the NW Adirondack Lowlands have been fruitful. Brown, C.E. (1978) made a reconnaissance of the high-calcium marble in the Beaver Creek area of St. Lawrence County. Cushing, H. P. and Newland (1925), Buddington, A. F. (1934), and Engel, A. E. J. (1956), respectively, studied the marble. Their studies revealed the presence of abundant silicate minerals in the marble such as phlogopite, tremolite, talc, and diopside and minor minerals such as graphite, sphene, apatite, pyrite, pyrrhotite, and spinel have been observed. Wollastonite in the marbles was found to be associated with the contact with syenitic intrusives. Pyroxene and amphibole were found to be common in the marble at contacts with granite and syenite gneiss. Wollastonite was found to be rare at granite-marble contacts. Agar (1923) studied contact metamorphism in the western Adirondack Lowlands. His work was concentrated in St. Lawrence, Jefferson, and Lewis Counties but he also mapped Hammond, Lake Bonaparte, Gouverneur, Rossie and Canton quadrangles.

The occurrence of wollastonite in marble associated with syenite contacts was also observed by Eskola (1914). He concluded that where wollastonite is present, the temperature

during metamorphism must have exceeded a certain limit which is a function of pressure. At atmospheric pressure, wollastonite can form above about 500°C but this increases to about 950°C at about 15,000 atmospheres. Engel and Engel (1953) also studied the effects of intrusive magmas on metasedimentary rocks. They observed that magmas have interacted with the metasediments to produce hybrid rocks and skarns.

Geothermometric and geobarometric work in the Adirondack Lowlands have received considerable attention. Most of this work has been based on mineral assemblages in the metamorphic rocks. Metamorphism occurred in this region during the Grenville Orogeny, about 1.1 to 0.9 b.y. ago, and attained the greenschist middle amphibolite grade (Wynne-Edwards, 1972). Essene and others (1978) estimated temperatures of about $600^{\circ}\text{C} \pm 50^{\circ}\text{C}$ for the Adirondack Lowlands on the basis of two-feldspar and Fe-Ti oxide thermometry. Metamorphism in the Adirondack region increases from lower amphibolite facies in the Lowlands to garnet granulite and upper amphibolite facies in the Highlands (deWaard, 1969). Values of pressure have been debated, but they are now tightly constrained in several localities. Estimates have ranged from 2-3 kb (Engel and Engel, 1960) to 8 to 10 kb (deWaard, 1969) in the Lowlands, and 7 to 12 kb (Jaffe et al., 1978) in the Highlands. DeWitt and Essene (1974) estimated the lithostatic

pressure to be about 6.5 kb in the Lowlands at Balmat. Bohlen et al. (1980) have estimated the minimum pressure in the Highlands at 6 ± 1 kb, in the western side, and 7 ± 1 kb, in the Mount Marcy Quadrangle within the main anorthosite massif.

The temperature estimates also vary greatly, ranging from 500°C to about 900°C. Engel and Engel (1953, 1960) estimated a gradual increase from 500°C at Emerysville, to about 600°C at Colton, from application of several geothermometers. The use of the calcite-dolomite solvus can only be regarded as a minimum. Essene and Valley (1980) have also applied the calcite-dolomite thermometer and found that the temperature is not less than 550°C to 575°C across much of the Lowlands. Brown et al. (1978) have determined a minimum calcite-dolomite temperature of 625°C at Balmat. Generally, scattered temperatures across the Lowlands (Bohlen et al., 1980), are uniformly greater than 600°C, thus further supporting the view that the carbonate temperatures are minimum values. The isotherms derived by Bohlen et al. (1980) are roughly concentric to the anorthosite massif with 750°C found around Saranac Lake, in the Highlands (Figure 6).

Engel and Engel's temperature estimate based on the K and Na content of K-feldspar-plagioclase pairs, can be used as estimates of minimum temperatures. Their microprobe determination was combined with their optically determined plagioclase

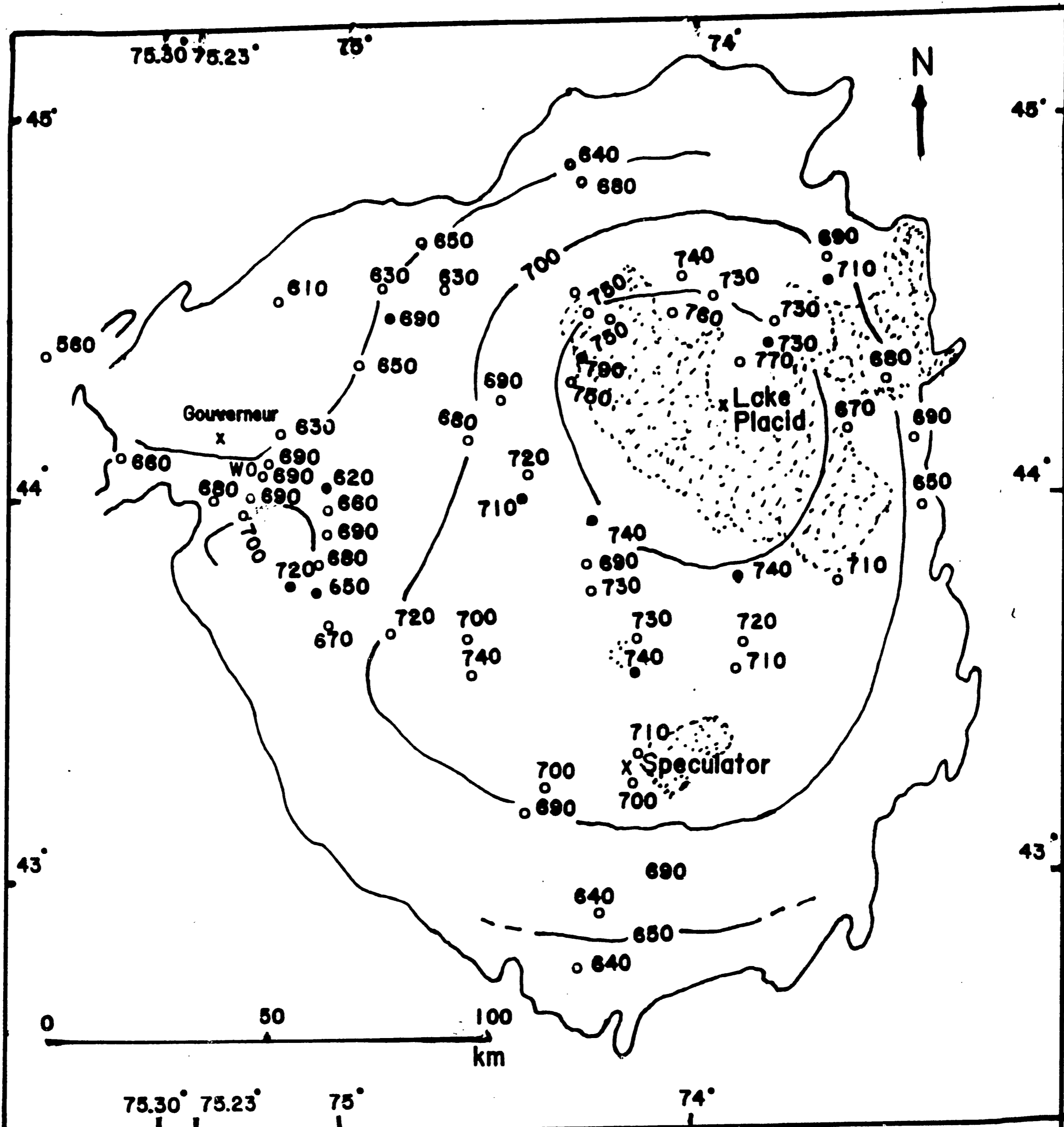


Figure 6. Adirondack Isotherms of Bohlen and others (1980), from magnetite, ilmenite(●) and K-feldspar-plagioclase(○) thermometry. The stippled zone represents anorthosite. wo indicates the position of the wollastonite deposit.

compositions. Using Stormer's (1975) curves adjusted to 6 kb, they obtained 500°C-600°C at Balmat-Emerysville and 600°C to 700°C at Colton.

The study of mineral assemblages supports maximum temperatures in the Lowlands that are not very much higher than the highest Fe-Ti-oxide or feldspar values cited above. The best estimates then show a regional trend which has a gradual eastward increase in pressure and temperature with 6.5 kb and 650°C at Balmat and 8.0 kb and 750°C in the Highlands. Also the absence of wollastonite and the co-existence of calcite + quartz, cited by the Engels (1960) is evidence that the temperature was less than 750°C at Colton, about 10-15 km north of the wollastonite deposit. This assumes that $P_{CO_2} < P_{total} \leq 3$ kb. However, at $P_{CO_2} = 6$ kb, the maximum stability of calcite + quartz is 930°C. Valley and Essene (1977, 1979) have shown that scattered localities of wollastonite do exist in both the Lowlands and Highlands and have suggested that they were stabilized during regional metamorphism by high X_{H_2O} rather than an unusually high temperature. Table 2 gives a brief summary of some of the previous work done in the area.

Table 2. SUMMARY OF PREVIOUS WORK

1. Brown, C. E. (1978) investigated the high-calcium marble in the Beaver Creek.
2. Cushing, H. P. and Newland (1925); Buddington, A. F., (1934); Engel, A. E. (1956) studied the marble and noted the various calc-silicate minerals and the association of wollastonite in marble in contact with syenite intrusives in the area.
3. Buddington and Smyth, 1926, mapped the Lake Bonaparte quadrangle.
4. Agar, 1923, studied contact metamorphism.
5. Engel and Engel (1953) the effects of intrusive magma on metasedimentary rocks.
6. Wynne-Edwards (1972) metamorphism is associated with Grenville Orogeny, about 1.1 to .9 b.y. ago and attained greenschist to lower to middle amphibolite facies.
7. Valley and Essene (1977, 1979) scattered occurrences of wollastonite; confirmed wollastonite stabilization by high X_{H_2O} rather than high temperature.
8. Essene et al. (1978) peak temperature of about $600^{\circ}\text{C} \pm 50^{\circ}\text{C}$ for the Adirondack Lowlands.
9. Engel and Engel (1953) temperature of 500°C to 600°C .
10. Brown et al. (1978) temperature of 625°C at Balmat from calcite-dolomite study; 550°C to 575°C by Essene and Valley (1980).
11. Bohlen et al. (1980) temperature greater than 600°C .
12. Engel and Engel (1960) pressure of 2-3 kb; deWaard (1969) 8-10 kb, in the Lowlands.
13. DeWitt and Essene (1974) lithostatic pressure of 6.5 kb in the Lowlands.

METHODS OF STUDY

The following methods were used to study the wollastonite deposit:

- (a) field mapping
- (b) petrographic methods
- (c) X-ray diffractometry
- (d) X-ray fluorescence analysis
- (e) electron microprobe analysis

Field Mapping

The field work was done between May 23 and 29, 1983. The deposit and the associated syenite gneiss were mapped. Representative samples for analyses were collected and the descriptions of the samples are given in Table 3. Figure 7 shows the sample locality map.

Petrographic Methods

Standard thin sections of some of the representative samples were prepared for petrographic study. Polished thin sections were prepared for electron microprobe analysis. Table 4 gives

Table 3. SAMPLE DESCRIPTIONS

Sample No.	Descriptions
CA-1	Medium to coarse-grained calcitic wollastonite. Contains specks or flakes of graphite, calcite, coarse-grained wollastonite (approx. 1-2 cm in length. The rock is greenish and diopsidic with the yellowish tint of epidote.
CA-2	Coarse-grained blue calcite with white prisms of wollastonite.
CA-3	Mainly blue calcite marble, medium to coarse grained with prisms of wollastonite and flakes of graphite (.5 -3 mm in size).
CA-4	Medium- to coarse-grained blue calcite marble with flakes of graphite (approx. 0.5-1 mm).
CA-5	Medium to coarse-grained blue calcite marble with flakes of graphite. Portions of the sample are pale greenish yellow and white with coarse-grained white wollastonite.
CA-6	Coarse-grained blue calcite marble consisting of thin layers or bands of dark blue calcite marble alternating with white feldspathic bands. The bands are lenticular and the band thickness varies between 1 and 3 cm.
CA-7	Thinly bedded blue calcite marble with graphite flakes.
CA-8	Blue calcite marble, medium- to coarse-grained, thinly layered with graphite flakes.
CA-9	Medium- to coarse-grained (1-5 cm) white decussate wollastonite and calcite grains with greyish green diopside.
CA-10	Same as Sample CA-9.

- CA-11 Coarse-grained white decussate wollastonite (2-5 cm in size) with calcite.
- CA-12 Medium- to coarse-grained white wollastonite containing calcite.
- CA-13 Medium- to coarse-grained white wollastonite.
- CA-14 Mainly coarse-grained blue calcite marble containing predominantly wollastonite (1-3 cm in size); some graphite flakes are present.
- CA-15 Greenish, medium-grained calcite marble which contains some wollastonite.
- CA-16 Coarse-grained blue calcite marble with a small amount of wollastonite.
- CA-17 Light greenish-white diopsidic medium-grained calcite marble with a little wollastonite and graphite flakes.
- CA-18 Coarse-grained pink syenite gneiss with K-spar, pink in color with grain size (1-2 cm) containing grains of epidote and amphibole.
- CA-19 Coarse-grained pink syenite gneiss with patches of granular epidote.
- CA-20 Pale greyish-white syenite gneiss. Porphyroblasts of K-feldspar (1-2 cm), and green mafic minerals such as epidote, amphibole, and augite.
- CA-21 Coarse-grained white to pink quartzite.
- CA-22 Sample at contact between the syenite gneiss and the wollastonite deposit from the wollastonite side. It is diopsidic with coarse-grained (2-5 cm) wollastonite.
- CA-23 Medium-grained white calcite marble.

- CA-24 Light pink, weathered, coarse-grained syenite gneiss.
- CA-25 Coarse-grained pink syenite gneiss with green patches of epidote, amphibole and pyroxene.
- CA-26 Coarse-grained decussate wollastonite with minor diopside.
- CA-27 Medium-grained yellowish green calcite marble with coarse-grained wollastonite.
- CA-28 Coarse-grained decussate (3-5 cm) wollastonite with diopside and calcite.
- CA-29 Light yellowish green diopsidic calcite marble.
- CA-30 Medium- to coarse-grained diopsidic calcite marble with prisms of wollastonite.
- CA-31 Coarse-grained pale greenish white diopsidic calcite marble obtained from a calcite vein (approx. 5 m long and 6 cm wide). The vein originates and disappears within the marble deposit and is in contact with coarse-grained (1-2 cm) wollastonite.
- CA-32 Coarse-grained decussate wollastonite (2-5 cm) with pale green diopsidic coarse-grained calcite marble.
- CA-33 Coarse-grained blue calcite marble containing veinlet of decussate wollastonite. It also contains graphite and diopside.
- CA-34 Very coarse-grained white decussate wollastonite (greater than 5 cm in length).
- CA-35 Medium- to coarse-grained massive blue calcite marble containing a few graphite flakes.
- CA-36 Coarse-grained decussate wollastonite with grain size 1-5 cm, containing some calcite grains.

- CA-37 Coarse-grained pale greenish white calcite marble containing a little wollastonite.
- CA-38 Medium- to coarse-grained pale greenish white diopsidic marble and non-graphitic blue calcite marble.
- CA-39 Coarse-grained white to blue calcite marble. It contains graphite and wollastonite.
- CA-40 Medium- to coarse-grained slightly weathered greyish white calcite marble.
- CA-41 Coarse-grained white wollastonite with pale greenish white diopsidic calcite marble.
- CA-42 Coarse-grained white decussate wollastonite (greater than 5 cm in size) with greenish white diopsidic calcite marble.
- CA-43 Coarse-grained (greater than 5 cm) white decussate wollastonite containing some diopsidic greenish white calcite marble.
- CA-44 Coarse-grained pink syenite gneiss with patches of epidote and amphibole.
- CA-45 Coarse-grained blue calcite marble with diopside and wollastonite.
- CA-46 Green epidote and white coarse-grained syenite gneiss.
- CA-47 Pale greenish white medium-grained diopsidic calcite marble.
- CA-48 Coarse-grained decussate white wollastonite.
- CA-49 Coarse-grained decussate wollastonite with blue calcite marble and specks of graphite.
- CA-50 Medium- to coarse-grained blue graphitic marble.
- CA-51 Coarse-grained decussate white wollastonite (greater than 5 cm in size).

- CA-52 Coarse-grained (1-3 cm) blue calcite marble with wollastonite. Collected at the entrance to the underground mine.
- B Layered white calcite marble in contact with green tremolite-epidote-diopside marble.
- M1A Coarse-grained white calcite marble collected at the of 750 foot level in the underground mine.
- M1B Greyish green medium- to coarse-grained calcite marble collected at the of 700 foot level in the underground mine.

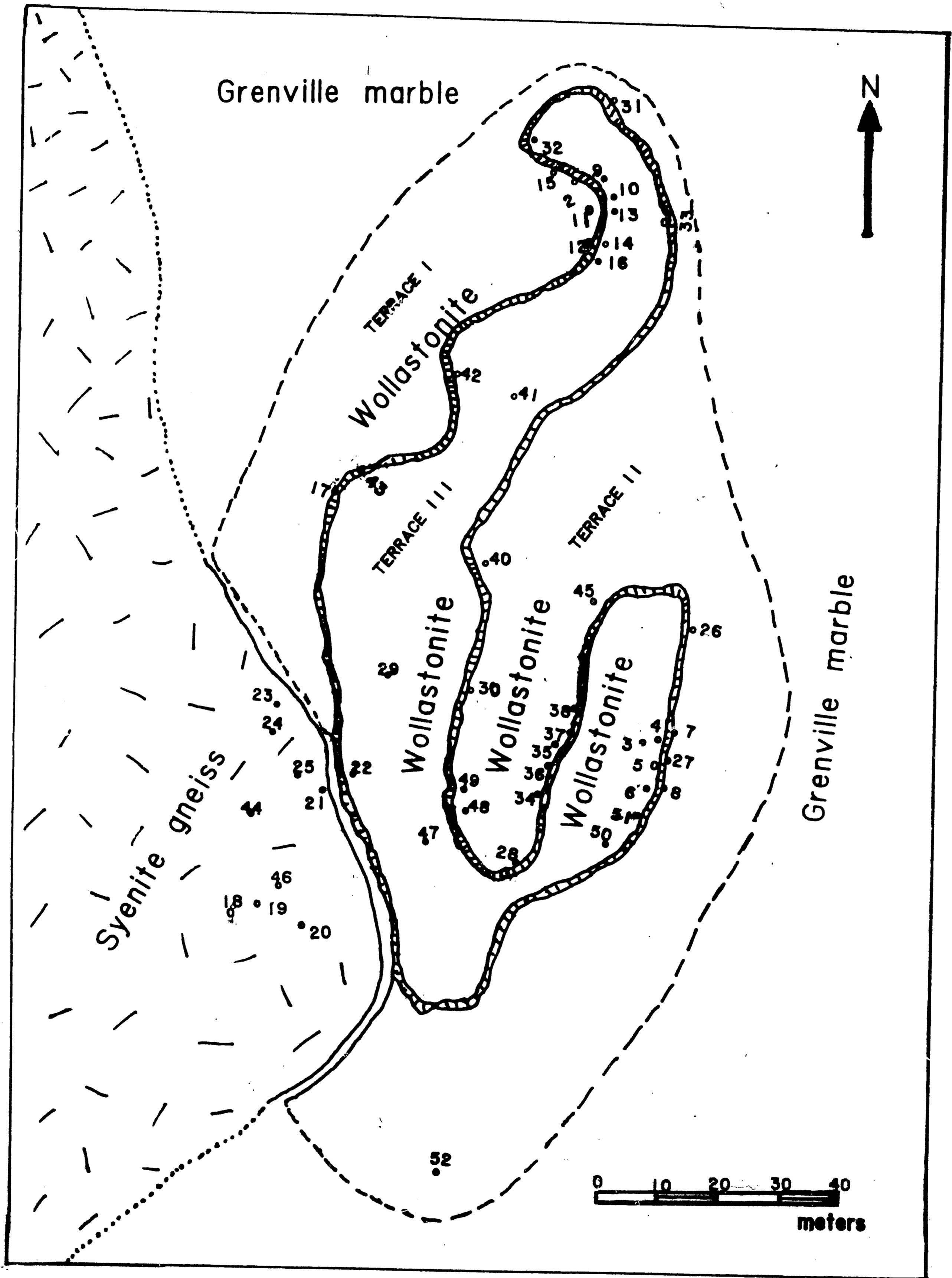


Figure 7. Lake Bonaparte Wollastonite Deposit Sample Locality Map

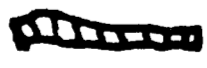
Key:  Cliff face (by 5/22/83)
 - 10 meters high between Terrace I and III
 - 4 meters high between Terrace II and III

Table 4. Mineral Assemblages in the Syenite Gneiss and the Wollastonite Deposit

Specimen No.	Outcrops	K-Spar	Pl	Micpt	Cc/Do	Di	Amph	Ep	Sph	Mag	Apat		
19	Pink Syenite Gneiss	X	X	X	X	X	X	X	X		X		
44	" " "	X	X	X			X	X	X	X			
25	" " "	X	X	X	X	X	X	X	X	X	X		
20	Grey Wh. " "	X	X	X			X	X	X	X			
Specimen No.	Outcrop	K-Spar	Pl	Wo	Cc/Do	Di	Phl	Ep	Sph	Tr	Chl	Gra Gr	CZO
22	Wollastonite			X	X	X	X	X	X	X			X
17	"			X		X	X	X		X			X
29	"			X	X	X		X	X				X
47	"	X			X	X		X	X				
41	"		X	X	X	X				X	X		X
36	"		X	X		X							
39	"			X	X	X						X	
15	"	X				X				X	X		
31	"	X		X	X	X			X	X			
14	"			X	X	X							
33	"			X	X	X			X				
13	"	X		X	X	X			X	X			
5	"	X			X		X				X	X	
6	"	X			X	X	X					X	
27	"		X	X	X	X			X	X			
MLA	"			X	X	X							
MLB	"		X	X		X							
B	"			X	X	X		X					

the mineral assemblages observed under the microscope. Table 5 gives the abbreviations for the identified minerals. Table 6 gives the modal analyses for both the syenite gneiss and the marble.

Table 5. Abbreviations and Formulae of Minerals Used in the Text.

Minerals	Abbreviations	Formulae
Albite	Ab	$\text{NaAlSi}_3\text{O}_8$
Amphibole	Amph	Any one specified
Anorthite	An	$\text{CaAl}_2\text{Si}_2\text{O}_8$
Apatite	Apat	$\text{Ca}_5(\text{PO}_4)_3(\text{F}, \text{Cl}, \text{OH})_2$
Calcite	Cc	CaCO_3
Chlorite	Chl	$\text{Mg}_5\text{Al}_2\text{Si}_3\text{O}_{10}(\text{OH})_8$
Clinzoisite	CZo	$\text{Ca}_2\text{Al}_3\text{Si}_3\text{O}_{12}\text{OH}$
Epidote	Ep	$\text{Ca}_2(\text{Al}, \text{Fe}^{3+})_3\text{Si}_3\text{O}_{10}\text{OH}$
Diopside	Di	$\text{CaMgSi}_2\text{O}_6$
Dolomite	Do	$\text{CaMg}(\text{CO}_3)_2$
Graphite	Graph	C
Grossularite	Gr	$\text{Ca}_3\text{Al}_2(\text{SiO}_4)_3$
Magnetite	Mag	Fe_3O_4
Microcline	Mi	KAlSi_3O_8
Microperthite	Micrpt	$\text{Na}(\text{AlSi}_3)\text{O}_8 - \text{K}(\text{AlSi}_3)\text{O}_8$
Phlogopite	Phl	$\text{KMg}_3\text{AlSi}_3\text{O}_{10}(\text{OH})_2$
Plagioclase	Pl	$(\text{NaSi}, \text{CaAl})\text{AlSi}_2\text{O}_8$
Pyroxene	Py	Any one specified
Potassium Feldspar	K-Spar	KAlSi_3O_8
Orthoclase	Or	KAlSi_3O_8
Quartz	Qt	SiO_2
Rutile	Ru	TiO_2
Sphene	Sph	CaTiSiO_5
Tremolite	Tr	$\text{Ca}_2\text{Mg}_5\text{Si}_8\text{O}_{22}(\text{OH})_2$
Wollastonite	Wo	CaSiO_3
Zoisite	Zo	$\text{Ca}_2\text{Al}_3\text{Si}_3\text{O}_{12}\text{OH}$

Table 6. Modal Analyses, (500 points per slide)
Wollastonite

Specimen No.	Wo	Cc	Di	Do	K-Spar	Pl	Tr	Ep	Czo,Zo	Sph	Chl	Graph	Phl	Apat	Gr
5		35		5	55						1	1	.5		
6		70	.4	25								2	.6		
13	25	15	8	6.2	40		1.7			5					
14	.2	80	.6	15											
15			7		70		70				5				
17	45	.3	35					16	2	.1	.8				
22	50	15	12	5			5	10	1				1		
27	56	4.2	28		.01	1	4			5					
29	80	8	3				3	3	.2	.6					
31	1	80	1.5	15			1			1.5					
33	70	25	2	1						.5					
36	95		2			.5									
39	2	70	20									2			
41	50	.5	26			4	2				5				10
47		3	7		70	.1		5		20				.2	
B	.4	.1	15					80							
MLA	90	.2	7												
MLB	50		47				.6								

39

Syenite Gneiss

Specimen No.	Cc	Di	K-Spar	Pl	Micpt	Ep	Amph	Sph	Mag	Apat
19	2	3	60	20	5	.1	4	5		.4
20		5	25	40	20	3	4.5	.2	.5	.5
25	5		20	50	10	.2	10	2.4	2.1	
44			65	10	5	4.2	8.2	2.5	3.6	

X-Ray Diffractometry

The X-ray diffractometric study was used as an aid in mineral identification. Selected samples for the analysis were ground to powder and sieved through an 80-mesh sieve. The powder was mounted on a glass slide using acetone slurry, and each sample was scanned on the Philips automated X-ray powder diffractometer APD3600. The generator setting was 45Kv and 30Ma current, at a step scan of about 0.020 degrees per second. Prominent X-ray diffraction peaks were identified using silicon ($d = 3.14\text{\AA}$) as reference point or internal standard. Table 4 shows the identified minerals. Calcite and dolomite diffraction peaks were difficult to differentiate. The presence of both was confirmed also by using a stain of Alizarin Red S dissolved in 0.2% cold HCl (0.2 gm/100 ml), applied to rock chips using the method of Friedman (1959) in which magnesian calcite stains dark red to purple and calcite turns white.

X-Ray Fluorescence Analysis

All the samples analyzed by X-ray fluorescence spectroscopy were ground in an automatic agate mortar (Spex-mill) until the entire sample appeared to be a homogeneous powder. The powder was sieved through a 200-mesh sieve. Large particles that could not pass through this sieve were reground until they passed

through the sieve aperture. The powder was then shaken for homogeneity and later was dried in the oven for about 24 hours. The dried sample was kept in a dessicator for about 12 hours. Then 0.40 gm of the powder was mixed with 3.60 gm of lithium tetraborate ($\text{Li}_2\text{B}_4\text{O}_7$) flux and fused to melting in a platinum crucible. The final product (the disk) for X-ray spectrographic analysis was made by pouring the liquid into a red-hot platinum crucible lid. The liquid solidified under atmospheric conditions. All the samples for analysis were prepared in this way. The results of this study was not totally conclusive but some analyses were used to interpret the distribution of some elements in certain localities (see Tables 7, 8, and 9 for the results).

Electron Microprobe Analyses

Quantitative analyses of mineral grains were made by wavelength-dispersive spectroscopic analysis (WDS) with a Jeol Superprobe 733, electron microprobe. All elements were analyzed at an excitation voltage of 15Kv. Sample current was 10Ma. Counting time ranged from 5 to 15 seconds, depending on the elements. LiF, PET, and TAP analyzing crystals were used and drift was controlled by a beam current digitizer. Silicate standards having compositions close to those of the unknowns were

Table 7. XRF Analyses

Sample No.	Syenite Gneiss				Wollastonite Marble							
	18	24	44	46	5	9	14	27	30	36	49	52
SiO ₂	60.37	60.19	61.36	59.22	56.77	49.34	8.53	47.55	43.29	49.24	43.72	15.77
Al ₂ O ₃	15.23	17.32	15.88	15.92	18.03	2.85	0.20	11.23	20.24	5.84	20.85	1.65
FeO	8.96	8.02	8.63	8.60	0.79	0.87	0.06	0.32	6.87	0.21	7.00	6.40
TiO ₂	1.57	1.40	1.46	1.43	0.03	0.02	0.01	0.03	1.09	0.03	1.10	1.08
MnO	0.15	0.14	0.15	0.15	0.03	0.03	0.01	0.03	0.12	0.02	0.14	0.12
MgO	3.63	3.35	3.22	3.55	1.77	11.39	4.06	3.10	4.39	5.30	4.48	8.29
CaO	4.02	4.65	3.00	5.49	11.24	22.72	16.92	21.72	26.80	20.42	26.14	60.21
Na ₂ O	4.41	3.74	4.43	3.91	1.50	3.48	5.34	3.21	3.42	2.81	3.64	7.14
K ₂ O	5.56	8.21	6.80	7.48	8.75	1.48	0.01	0.09	0.15	0.01	0.14	0.20
P ₂ O ₅	0.38	0.36	0.35	0.37	0.15	0.62	0.45	11.23	20.24	0.29	0.34	0.42
	104.32	107.37	105.28	106.12	99.06	92.83	35.61	87.51	106.70	84.17	107.55	101.29

(Analytical results before recalculation to 100%)

TABLE 8. XRF Analyses Recalculated to 100%.

Sample No.	Syenite Gneiss				Wollastonite Marble							
	18	24	44	46	5	9	14	27	30	36	49	52
SiO ₂	57.87	56.05	58.28	55.80	56.78	52.71	22.34	52.48	40.30	57.56	40.46	15.42
Al ₂ O ₃	14.62	16.13	15.08	15.00	18.03	3.04	.51	12.39	18.84	6.83	19.29	1.60
FeO	8.59	7.47	8.20	8.12	.79	.93	.17	.36	6.40	.25	6.48	6.26
TiO ₂	1.51	1.30	1.39	1.35	.03	.02	.02	.06	1.01	.03	1.02	1.06
MnO	.15	.13	.14	.14	.03	.03	.02	.03	.12	.03	.13	.12
MgO	3.48	3.12	3.06	3.35	1.77	12.17	10.63	3.42	4.09	6.20	4.15	8.11
CaO	3.85	4.33	2.85	5.17	11.24	24.27	44.30	23.97	24.95	23.87	24.19	58.87
Na ₂ O	4.23	3.48	4.21	3.68	1.50	3.72	13.98	3.54	3.18	3.29	3.37	6.98
K ₂ O	5.33	7.65	6.46	7.05	8.75	1.58	.03	.10	.14	.02	.13	.20
P ₂ O ₅	.37	.34	.33	.34	.15	.67	1.20	.25	.30	.33	.31	.41
CO ₂					.93	.94	6.76	3.42	.67	1.50	.47	.97

Table 9. XRF Norms, Calculated Weight %

	Syenite Gneiss				Wollastonite Marble							
	18	24	44	46	5	9	14	27	30	36	49	52
Qt	3.1		1.32									
Or	32.86	48.52	40.19	44.21	51.71	6.09				.12		
Ab	37.32	27.14	37.49	29.09	7.84					10.41		
An	5.40	6.23	3.36	3.80	16.62			17.49	36.72	3.81	37.13	
Pl	An ₁₃	An ₁₉	Ang	An ₁₂	An ₆₈			An ₁₀₀	An ₁₀₀	An ₂₇	An ₁₀₀	
Di	5.58	7.89	3.68	12.96	9.51	65.41		18.37		33.30		
Apat	.89	.84	.81	.85	.35	1.55	2.78	.58	.7	.76	.72	.95
Wo					8.38	10.88		23.69		25.13		
Ne		2.44		2.17	2.63	3.71	1.33	16.36	14.58	9.44	15.45	.36
Per		2.12		2.15				.04	1.49		1.49	1.57
Ilm	.32	.29	.32	.32	.06	.04	.04	.06	.26	.06	.28	.26
Hem	8.96	8.02	8.63	8.60	.78			.36	6.40	.24	6.48	
Le						2.55		.46				
Ol		3.28		1.98		2.69	.49					
Acm												
Kal							.10	.10	.47	.47	.44	.67
Wus							24.05		9.42		9.37	48.89
Hyp	6.45		6.31									
Ru	3.43		3.17									
Nms		1.24				5.02	26.83	26.83	26.83	26.83	26.83	7.31
Cc					2.13	2.16	15.50			3.44		
Cos							52.38	5.99	25.40		24.09	88.58

44

Legend to abbreviation symbols not in the text follow this page.

Abbreviation Legend

Acm:	Acnite	--	$\text{NaFeSi}_2\text{O}_6$ (cpx)
Hem:	Hematite	--	Fe_2O_3
Hyp:	Hypersthene	--	$(\text{Mg}_1\text{Fe}^{2+})_2\text{Si}_2\text{O}_6$
Ilm:	Ilmenite	--	FeTiO_3
Kal:	Kalsilite	--	KAlSiO_4
Le:	Leucite	--	KAlSi_2O_6
Ne:	Nepheline	--	$\text{Na}_3\text{K}(\text{AlSiO}_4)_4$
Ol:	Olivine	--	$(\text{Mg}_1\text{Fe})\text{SiO}_4$
Per:	Periclase	--	MgO
Wus:	Wustite	--	Fe_{1-x}O
Nms:	Sodium Metasilicate	--	$\text{Na}_2\text{O} \cdot \text{SiO}_2$
Cos:	Calcium Orthosilicate	--	$2\text{CaO} \cdot \text{SiO}_2$

used. Pyroxenes, wollastonite, amphibole, feldspars, epidote and carbonate phases were analyzed as shown in the tables.

Stoichiometric calculations on the basis of 6(0) for the pyroxenes, 23(0) for amphiboles, 6(0) for wollastonite, 8(0) for feldspars and 3(0) for the carbonates were made. The mole fractions of K-feldspar, albite, anorthite, and enstatite, ferrosilite and wollastonite (for pyroxenes) were calculated. Minerals were renormalized using the accepted stoichiometry following Deer, et al. (1966).

In pyroxene, the formula, $Y_2Z_2O_6$, assumes that $Z^{IV} = Si, Al$; $Y^{VI} = Mg, Ca, Fe^{2+}, Al, Ti, Mn, Na$. Normalization is based on four IV and VI cations with no site vacancies from charge balance; it is assumed that $Fe^{3+} = Al^{IV} + K - Na - 2Ti$. In amphibole in the formula $A_{0-1}X_2Y_5Z_8O_{22}(OH, F, Cl)_2$, it is assumed that $Z^{IV} = Si, Al$; Y, the M1, M2; all M3^{VI}-sites = $Fe^{2+}, Fe^{3+}, Al, Mg, Ti, Mn$; and that X, the M4^{VIII}-site = Ca, Na ; and that A-site = Na, K , above which is necessary to fill M4. Normalization is based on 13IV+VI cations with vacancies only on the A-sites (Leake, 1968). From the charge balance, it is assumed that $Fe^{3+} = Al^{IV} - Al^{VI} + Na^{VIII} - K^A - Na^A - 2Ti$; also $OH + F + Cl = 2$. Generally, the number of cation sites on the basis of 23(0) in a typical calcic amphibole may be broken down as follows:

- (a) Eight tetrahedral sites (T-sites) occupied by Si+Al

- (b) Five small octahedral sites (M1), (M2), and (M3),
occupied by Mg, Fe, Al + Mn (+Ti)
- (c) Two large octahedral sites, occupied by
Ca+Na+Fe²⁺+Mg+Mn
- (d) One A-site, occupied by Na+K

Electron microprobe analyses of these minerals are given in Table 10.

Mineralogy and Texture

The distribution of mineral assemblages reflects the general bulk chemical composition in the wollastonite deposit. Field observation of the entire deposit shows the dispersed abundant distribution of wollastonite and subordinate light greenish diopside. Besides these two minerals, others include potassium feldspars (mainly microcline), minor plagioclase, epidote (grouped as clinozoisite, zoisite), tremolite, phlogopite, calcite and a little dolomite. Sphene, graphite, chlorite, grossularite and accessory apatite have also been identified.

Phlogopite occurs as micaceous platy crystals, wollastonite is decussate or granoblastic or fibrous, and aggregates of epidote, sphene, tremolite and chlorite were also observed. Graphite flakes range in size between .1 to 5 mm in diameter and are disseminated in the blue calcite zone. Wollastonite grains

Table 10. Electron Microprobe Analyses of Feldspar

Sample No.	Pink Syenite	Greyish White Syenite			
	19e	20(1a)	20(IIb)	20(IIIId)	20(IVg)
SiO ₂	65.22	68.43	68.45	63.57	68.10
Al ₂ O ₃	19.01	20.23	20.06	19.23	20.36
FeO	0	0	.030	0	0
TiO ₂	.08	.18	.04	0	.11
MgO	.01	0	0	0	.0
CaO	.20	.11	.100	.06	.15
Na ₂ O	.84	11.19	11.69	.30	11.28
K ₂ O	16.46	.09	.09	16.38	.10
TOTAL	101.84	100.22	100.45	99.54	100.10
Cation Proportions Normalized to 32 (O)					
Si	11.876	11.904	11.908	11.831	11.874
Al	4.080	4.148	4.114	4.218	4.184
Fe ³⁺	.002	0	0	.003	.003
Ti	.012	.024	.005	0	.014
Mg	.003	0	0	0	0
Fe ²⁺	0	0	.004	0	0
Ca	.039	.040	.018	.012	.029
Na	.296	3.775	3.942	.109	3.812
K	3.824	.020	.020	3.888	.022
Si+Al+[ti]	15.96	16.052	16.022	16.049	16.061
Na+Ca+K	4.159	3.836	3.980	4.009	3.863
100Ca/Ca+Na+K = An	.938	1.043	.452	.299	.751
100Na/Na+Ca+K = Ab	7.112	98.410	99.045	2.719	98.680
100K/K+Ca+Na = Mi	91.945	.521	.503	96.982	.570

Table 10. Feldspars (Contd.)

Sample No.	Pink Syenite		Grey-White Syenite		
	44(Ib)	44(IIc)	46(1b)	46(IIc)	46(IIId)
SiO ₂	66.54	66.44	61.40	62.87	62.26
Al ₂ O ₃	19.98	20.20	18.32	18.84	18.46
FeO	.11	.11	.02	.13	.12
TiO ₂	.26	0	0	.34	0
MgO	.01	0	0	0	0
CaO	.11	.12	0	0	0
Na ₂ O	11.80	11.93	.47	.99	.56
K ₂ O	.08	.07	15.23	14.79	15.02
TOTAL	98.90	98.86	95.43	97.96	96.42
Cation Proportions Normalized to 32 (O)					
Si	11.795	11.784	11.881	11.83	11.903
Al	4.175	4.222	4.177	4.178	4.159
Fe ³⁺	.003	0	.001	.001	.003
Ti	.034	0	0	.048	0
Mg	.004	0	0	0	0
Fe ²⁺	.013	.016	.001	.020	.016
Ca	.022	.022	0	0	0
Na	4.054	4.103	.178	.363	.208
K	.018	.016	3.759	3.549	3.662
	15.97	16.010	16.059	16.010	16.07
	4.094	4.141	3.937	3.912	3.870
An	.537	.531	0	0	0
Ab	99.023	99.082	4.521	9.279	5.375
Mi	.440	.386	95.479	90.721	94.625

Table 10. Feldspars (Contd.)

Sample No.	Wollastonite Marble				
	15(Ia)	15(IIb)	15(IIIc)	15(IVd)	15(VM)
SiO ₂	62.53	63.59	62.93	60.86	62.65
Al ₂ O ₃	18.99	19.17	18.78	18.57	18.27
FeO	0	.05	.04	0	.02
TiO ₂	0	.11	0	.11	0
MgO	0	0	0	0	0
CaO	.03	0	0	0	.04
Na ₂ O	.74	.91	.39	.91	.65
K ₂ O	16.19	15.02	15.48	14.92	15.21
TOTAL	98.47	98.84	97.62	95.99	96.83
Cation Proportions Normalized to 32 (0)					
Si	11.792	11.848	11.891	11.794	11.934
Al	4.220	4.210	4.182	4.242	4.102
Fe ³⁺	.001	.002	.001	.002	.002
Ti	0	.016	0	.016	0
Mg	0	0	0	0	0
Fe ²⁺	0	0	0	0	0
Ca	.006	0	0	0	.009
Na	.269	.328	.142	.341	.239
K	3.893	3.570	3.732	3.688	3.695
	16.013	16.058	16.074	16.038	16.036
	4.168	3.914	3.874	4.040	3.943
An	.144	0	0	0	.228
Ab	6.454	8.380	3.804	8.441	6.061
Mi	93.402	91.211	96.334	91.728	93.710

Table 10. Electron Microprobe Analyses of Amphibole (Contd.)

Sample No.	Pink Syenite		Pink Syenite			
	25(IV)	25(V)	44(II)	44(IV)	44(X)	
SiO ₂	50.04	50.60	42.42	51.89	51.50	
Al ₂ O ₃	1.75	.86	10.10	.98	1.57	
FeO	22.45	21.65	20.38	20.95	22.72	
TiO ₂	.05	.27	.61	.05	.08	
MgO	10.10	11.41	9.35	11.52	10.15	
MnO	.35	.41	.57	.26	.45	
CaO	11.73	12.56	11.38	12.03	11.62	
Na ₂ O	.42	.23	.95	.33	.35	
K ₂ O	1.92	.10	.91	0	.10	
TOTAL	98.81	98.09	96.67	98.00	98.53	
Total Cations Recalculated to 13 Exclusive of K, Na, Ca, on the Basis of 23 (O).						
8	Si	7.540	7.533	6.394	7.664	7.613
T	Al	.311	.152	1.606	.171	.273
	Fe ³⁺	.149	.315	-	.165	.114
5	Al	-	-	.188	-	-
	Fe ³⁺	.821	.336	1.150	.434	.482
	Ti	.002	.030	.070	.005	.009
C	Mg	2.184	2.532	2.101	2.536	2.238
	Fe ²⁺	1.942	2.044	1.418	1.988	2.212
	Mn	.057	.051	.073	.033	.056
2	Ca	1.892	2.003	1.837	1.903	1.870
B	Na	.108	-	.163	.094	.101
0 ≤ 1	Na	.016	.065	.114	-	-
A	K	.369	.018	.174	-	.019
	Mg/Fe+Mg	.429	.484	.450	.495	.444
	Fe/(Fe+Mg)	.571	.516	.550	.505	.556
	Ca+Fe+Mg	6.988	7.230	6.506	7.026	6.916
	Mg/(Mg+Fe+Ca)	.313	.350	.323	.361	.324
	Fe/(Mg+Fe+Ca)	.417	.373	.395	.368	.406
	Ca/(Mg+Fe+Ca)	.271	.277	.283	.271	.270

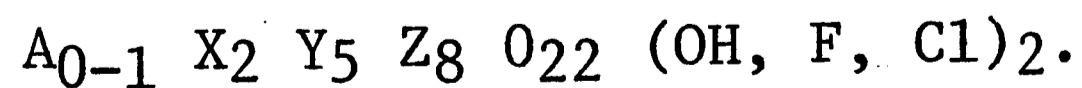


Table 10. Electron Microprobe Analyses of Pyroxenes (Contd.)

Sample No.	Pink Syenite			
	19(II)	19(III)	19(IV)	
SiO ₂	50.22	50.92	48.66	
Al ₂ O ₃	1.21	.04	.31	
FeO	14.55	16.18	19.48	
TiO ₂	0	0	0	
MgO	9.02	8.23	6.39	
MnO	.35	.40	.41	
CaO	20.12	23.86	22.17	
Na ₂ O	.48	.16	.74	
TOTAL	95.95	99.79	98.16	
<u>Cation Proportions on the Basis of 6 (O).</u>				
Z { Si	2.002	1.987	1.966	
T { Al	.057	.002	.015	
2 { Fe ³⁺	0	.001	.001	
X+Y=2 {	Al	.057	-	-
	Fe ³⁺	.001	-	-
	Ti	0	0	0
	Mg	.536	.479	.385
	Fe ²⁺	.484	.527	.657
	Mn	.012	.013	.014
	Ca	.859	.997	.959
Na	.037	.012	.058	
En = 100Mg / (Mg+Fe+Ca)	28.511	23.914	19.231	
Fs = 100Fe / (Mg+Fe+Ca)	25.798	26.311	32.867	
Wo = 100Ca / (Mg+Fe+Ca)	45.691	49.775	47.902	
Mg / (Mg+Fe)	.525	.476	.369	
Fe / (Mg+Fe)	.475	.477	.631	

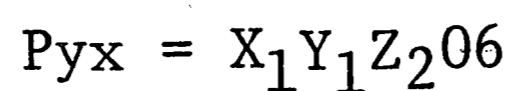


Table 10. Electron Microprobe Analyses (Contd.)

Sample No.	Diopside				Epidote
	36(a)	36(c)	36(d)	31(d)	47
SiO ₂	55.05	55.31	56.03	54.77	37.80
Al ₂ O ₃	.33	.33	.21	.40	20.95
FeO	.50	.40	.36	2.64	14.47
TiO ₂	1.09	0	0	0	.03
MgO	17.89	17.99	18.17	16.36	0
MnO	0	.03	.05	.10	.08
CaO	24.67	25.46	25.01	23.75	22.92
Na ₂	.26	.20	.17	.27	0
TOTAL	99.80	99.72	100.01	98.29	96.25
Cation Proportions on the Basis of 6 (0).					
Si	1.9886	2.0008	2.0150	2.0205	1.518
Al	.0114	-	-	-	.482
Fe ³⁺	-	-	-	-	-
Al	.0025	.0139	.0090	.0175	.510
Fe ³⁺	-	-	-	-	.486
Ti	.0297	0	0	0	.001
Mg	.9635	.9705	.9740	.8997	0
Fe ²⁺	.0152	.0121	.0110	.0814	-
Mn	0	.0010	.0016	.0030	.003
Ca	.9547	.9866	.9637	.9387	.986
Na	.0179	.0144	.0122	.0192	0
En=100Mg/(Mg+Fe+Ca)	49.83	49.30	49.98	46.86	-
Fs=100Fe/(Mg+Fe+Ca)	0.79	0.61	0.56	.042	-
Wo=100Ca/(Mg+Fe+Ca)	49.38	50.10	49.45	48.90	-
Mg/Mg+Fe	0.984	.988	.989	.917	-
Fe/Mg+Fe	0.016	.012	.011	.083	-

Table 10. Electron Microprobe Analyses of Wollastonite (Contd.)

Sample No.	36(b)	36(d)	36(e)	36(g)	31
SiO ₂	51.08	51.47	51.37	50.93	51.06
Al ₂ O ₃	.01	0	0	0	0
FeO	.18	.06	0	0	.07
TiO ₂	0	0	0	0	0
MgO	0	.02	0	0	.05
MnO	0	0	.03	.10	.02
CaO	46.71	46.69	46.54	46.85	45.70
Na ₂ O	0	.08	0	.05	.05
TOTAL	97.99	98.33	97.93	97.92	96.95
<u>Cation Proportions on the Basis of 6 (O).</u>					
Si	2.0112	2.0168	2.0194	2.0078	2.0251
Al	.0007	0	0	0	0
Fe	.0060	.002	0	0	.0023
Ti	0	0	0	0	0
Mg	0	.0011	0	0	.0027
Mn	0	0	.0009	.0033	.0006
Ca	1.9704	1.9600	1.9602	1.9790	1.9419
Na	0	.0061	0	.0036	0.0041
Mg/Mg+Fe	0	.35	0	0	.54

Table 10. Electron Microprobe Analyses of Carbonates (Contd.)

Sample No.	(14(a))	(14(c))	14(f)	14(g)	14(k)	14(l)	31(b)	31(d)
CaO	50.40	50.84	50.44	50.93	52.05	50.99	51.40	48.68
MgO	.11	.06	.04	.14	.12	.14	0	.04
FeO	0	.03	0	0	.08	0	0	.01
SiO ₂	.01	0	0	0	.01	0	0	.05
Total	50.52	50.94	50.48	51.07	52.26	51.14	51.40	48.78
CO ₂	49.48	49.06	49.52	48.93	47.74	48.86	48.60	51.22

Cations proportions on the basis of 3(O)

Ca	2.989	2.993	2.996	2.988	2.985	2.988	3.000	2.990
Mg	.009	.005	.004	.012	.009	.012	0	.004
Fe	0	.002	0	0	.04	0	0	.001
Si	.005	0	0	0	.005	0	0	.003
CaCO ₃	99.70	99.78	99.88	99.61	99.58	99.61	100	99.86
MgCO ₃	.30	.17	.12	.39	.31	.39	0	.02
FeCO ₃	0	.05	0	0	.11	0	0	.02
Temp. Est.	350°C		400°C		400°C			

Table 10. Electron Microprobe of Epidote Grain (Contd.)

Sample No.	47
SiO ₂	37.80
Al ₂ O ₃	20.95
FeO	14.47
TiO ₂	.03
MgO	0
MnO	.08
CaO	22.92
Na ₂ O	0
TOTAL	<u>96.25</u>

Cation Proportions on the Basis of 13(O).

Si	1.518
Al	.482
Fe ³⁺	-
Al	.510
Fe ³⁺	.486
Ti	.001
Mg	0
Fe ²⁺	-
Mn	.003
Ca	.986
Na	0

range in size from about 1 mm up to more than 3 cm. Calcite grains are subhedral sometimes with twin lamellae and also occur with well-developed fine-grained mortar texture. Quartz was not observed. (See Figures 8 and 9.)

Most grains appear optically homogeneous apart from the presence of fluid inclusions. A few crystals of K-feldspar appear zoned. The zoning may be caused by metasomatic effects during or after crystallization. Some calcite and feldspar grains in the marble, and feldspar grains in the syenite gneiss are deformed. This effect may be due to external stress. The deformation might be associated with the regional deformation and metamorphism which affected the rocks of the Lowlands.

Textural evidence shows that most of the minerals have formed during prograde contact metamorphism. Because of intense recrystallization and annealing of the marble during this metamorphic event or during the superimposed regional metamorphism, rock texture alone is not very useful in determining the prograde reaction sequence. The decussate wollastonite, calcite, diopside, and phlogopite may be associated with peak metamorphism. There is no evidence to establish the prograde or retrograde metamorphic process where wollastonite is fibrous or calcite develops mortar overgrowth.

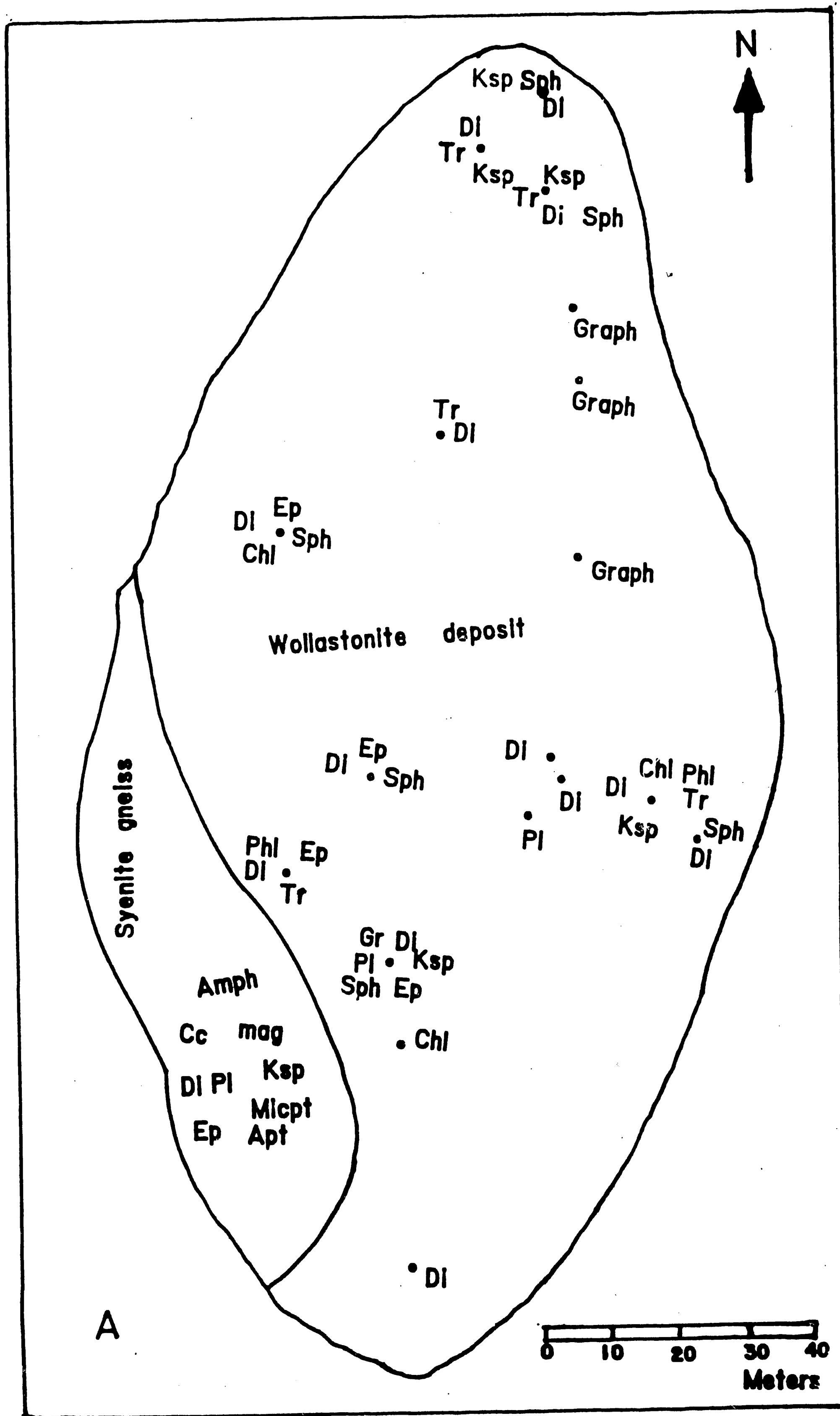


Figure 8. Distribution of mineral phases in the syenite gneiss and wollastonite deposit. Wollastonite and calcite present in almost all optically studied samples in the wollastonite deposit.

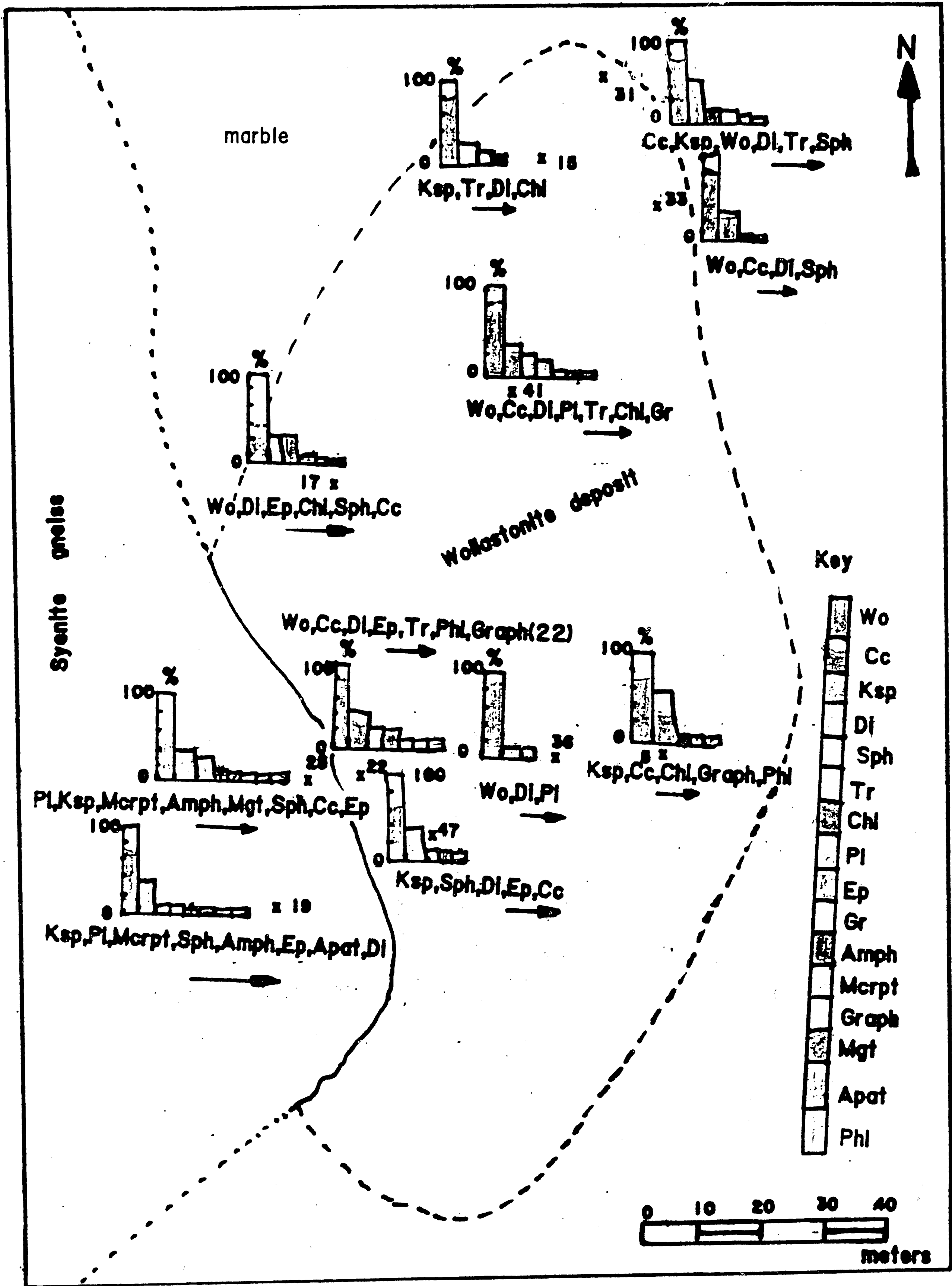


Figure 9 . Mineral distribution and abundance in some representative samples in the wollastonite deposit and syenite gneiss. Abundance is estimated in percentages. The arrows indicate that the listed minerals decrease in abundance in that order.

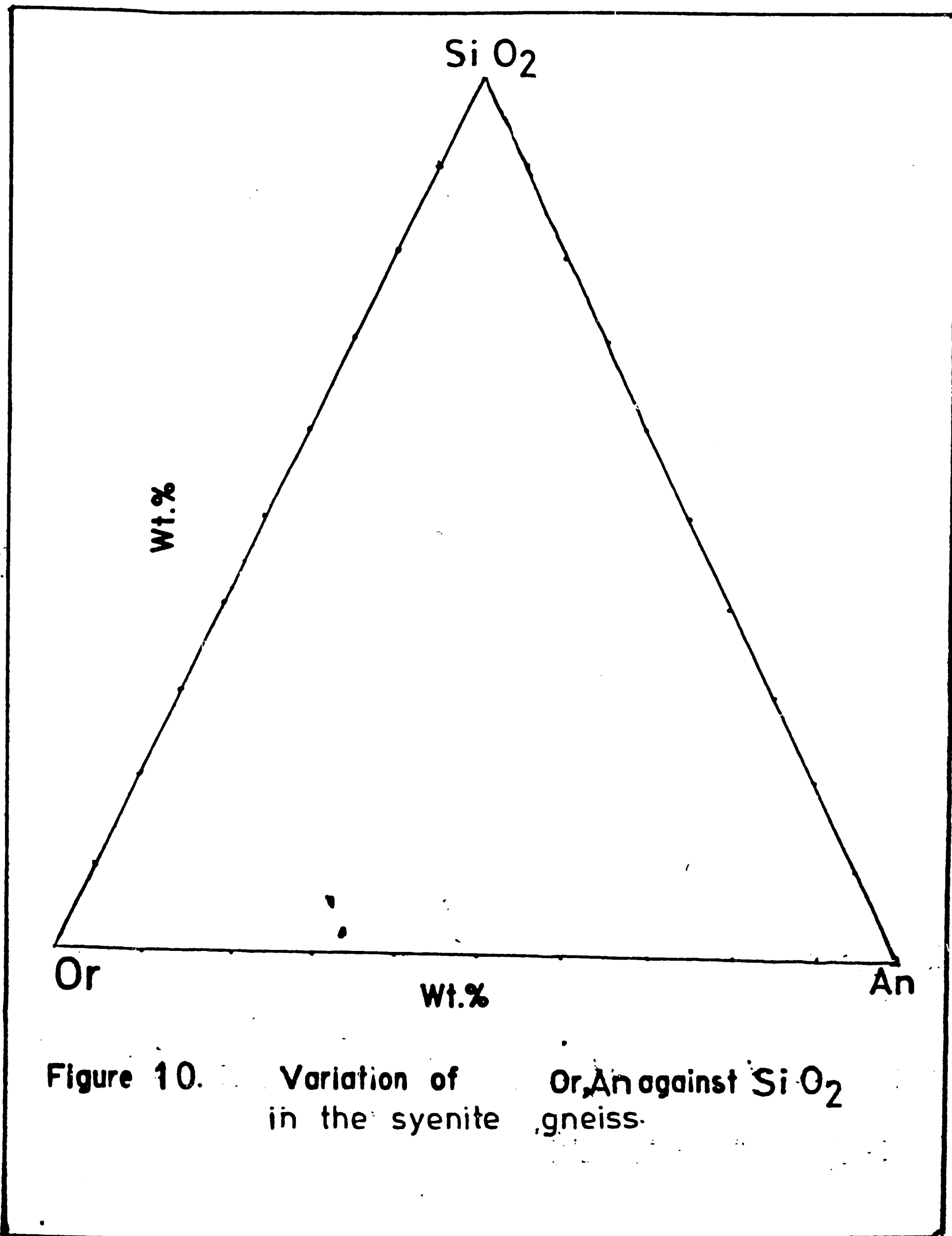
The diopside grains are typically engulfed by wollastonite. This may indicate the later formation of wollastonite. In some thin sections, the diopside grains show fine-grained texture around their rims. Small grains of tremolite are mainly anhedral and discrete. Retrograde reactions under dwindling temperature at constant pressure would have resulted in the formation of some of the minerals such as tremolite, epidote and sphene.

Mineral Chemistry

The mineral phases observed optically appear homogeneous. Most of them possess sharp boundary contacts with one another. There could have been limited diffusion of elements especially at high temperature. Moreover, it is known that solid solution can significantly extend or restrict the stability of one mineral assemblage relative to one another. To investigate these problems, some phases such as wollastonite, diopside carbonate, epidote, and K-feldspar in the marble were chemically analyzed.

The results of these analyses are shown in Table 10. These reflect the homogeneous nature of the phases. Core to rim analysis was made on the grains but no appreciable zonation of elements was found. Chemical compositional variations within grains were not observed within the phases both in the syenite gneiss and in the marble. In the syenite gneiss, where the field

observation shows color variation from pink to grey-white (e.g. samples 19, 25, 44 for pink syenite and samples 20 and 46 for grey-white syenite), the weight percent of cations such as Si, Al, Fe, Ti, Mg, Cr, Na, and K show no systematic variation. It thus makes it difficult to decide what impurity in the crystal lattice of the feldspar could cause the color change at this level of detection. Therefore, the problem of the color change remains unsolved. The absence of some elements or their cation proportion could be interpreted to indicate apparent minor-element substitution within the crystal lattice. But the amount of substitution appears too small to explain any large scale zoning. Amphibole analyses also show appreciable homogeneity. The amphibole ranges in composition from actinolite to actinolitic hornblende, based on the classification by Leake, 1968. The Mg/(Mg+Fe) ratios vary between 0.429 and 0.495. The feldspars in the wollastonite marble are mainly microcline. The plagioclase grains were too small to be chemically analyzed. The K-feldspar contains little Ca or Na. The Al content shows no variation between feldspars from the syenite gneiss and from the marble. The variation in the plot of SiO₂, An and Or in the syenite gneiss is shown in Figure 10. The plot indicates that this composition places the rock in the syenite group.



The ratio of $Mg/(Mg+Fe)$, $Fe/(Mg+Fe)$, $Ca/(Mg+Fe+Ca)$, places the analysed pyroxene on the diopside side of the quadrilateral. The $Mg/(Mg+Fe)$ ratio for the pyroxene ranges between 0.917 to 0.989 in the marble and 0.369 to 0.525 in the syenite gneiss. In the marble diopside, the Si, Mg, and Ca values are higher than those of the diopside of the syenite gneiss. But this is reversed for Al, Fe and Na. In both rock types Mn is either absent in the analysis or the proportion is too low to be detected. Ti is also very low. Ca and Si are, of course dominant in the wollastonite which appears to be a pure end-member phase. (See Figure 11.)

The fact that wollastonite is not uniformly distributed in the marble may be the result of insufficient SiO_2 . The SiO_2 might have been original in the parent limestone or introduced in a siliceous fluid supplied by the magmatic syenite. The blue calcite is virtually free of siliceous impurities, and wollastonite is less abundant within the blue calcite layer. The Mg content of the carbonate is very low and Fe is almost absent.

The plagioclase content of the wollastonite marble is very low. Presumably, the Al+Si left over after the formation of other silicate phases at medium temperature was not enough for plagioclase to form. Moreover, it appears that at high temperature, there is competition for Si and Al between either

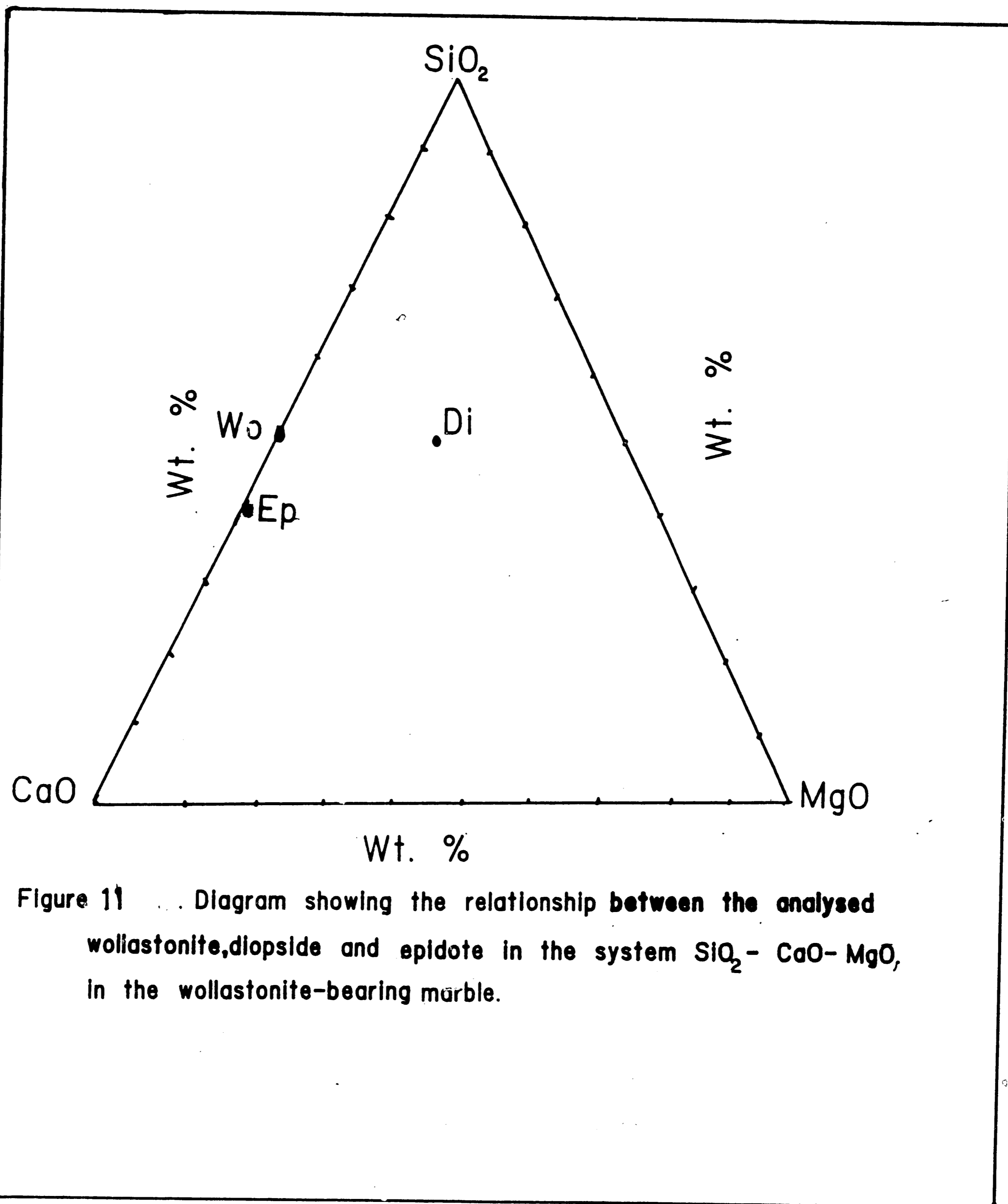


Figure 11 . . . Diagram showing the relationship between the analysed wollastonite, diopside and epidote in the system $\text{SiO}_2 - \text{CaO} - \text{MgO}$, in the wollastonite-bearing marble.

plagioclase or grossularite. The Al+Si would form K-feldspar, depending on the amount of Ca available to go into plagioclase or grossularite. The fact that neither grossularite nor plagioclase is abundant may be explained by this limitation.

The presence of quartz often renders grossularite unstable at high temperatures (Yoder, Jr., 1950), but this reaction is also $p\text{CO}_2$ dependent.

The results of XRF analysis was not very useful for the interpretation of the mineral chemistry. The oxide total values came out too low. On the other hand, a few results were useful to show the variation of Na_2O , K_2O , FeO, CaO and Al_2O_3 against SiO_2 (Figure 12) for the marble and the syenite and $1/3 \text{SiO}_2 + \text{K}_2\text{O}-\text{MgO}-\text{CaO}-\text{FeO}$ against $\text{MgO}+\text{FeO}+\text{CaO}$ in the syenite gneiss (Figure 13). This plot shows the lack of homogeneity in the distribution of elements in the marble. This is only a function of bulk chemical composition. It does not reflect any gradational change between the syenite gneiss and the wollastonite marble as was expected.

An ACF diagram (Figure 14) was plotted based on the XRF results from the syenite gneiss. The clustering of plotted points might represent chemical equilibrium attained between different phases.

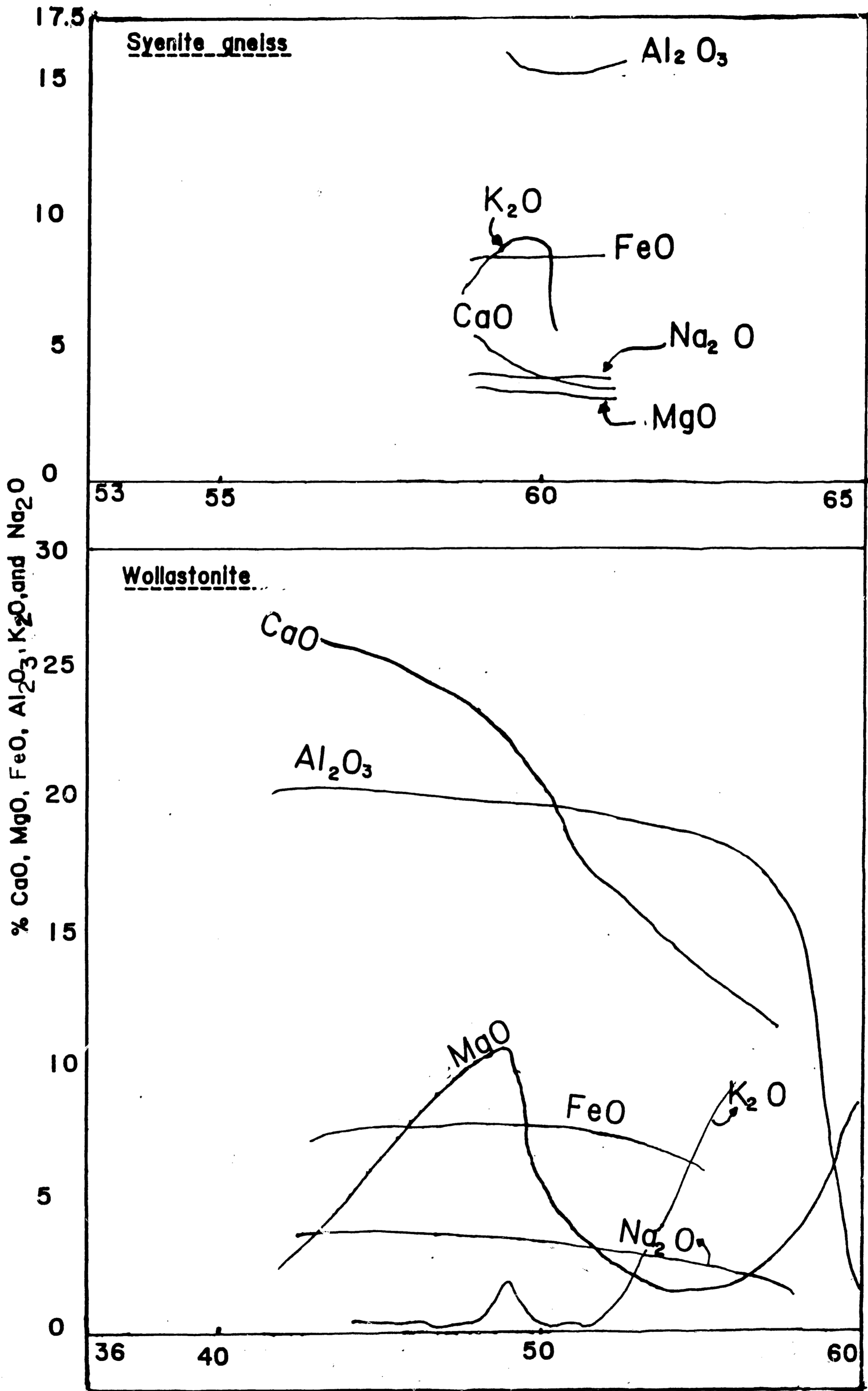


Figure 12. Variation of CaO, MgO, FeO, Al₂O₃, K₂O, Na₂O against SiO₂ from XRF chemical analysis.

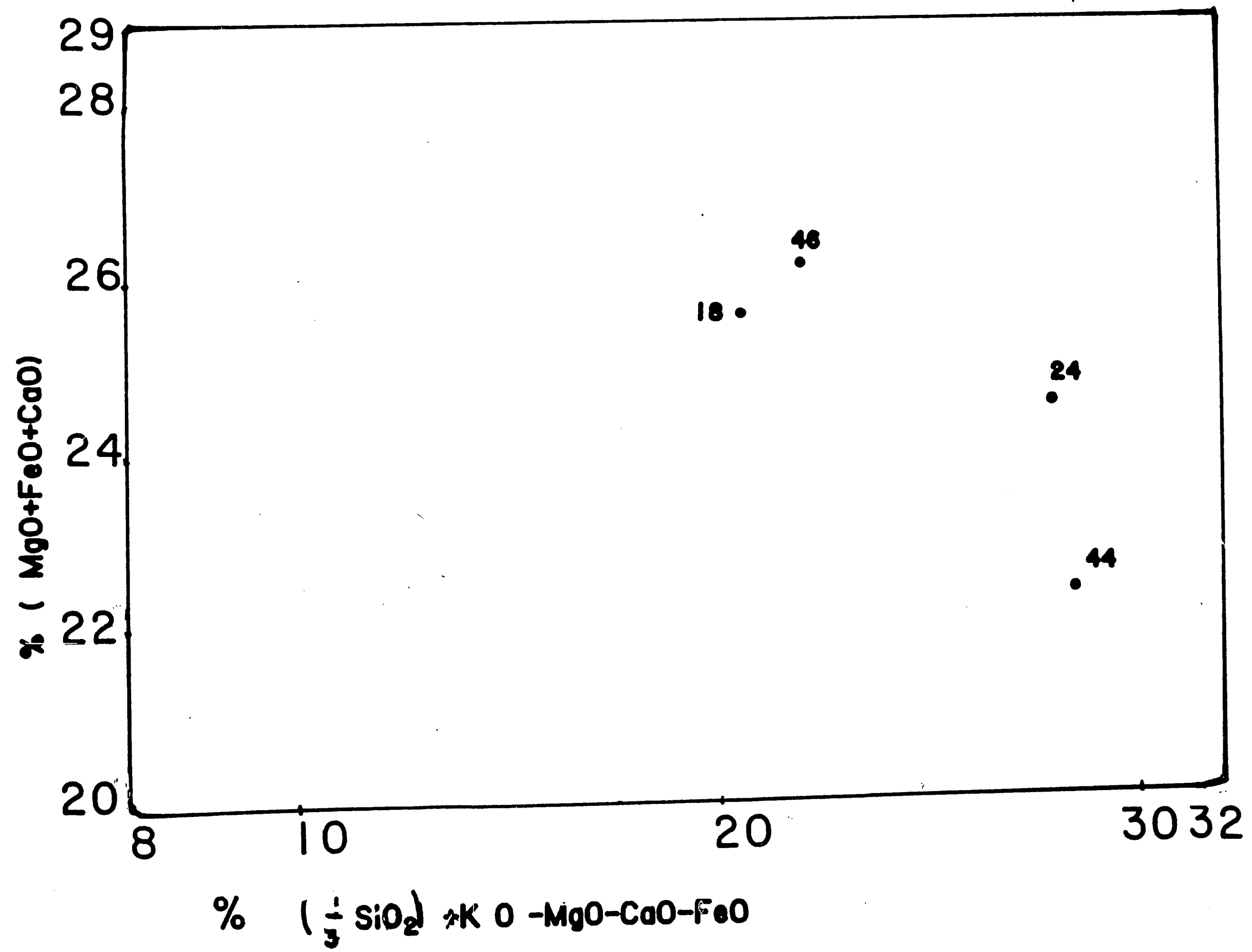
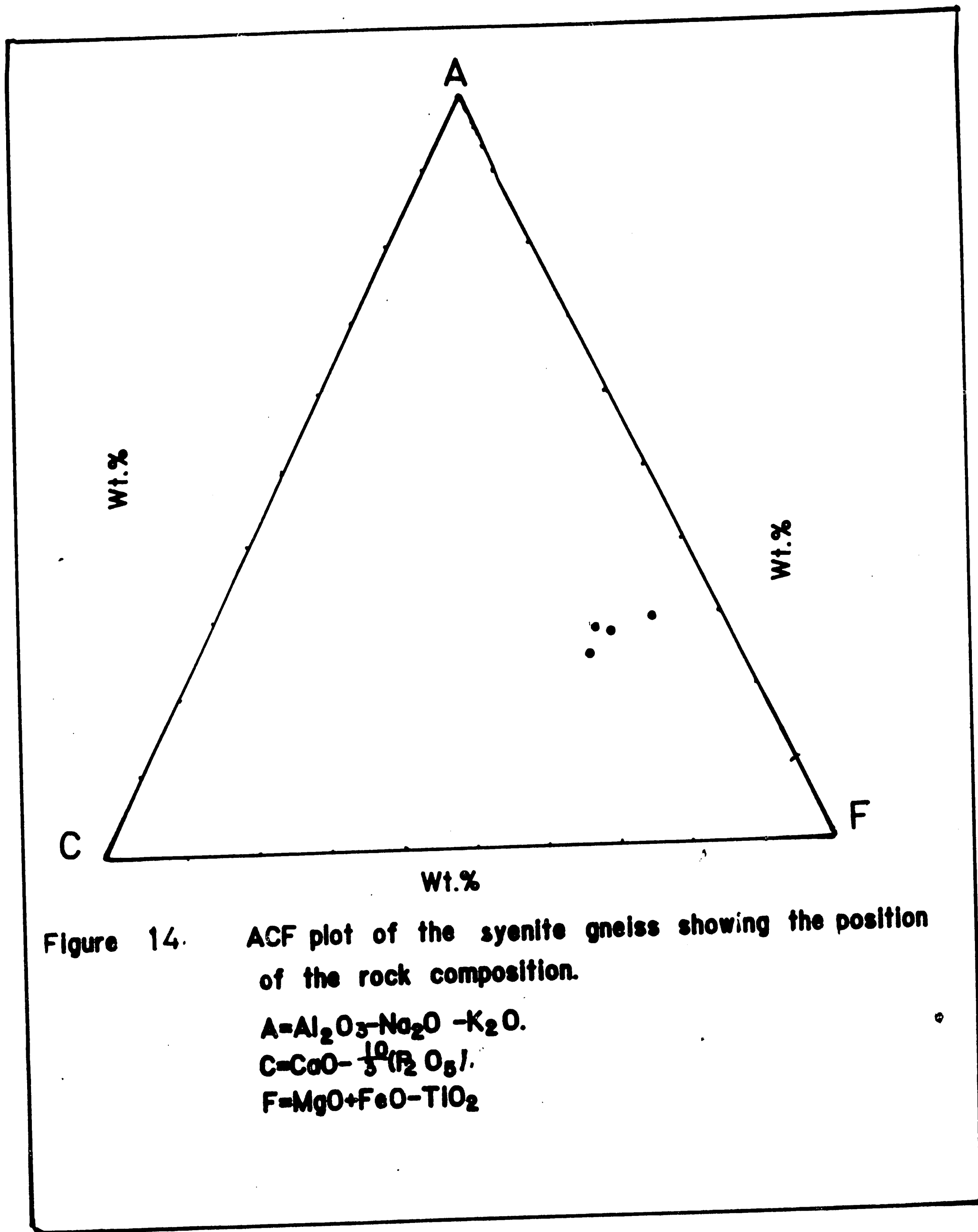


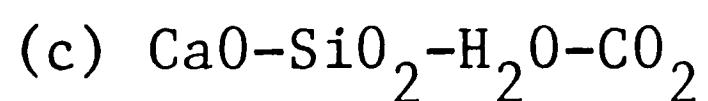
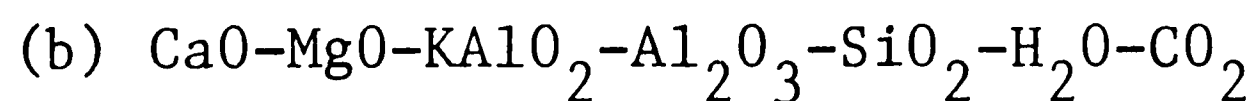
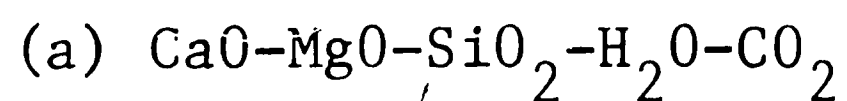
Figure 13. Diagram showing the relation between $\frac{1}{3} \text{SiO}_2 + \text{K}_2\text{O} - \text{MgO} - \text{CaO} - \text{FeO}$ and $\text{MgO} + \text{FeO} + \text{CaO}$, in the syenite gneiss. Numbers correspond to sample localities.



MINERAL EQUILIBRIA

Introduction

The relative stability of the carbonate-silicate metamorphic assemblages is purely temperature and pressure dependent. The presence of a fluid phase is important in this consideration. In the wollastonite deposit, the following systems can be inferred from the existence of the identified mineral phases.



Combinations of different mineral assemblages have been found in several samples. In the system, $\text{CaO-MgO-SiO}_2\text{-H}_2\text{O-CO}_2$, calcite dolomite, quartz, tremolite, diopside, and wollastonite may coexist at equilibrium, if temperature, total rock pressure and chemical potentials of H_2O and CO_2 are externally controlled. That is, if there are four independent variables, if $P = C+2-F=3$, where P = number of phases, C = components, F = number of degree of freedom ($C = 5$, $F = 4$). These conditions are inherent assumptions in Goldschmidt's mineralogical phase rule, and in Korzhinskii's classification of CO_2 and H_2O as "preferred mobile" components during metamorphism.

If four minerals coexist in a five-component system involving two volatile components, a devolatilization reaction

can be written between them (Korzhinskii, 1959). These reactions and their invariant point may be schematically portrayed as a function of two variables only by assuming all other variables constant. For two volatile systems, a plot of the reactions as a function of one composition of the coexisting volatile phase and temperature at fixed total pressure is particularly useful in interpreting metamorphic conditions.

Stable Reaction Equilibria

The equilibrium mineral assemblages listed in Table 11 and their reactions are possible in this wollastonite deposit. The table does not include equilibrium reactions involving talc. Talc may not constitute one of the major phases since it has not been optically observed. It is mentioned here because it has shown up in the x-ray diffractometric study. Even then, it shows only a weak peak. Talc is common in the low-temperature portion of contact aureoles in impure carbonate rocks (Cooper, 1957). The absence of talc might be related to the initial low volatile content in the marble, so that its stability field was not achieved during metamorphism. Its presence is controlled by pore fluid rather than by temperature (Greenwood, 1962).

The initial water content in the marble is, therefore, important during subsequent equilibrium reactions. The list shows that most reactions form diopside directly. Others form it

Table 11. Equilibrium Reactions

Reactions	Stable Reaction Equilibria	Possible Sources from Specimens
1	$5Do + 8Qt + H_2O = Tr + 3Cc + 7CO_2$	Sample 1, M1B
2	$Do + 2Qt = 5Di + 2CO_2$	6
3	$Tr + 3Cc + 2Qt = Di + H_2O + 3CO_2$	6
4	$Ru + Cc + Qt = Sph + CO_2$	B, 22, 27
5	$Tr + 2Do + K-Spar = Phl + 4Di + 4CO_2$	5, 6
6	$3Tr + 6Cc + K-Spar = 12Di + Phl + 2H_2O + 6CO_2$	5, 6
7	$3Do + K-Spar + H_2O = Phl + 3Cc + 3CO_2$	5, 6
8	$Phl + 2Do + Qt = Tr + K-Spar + 4CO_2$	5
9(a)	$5Phl + 6Cc + 24Qt = 3Tr + 5K-Spar + 2H_2O + 6CO_2$	5, 15, 22
9(b)	$Phl + 3Cc + 6Qt = Di + K-Spar + H_2O + 3CO_2$	5, 15, 22
10	$Phl + 2Di + 4Qt = 3Tr + K-Spar$	15, 22
11	$2Zo + CO_2 = Cc + 3An + H_2O$	27, 29, 41
12	$10Cc + 21Qt + 3chl = 2Zo + 3Tr + 8H_2O + 10CO_2$	22
13	$2An + 15Cc + 9Tr = 35Di + 2chl + H_2O + 15CO_2$	22
14	$5An + 6Cc + 4chl = 11Di + 9Sph + 16H_2O + 6CO_2$	B, 13, 17, 27, 47
15	$3Cc + 3Di + K-Spar + H_2O = 6Wo + Phl + 3CO_2$	22
16	$Cc + Qt = Wo + CO_2$	36, 27, 31, M1A, M1B
17	$Cc + An + Qt = Gr + CO_2$ (High T)	41
18	$Gr + Qt = 2Wo + An$ (High T)	41
19	$Gr + CO_2 = Cc + An + Wo$ (Low T)	41
20	$4Zo + Qt = 5An + Gr + 2H_2O$	41
21	$12Zo + 4chl = 11Di + 9Sph + 13An + 22H_2O$	B, 17, 47
22	$Gr + chl = 3Di + 2Sph + 4H_2O$	B, 17, 47
23	$7An + 5Di + 8chl = 6Tr + 15Sph + 26H_2O$	B, 17, 47
24	$Tr + 3Cc = 4Di + Do + CO_2 + H_2O$	1, 6, 8

through intermediate reactions involving tremolite (e.g. 3, 5, 6). These two paths are evidently related to the initial volatile content of the marble. Reaction 2 does not involve H_2O and so diopside forms directly. Reactions 1, 8, 9, 10 and 12 show that tremolite may form due to favorable volatile composition in the marble at constant total rock pressure. This condition has been demonstrated in the plot of CO_2-H_2O chemical potentials at constant temperature and pressure (Korzhinskii, 1959).

In reaction 3, the composition of fluid phase is maintained at a molar ratio of $CO_2/H_2O = 3/1$. This is the ratio at which the reaction proceeds at the maximum temperature for a given pressure (Greenwood, 1962). Such buffering will continue until either calcite or tremolite is completely eliminated. The rapid equilibration of the assemblages might be enhanced by diffusion through fractures or intergranular fluids in the marble.

In the system $CaO-MgO-KAlO_2-Al_2O_3-SiO_2-CO_2-H_2O$, the components such as TiO_2 (in sphene), Na_2O (in plagioclase) are neglected because they are not involved in discontinuous reactions, that is, the reactions which produce new phases at the expense of others. Components such as FeO and MnO , which are present in minor amounts, probably substitute for MgO or CaO , and do not result in additional new phases, are also neglected.

Small amounts of Fe_2O_3 in the epidote or K-feldspar are also neglected. The component KA10_2 (for K_2O) is preferred because reactions involving phlogopite and K-feldspar involve transfer of K_2O and Al_2O_3 as a single component (KA10_2). Similarly, CO_2 and H_2O , where they are "perfectly mobile" do not give rise to additional phases directly, except for CO_2 in zoisite and grossularite (reactions, 11, 19). Thus the system can be expressed in terms of $\text{CaO-MgO-KA10}_2\text{-Al}_2\text{O}_3\text{-SiO}_2$. The major phases in this system include K-feldspar, quartz, diopside, tremolite, phlogopite, wollastonite, sphene and plagioclase. Each may be present as reactants and as products of a solid-solid reaction. If these minerals have end-member compositions, then the phase rule requires an isobaric invariant point in the ideal six-component system $\text{CaO-MgO-KA10}_2\text{-SiO}_2\text{-H}_2\text{O-CO}_2$. The stability of this invariant point would indicate the intersection of reactions in a T-XCO_2 space. Reactions 3, 6, 9, 10, 12, 13, 14, 15, 17, 18, 19 and others constitute this system. Hewitt (1973) and Thompson (1975) agreed that reactions 3 and 9 are stable at contact and regional metamorphic conditions and that they do not intersect.

Sphene is a common accessory mineral in this marble; samples 29, 31, 41, 47 and MIB contain sphene. The presence of sphene is restricted to the high fluid composition side of the

reaction (see reactions 4, 14 and 21) at the lowest P-T conditions (Hunt and Kerrick, 1976).

A number of reactions involve dolomite; for example, reactions 1, 2, 5 and 7. Optically, dolomite is not abundant in this deposit, and, therefore, not all its reactions will be considered to have occurred although it occurs often associated with calcite. The diopside-rich phase occurs in samples 7, 15, 17, 27, 41 and MIB and this suggests that reactions 2, 3, 5, 6 and others were possible during metamorphism.

Most equilibria, like 3, 6, and 9 constitute dehydration reactions of interest in the P-T plane. Their intersections as temperature-pressure curves form invariant points. Epidote occurs in samples 17, 22, 47, B and MIB with the assemblages

(a) WO + Di + Cc

(b) WO + Di + Cr + Chl + Sph

(c) WO + Di + Cc + Pl + Sph.

This suggests that epidote has a wide range of stability in the system $\text{CaO-MgO-KAlO}_2\text{-Al}_2\text{O}_3\text{-SiO}_2\text{-H}_2\text{O-CO}_2$. The epidote producing reactions are 11, 12, 20, and 21. It appears that low-temperature conditions may favor the formation of epidote in this environment, inasmuch as epidote occurs in the reactant sides. In thin section, the epidote grains are mainly anhedral and this suggests secondary products during declining temperature. From

the presence of wollastonite, grossularite and some plagioclase, the elevated temperatures must have prevailed in the deposit. The peak temperature might not have favored stable formation of epidote as a primary or prograde product. Rice (1983) showed that at pressures less than 2.5 kb, $An + Gr + Chl + H_2O$, is stable relative to $Zo + Di + Sph + H_2O$, whereas at higher pressures $Di + Sph + H_2O$ is stable relative to the low-pressure counterpart. The sequence of dehydration reactions encountered during progressive metamorphism is also distinctly different depending on the pressure. The stability of epidote is about 200° to 610°C at 2 kb or 2.5 kb. For the reaction $2Zo + CO_2 = 3An + Cc + H_2O$, the stability range at 5 kb is greater than 500° to 700°C. Under the temperature and pressure that prevailed in this deposit, the epidote (zoisite) is a retrograde product and probably formed by replacing plagioclase. Where epidote or zoisite occurs, the plagioclase seems to have been eliminated. Based on observation and the experimentally determined portion of the equilibria (Skippen, 1974), the reaction $2Zo + CO_2 = Cc + 3An + H_2O$, $Tr + Cc + 2Qt = 5Di + H_2O + 3CO_2$ (Hoschek, 1973), it is suggested that at temperatures greater than 400°C and pressure greater than 2 kb, epidote is stable in metamorphic rocks if the XCO_2 of the fluid phase is less than 0.10 to 0.20, in contrast to

a value of 0.03 determined experimentally by Johannes and Orville (1972).

The reaction $Cc + SiO_2 = CaSiO_3 + CO_2$ consists of three components: $CaO-SiO_2-CO_2$ existing in four phases $Cc + SiO_2 + Wo + CO_2$. A P-T curve can be drawn to show the behavior of the four phase at equilibrium. For all values of temperature and pressure which do not lie on this curve (Figure 15) (Greenwood, 1973), not more than three phases can coexist in equilibrium. Thus this curve separates two areas of divariant equilibria. The equation for the reaction can help in fixing the phase which can exist in each of the fields. If $Qt + Cc$ represents the low-temperature pair at any pressure, the assemblage $Wo + CO_2$ would represent the high temperature phase. But the association of $Cc + Qt +$ either Wo or CO_2 , (not both), can occur in the low temperature side. Also, $Wo + CO_2 +$ either Cc or Qt (not both), can occur on the high temperature side. Thus we can have three possible phase assemblages at a time, the low and high temperature assemblages. On the low-temperature side of the equilibrium curve, there are two degrees of freedom and any arbitrary bulk composition will crystallize to an assemblage of three phases ($CaO + CaCO_3 + Wo$), ($CaCO_3 + Wo + Qt$), and ($CaCO_3 + Qt + CO_2$), but Wo is not in equilibrium with CO_2 . On the high-temperature side (two degrees of freedom prevails), with the difference that $Wo + CO_2$ can

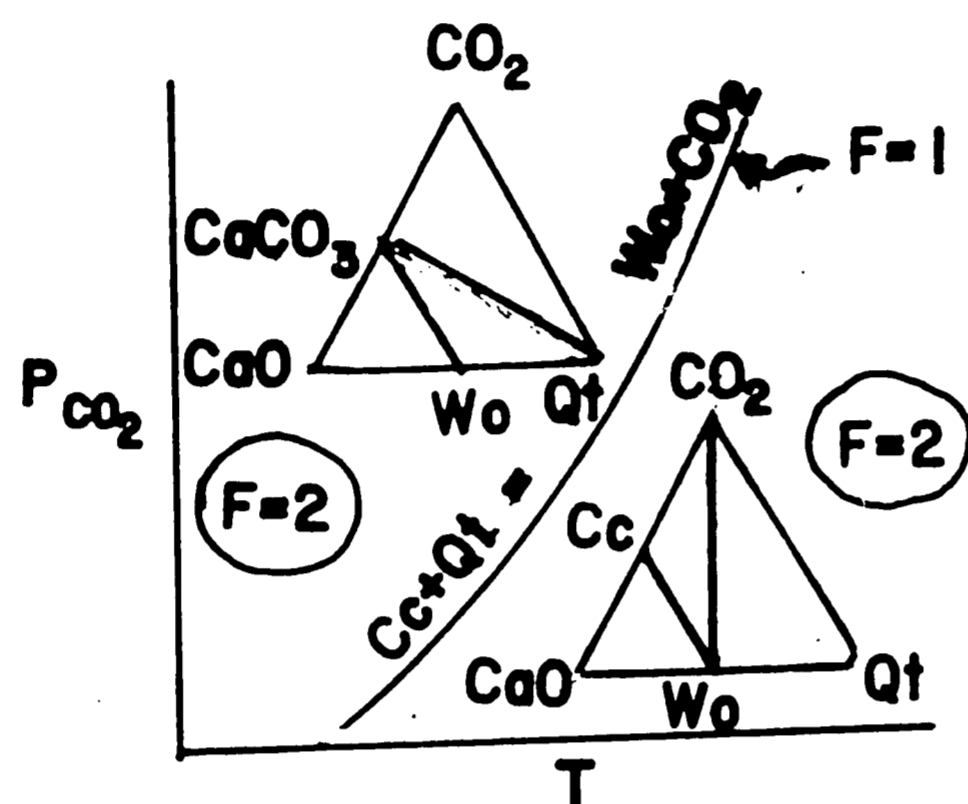


Figure 15. Illustration of the phase rule, applied to the three-component system $\text{CaO}-\text{CO}_2-\text{SiO}_2$. On the low-temperature side of the equilibrium curve there are 2 degrees of freedom, and any arbitrary bulk composition will crystallize to an assemblage of three phases ($\text{CaO}+\text{CaCO}_3 + \text{Wo}$), ($\text{CaCO}_3+\text{Wo}+\text{Qt}$), ($\text{CaCO}_3+\text{Qt}+\text{CO}_2$), but note that Wo is not at equilibrium with CO_2 . On the high-temperature side $F=2$, with the difference that $\text{Wo} + \text{CO}_2$ can coexist, and $\text{CaCO}_3 + \text{Qt}$ cannot. Along the equilibrium curve we have a 4-phase assemblage and only 1 degree of freedom.

coexist, and $\text{CaCO}_3 + \text{Qt}$ cannot. But along the equilibrium curve, there is a four-phase stable assemblage, only one degree of freedom is possible, and Cc, Qt, Wo, and CO_2 can all coexist if PCO_2 is fixed or given. This suggests that wollastonite can form under variable conditions of temperature and pressure, and the reaction for Wo-formation is XCO_2 -dependent.

Methods of Equilibria Calculations

Introduction:

Many workers have studied some of the equilibrium reactions experimentally with synthetic or natural mineral assemblages. Goldschmidt (1912), Danielson (1950), Ellis and Fyfe (1956), Hasker and Tuttle (1956), Greenwood (1962, 1967b), G. B. Skippen (1974, 1977), and many others, have investigated the wollastonite-forming reactions under different temperature, pressure and XCO_2 conditions. Their results were always displayed on a T- XCO_2 plot at different fluid pressures. This forms the basis for understanding the conditions that favor the formation of wollastonite amidst other mineral phases. In the NW Adirondack Lowlands, where the wollastonite deposit is located, Fisher (1977), has estimated that about 20 km of overburden was eroded away to expose the wollastonite deposit. From the estimates of Osborne (1936a), Buddington (1939), Engel and Engel (1939 and 1958b), about 1.6 km to 3.3 km thickness of marble

exists in this locality. This total thickness in addition to the overburden thickness, would probably have contributed to about 6.0 to 6.5 kb of total rock pressure in this locality at the time of intrusion. This would imply that the contact or regional metamorphism would have taken place at this total pressure.

Calculations of Equilibria

The mineral assemblages shown in Table 4, probably formed through one or more of the reactions listed in Table 11. Some of these reactions are univariant at constant pressure or constant fluid content and will be best displayed in a plot of T versus X fluid. The calculation for such a plot involves the thermodynamic data, making the assumption that the total rock pressure = $P_{H_2O} + P_{CO_2} = 6.0 - 6.5$ kb. For the assemblages with one degree of freedom, in a P - X fluid space, the term isobarically univariant, will be used. If the fluid composition is not fixed, such reactions will correspond to two degrees of freedom on a P - T plot. Reactions 3, 4, 9, 10, have been experimentally reversed by Valley and Essene (1980), and thus these and other reactions which have available thermodynamic data can be accurately calculated at various pressures. The approach to these calculations involves the use of thermodynamic data at standard states. Table 12 shows the symbols for the thermodynamic data used.

Table 12. Thermodynamic Data Symbols

T	=	Temperature in degrees centigrade ($^{\circ}\text{C}$)
P	=	Pressure under consideration
P°	=	Pressure at standard state condition
R	=	Gas constant
S°	=	Entropy at standard state (298 .15K), 3rd law of entropy of a phase
ΔS	=	Standard state entropy of change of a reaction
G°	=	Standard state free energy of a reaction
V	=	Molar volume of phases reacting
ΔV°	=	Standard state volume for solid phases in a reaction
n	=	Stoichiometric coefficient of component i in a balanced chemical reaction
H	=	Standard state entropy of reaction
K	=	Equilibrium constant, standard state unspecified
X	=	Mole fraction of component
a	=	Activity of component

Since the reactions are reversible, then

$$G_r = 0 = G_f + RT \ln K = H_f - T S_r + RT \ln K \quad (1)$$

The symbols are explained in Table 12. Then rearranging,

$$\ln K = -\frac{H_f}{RT} + \frac{S_r^0}{R} \quad (2)$$

$$\text{or } \ln K = -\frac{H_f}{RT} + \frac{S_f}{R} - \frac{V_s(P-P^0)}{RT} \quad (3)$$

$$\text{or } \ln k = \frac{A}{T} + B + C \frac{(P_T - P_r^0)}{T} \quad (4)$$

Kerrick and Slaughter, 1976).

Where A, B and C are constants calculated from the relations:

$$A = -\Delta H^0 / 2.303R \quad (5)$$

$$B = \Delta S^0 / 2.303R \quad (6)$$

$$C = -\Delta V_s / 2.303R \quad (7)$$

where s indicates solid phases. Equation (4) can be used to calculate the position of equilibrium of equilibrium reactions in T - XCO₂ space at isobaric conditions at standard state. Log K may be calculated if the values of A, B and C are known and the activities of components in the solid phases are estimated or calculated. If the activity terms for the solids are considered, Trommsdorff and Evans (1972) used the relation

$$B^1 = B + \log \left[\frac{(a_A)^a}{(a_C)^c} \right] \left[\frac{(a_B)^b}{(a_D)^d} \right] \quad (8)$$

and A and B terms are unchanged and

$$\log K \text{ becomes } \frac{A}{T} + B^1 + C(P-P^0)/T \quad (9)$$

where a, b, c and d are activities of the solids A, B, C, D in the parenthesis.

Kerrick and Slaughter (1976) have developed equations that involve free energies of CO_2 and H_2O by reformulating and differentiating equation (1):

$$d Gr = 0 = V_f dP - S_f dT + d(RT \ln k) \quad (10)$$

and integrating to

$$Gr=0 = \int_{P_1}^{P_2} V_f dP - \int_{T_1}^{T_2} S_f dT + RT_2 \ln k_2 - RT_1 \ln k_1 \quad (11)$$

and expanding the terms V_f and S_f therefore:

$$\begin{aligned} Gr = 0 = & \int_{P_1}^{P_2} V_{\text{H}_2\text{O}} dP + n_{\text{CO}_2} \int_{P_1}^{P_2} V_{\text{CO}_2} dP \\ & + n_{\text{H}_2\text{O}} \int_{P_1}^{P_2} V_{\text{H}_2\text{O}} dP - \int_{T_1}^{T_2} S_f dT \\ & - n_{\text{CO}_2} \int_{T_1}^{T_2} S_{\text{CO}_2} dT - n_{\text{H}_2\text{O}} \int_{T_1}^{T_2} S_{\text{H}_2\text{O}} dT \\ & + RT_2 \ln k_2 - RT_1 \ln k_1 \end{aligned}$$

Since $n_1 \int_{P_1}^{P_2} V_1 dP - n_1 \int_{T_1}^{T_2} S_1 dT = n_1 (G_1)_{P_1}^{P_2} - n_1 (G_1)_{T_1}^{P_2}$

then
$$\begin{aligned} Gr=0 = & \int_{P_1}^{P_2} V_{\text{H}_2\text{O}} dP - \int_{T_1}^{T_2} S_{\text{H}_2\text{O}} dT \\ & + n_{\text{H}_2\text{O}} [(G_{\text{H}_2\text{O}})_{P_2}^{P_2} - (G_{\text{H}_2\text{O}})_{T_1}^{P_1}] \\ & + n_{\text{H}_2\text{O}} [RT_2 \ln(X_{\text{H}_2\text{O}})_{T_2}^{P_2} - RT_1 \ln(X_{\text{H}_2\text{O}})_{T_1}^{P_1}] \\ & + n_{\text{CO}_2} [(G_{\text{CO}_2})_{T_2}^{P_2} - (G_{\text{CO}_2})_{T_1}^{P_1}] \\ & + n_{\text{CO}_2} [RT_2 \ln(X_{\text{CO}_2})_{T_2}^{P_2} - RT_1 \ln(X_{\text{CO}_2})_{T_1}^{P_1}] \end{aligned} \quad (12)$$

The equation for isobaric extrapolation readily derived from equation (12) is

$$\begin{aligned}
 0 = & - \int_{T_1}^{T_2} S_g dT + nH_2O [(GH_2O)_{T_2}^P - (GH_2O)_{T_1}^P] \\
 & + nH_2O [RT_2 \ln(1-X_2) - RT_1 \ln(1-X_1)] \\
 & + nCO_2 [(GCO_2)_{T_2}^P - (GCO_2)_{T_1}^P] \\
 & + nCO_2 [RT_2 \ln X_2 - RT_1 \ln X_1]. \quad (13)
 \end{aligned}$$

for non-ideal gas mixtures.

The equilibria of the listed reactions have been computer calculated for the various devolatilization reactions using "EQUILI", by Wall and Essene (1972). This program starts with $Gr = 0$, at an experimentally reversed P-T-X, and assumes $P_{total} = PH_2O + PCO_2$, and solves the equation:

$$\begin{aligned}
 & Gr (P_2 T_2 XH_2O^2) - Gr (P_1 T_1 XH_2O^1) \\
 = & - \int_{T_1}^{T_2} S_g dT + \int_{P_1}^{P_2} P_g dP \\
 & + Gr_{fluids} (P_2 T_2 XH_2O^1) \\
 & - Gr_{fluids} (P_1 T_1 XH_2O^1) \quad (14)
 \end{aligned}$$

The sources for the data used for these calculations are

- (a) S and V, from Robie et al. (1978).
- (b) Thermal expansion (α), is calculated from the data in Skinner (1966).
- (c) Compressibility, β , if required, from Birch (1966), Slaughter, Kerrick and Wall (1975).
- (d) Molar Volumes, from Robie, Bethke and Beardsley (1967).

- (e) High temperature entrophies from Robie and Waldbaum (1968).
- (f) H_2O free energy, from Burnham, Holloway, and Davis (1969).
- (g) CO_2 free energy, from Burnham and Wall, unpublished data and from Greenwood (1973).

In most calculations, thermal expansion and compressibility data for solid phases are lacking, and as such, calculations are often made with V_s calculated from 25°C, 1 atm. data. However, good results have always been obtained. Also, most calculations assume ideal mixing for the binary fluids $H_2O + CO_2$. Deviations from ideality are possible at low temperatures and high pressures and these often introduce errors into different calculated values at the extrapolated equilibrium points. If necessary, this source of error can be reduced by using the modified Redlich-Kwong equation of state as treated by Holloway (1977). Errors are also possible due to lack of accurate activity coefficients for some solids. Also the presence of graphite in the marble can result in the presence of CH_4 at all oxygen fugacities (Ohmoto and Kerrick, 1977). But if the amount of CH_4 is assumed to be insignificant and that it does not act as one of the diluents of CO_2 , then the assumption that $P_{total} = P_{fluid} = P_{H_2O} + P_{CO_2}$, is justified.

Results of Equilibrium Calculations

The thermodynamic equilibrium calculations make it possible to establish some of the physical conditions such as temperature, pressure, and fluid compositions that existed to favor the formation of silicate minerals. The conditions vary from place to place depending on the available parameters. From such calculations, Greenwood (1973) showed (see Figure 15) the behavior of the equilibrium curve (reaction boundary) for the reaction: $Cc + Qt = Wo + CO_2$. The equilibrium for this reaction will be maintained only under one condition, namely, either pressure or temperature is fixed. If this condition is applied to natural geological environments, any contradiction of the phase rule will imply a state of disequilibrium. But in nature, it is difficult to know how many components actually exist during any reaction. Then the phase rule may not necessarily apply, but is only inferred. The same reaction has been studied by Skippen (1974), at various temperatures and pressures (Figure 16).

Figures 17 and 18 show the effect of geologically diluting CO_2 by other gas species or H_2O at fixed total pressure. In Figure 18, Kerrick and Slaughter plotted a $P-XCO_2$ diagram using experimental data of Greenwood (1967b) and using calculation results from equation 13 at 2 kb and 1 kb. They assumed ideal and non-ideal

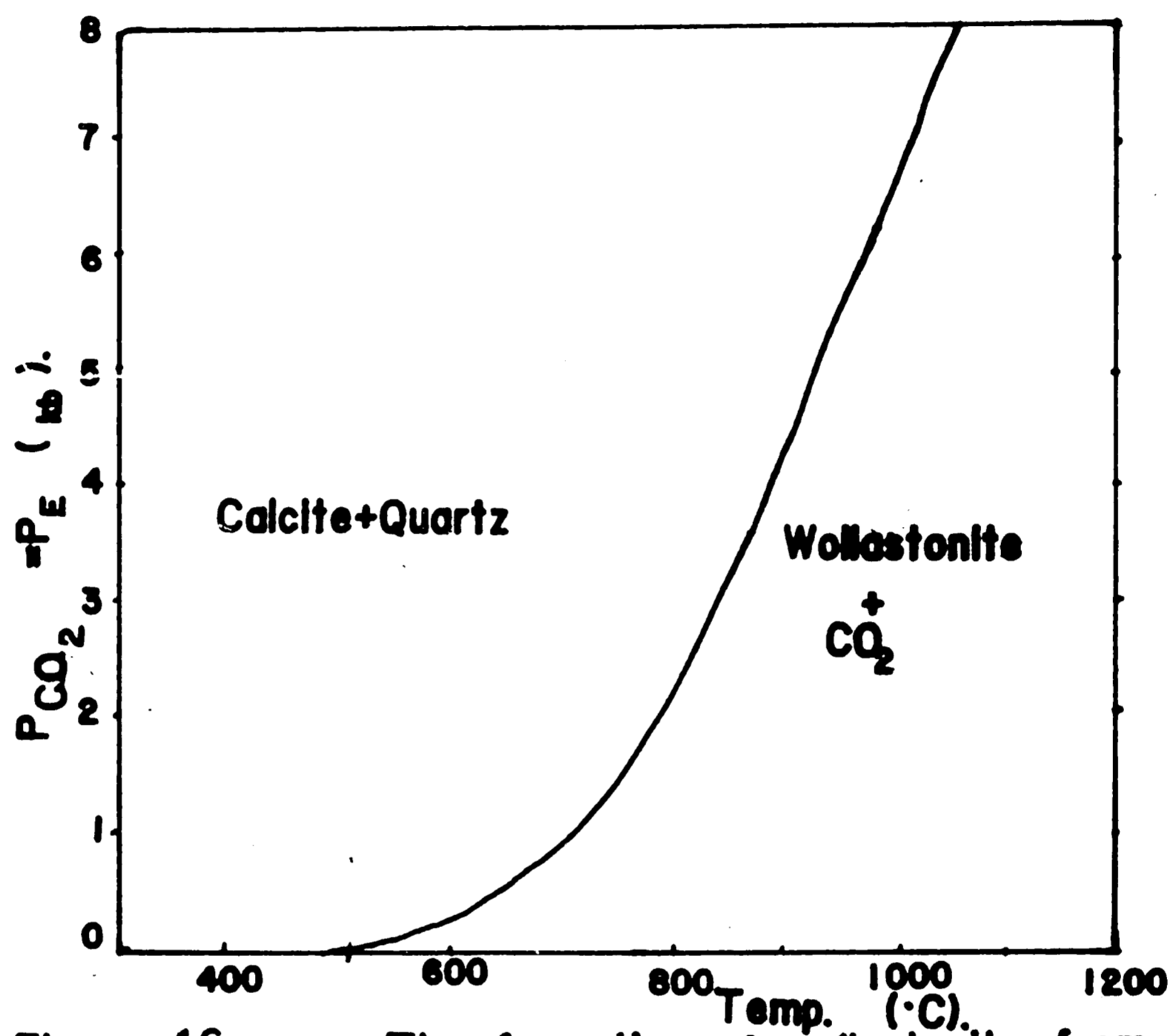


Figure 16. The formation of wollastonite from calcite and quartz as a function of temperature and pressure with CO₂ pressure (P_{CO₂}) = total pressure (P_E). (Skippen, 1974).

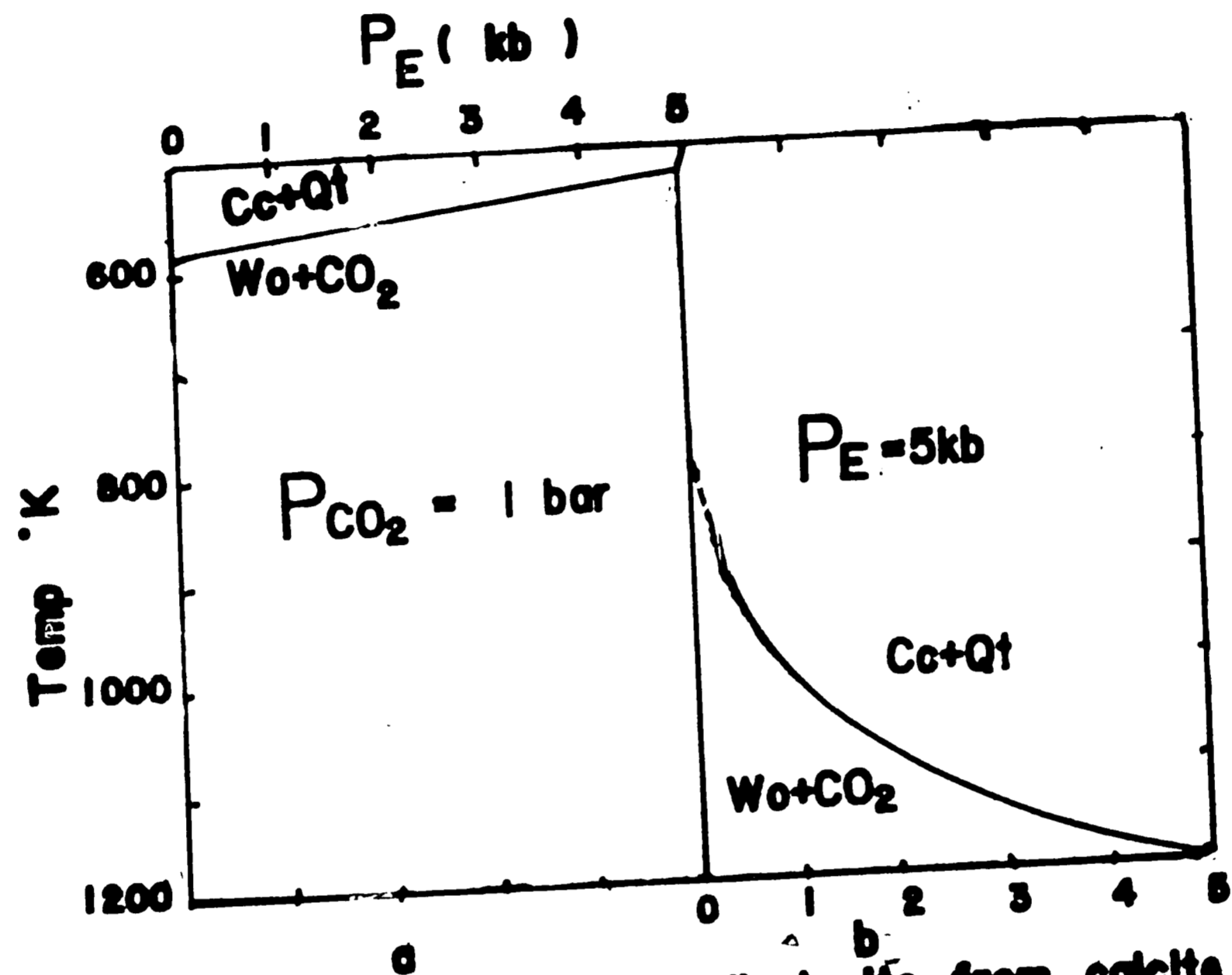


Figure 17. The formation of wollastonite from calcite + quartz
 a. Total pressure P_E vs. temperature at a fixed CO_2 pressure of 1 bar. b. CO_2 pressure P_{CO_2} vs. temperature at a fixed pressure of 5 kb. (Skippen, 1974).

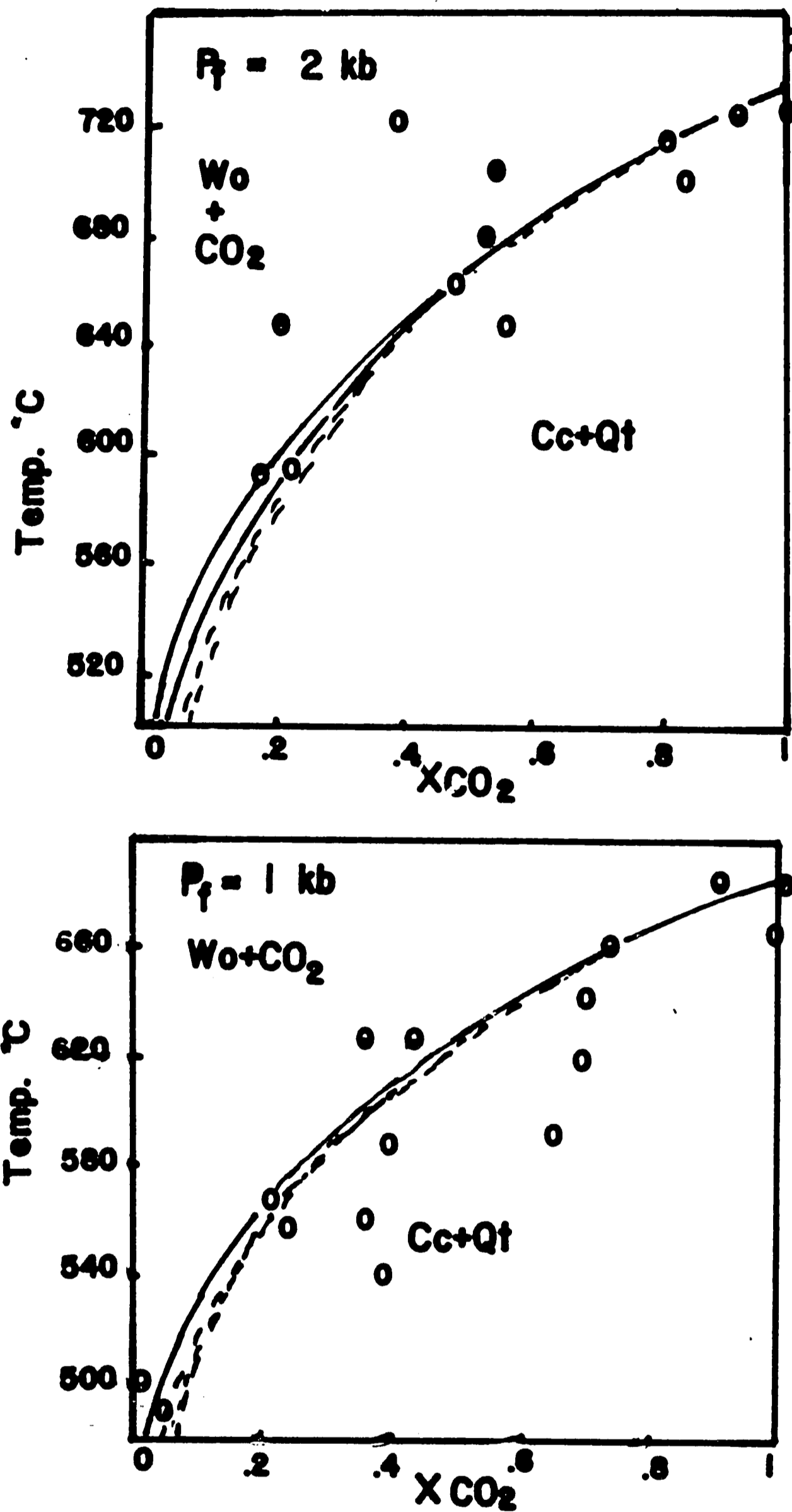


Figure 18. T-X diagrams for the reaction: $Cc+Qt = Wo+CO_2$ showing experimental data of Greenwood, 1967b. Stippled circles - wollastonite-stable, open circles, Cc+Qt-stable. The solid curves were calculated assuming non-ideal gas mixing, the dotted curves assume ideal gas mixing. The solid and dashed curves were calculated from the maximum and minimum uncertainties at standard entropies. (After Kerrick & Slaughter, 1976)

gas mixing. The dotted line was calculated using Greenwood's equation

$$-\frac{1}{T} = A + \frac{R}{dH_T^0} [n\text{CO}_2 \ln X_{\text{CO}_2} + n\text{H}_2\text{O} \ln X_{\text{H}_2\text{O}}]$$

where A = integration constant evaluated at the starting point.

The maximum uncertainties in S_f are assumed. This demonstration was used to study the stability of wollastonite in $\text{H}_2\text{O} - \text{CO}_2$ mixtures and its occurrence in a contact metamorphic aureole near Salmo, in British Columbia, Canada. Figure 19 after Greenwood, also assume ideal mixing of CO_2 and H_2O . Both diagrams (Figures 18 and 19) illustrate the fact that the equilibrium curve is a function of constant total rock pressure. The position of the equilibrium curve will rise with increase in pressure. Figure 20 also shows that the presence of other species can depress the position of equilibrium curve and the effect caused by considering the activity coefficients of the species when the pressure changes. In Figure 21, Greenwood (1962) showed that the isothermal coexistence of the assemblages $\text{Tr} + \text{Cc} + \text{Qt}$ and $\text{Qt} + \text{Do}$, do require volatile compositional gradients at their contacts. In this consideration, if the CO_2 and H_2O were homogenized (ideal mixing), then only one of the assemblages would be stable unless the volatile composition coincided with the curve labeled I. The condition for such assemblages is the presence of pore fluid rather than the temperature. The

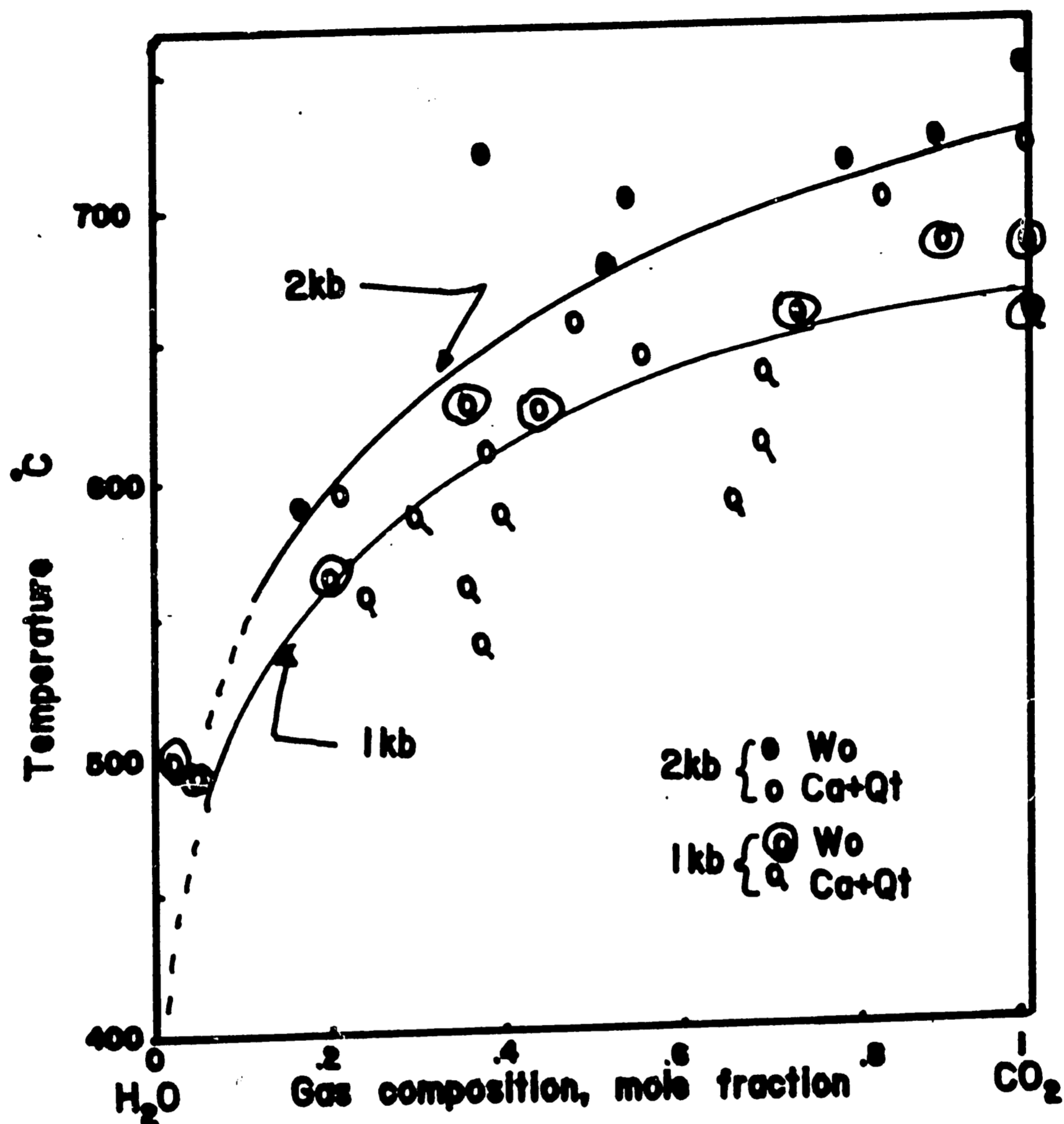


Figure 19. Stability relations of calcite, quartz, and wollastonite in supercritical mixtures of H_2O and CO_2 . Upper curve, 2kb, lower curve 1kb. Total pressure equals fluid pressure, gas compositions in mole fraction of CO_2 . Curves calculated assuming ideal mixing of CO_2 and H_2O . Pure CO_2 points from Harker & Tuttle, 1956. (After Greenwood, 1967 a).

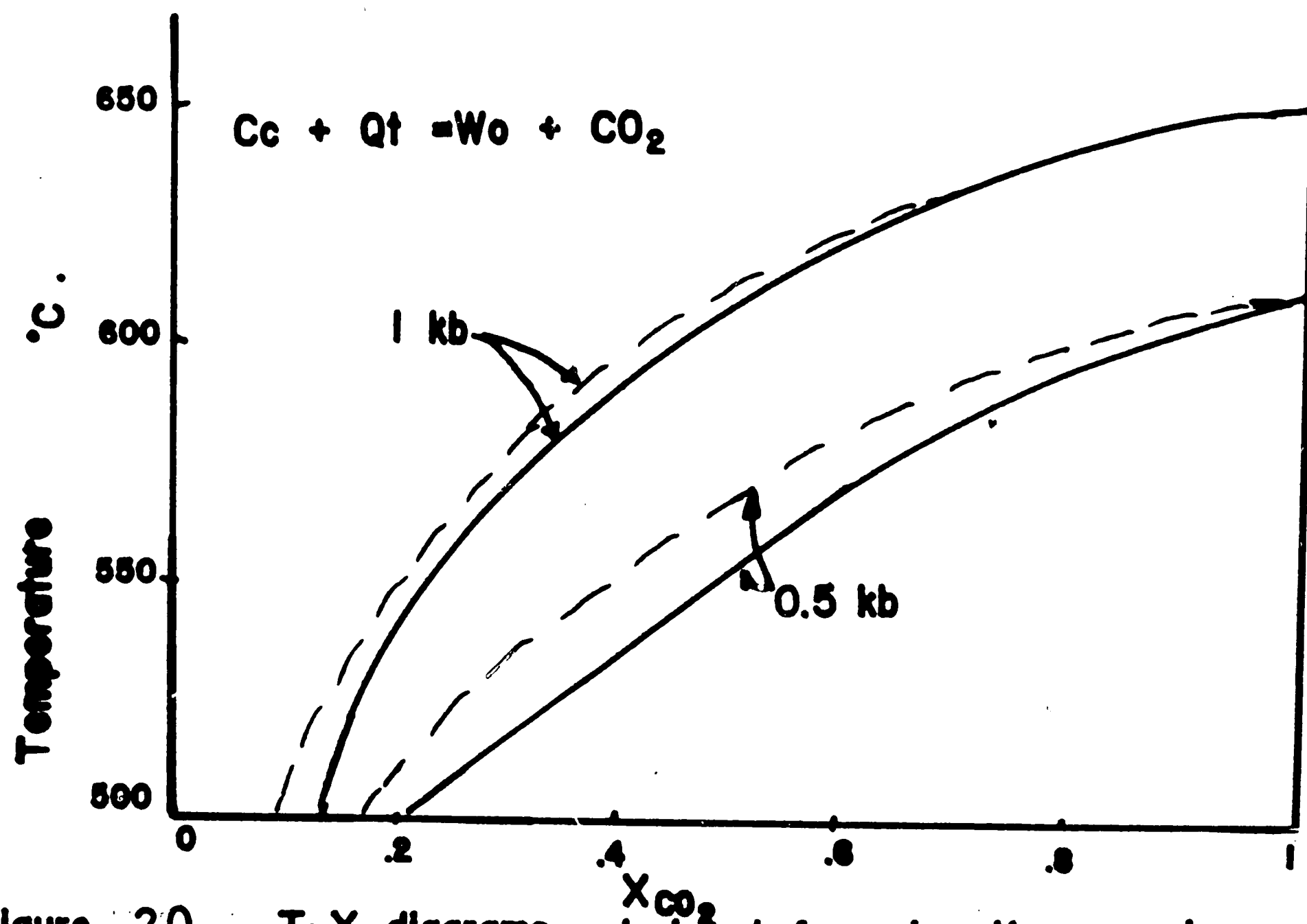


Figure 20. T-X diagrams calculated from log K expressions derived from experimental data at 2 kb.

The dashed lines were calculated assuming that the activity coefficients of gas species remain constant with changing pressure. The solid curves were derived by correcting for the change in activity coefficients with changing pressure.

(After Greenwood, 1962).

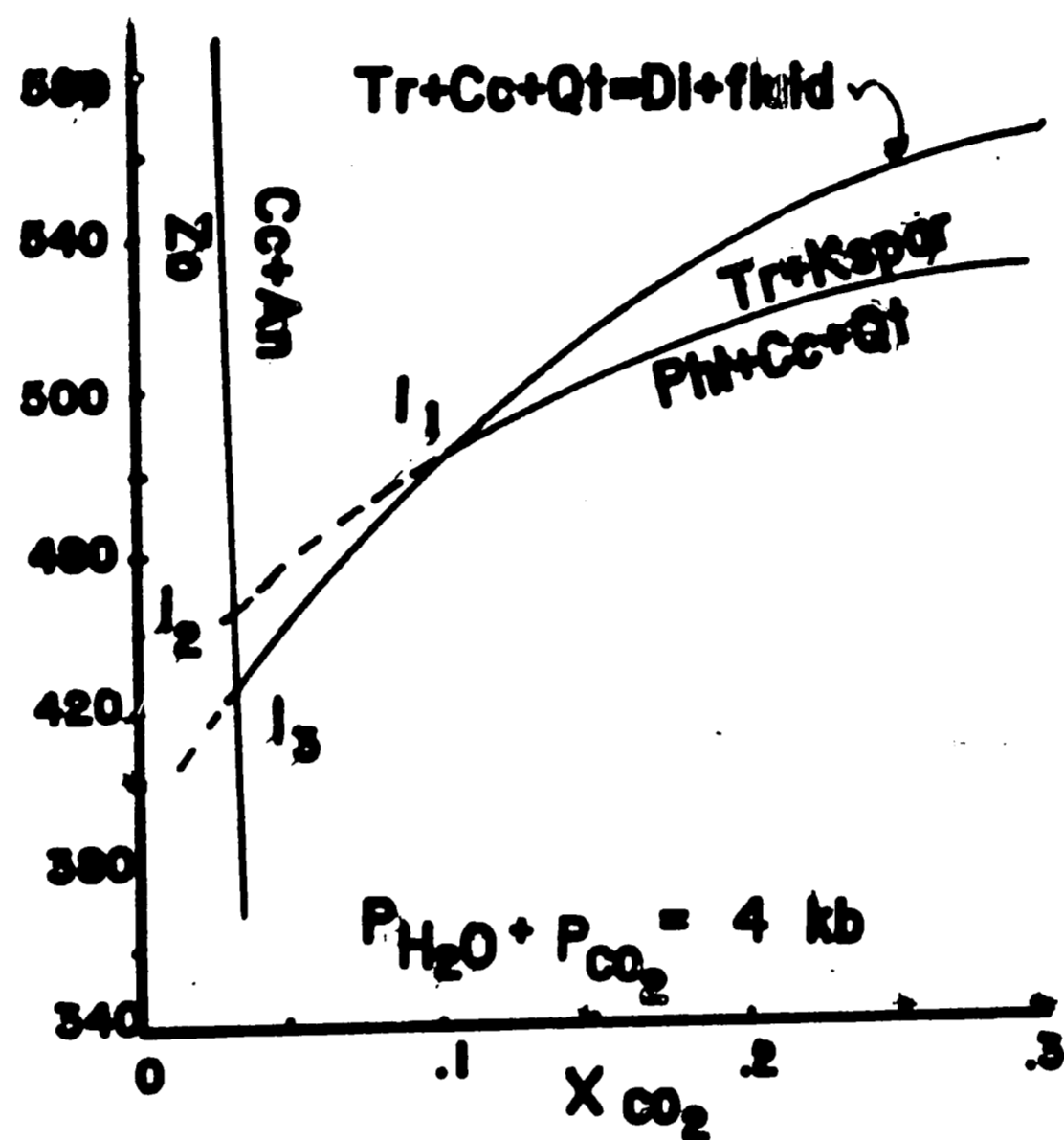


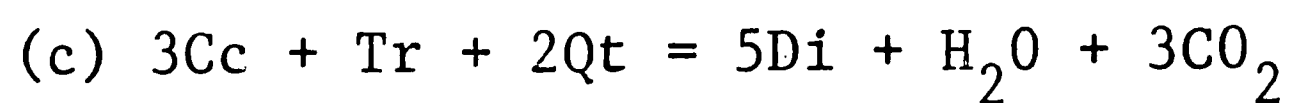
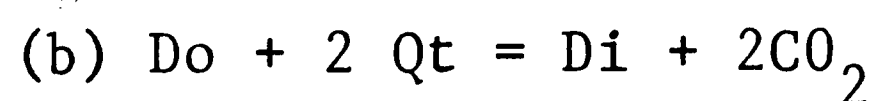
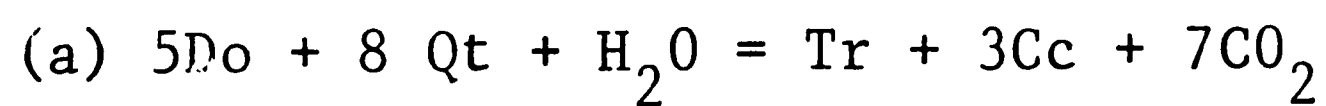
Figure 21. The position of the Tr-Ksp+P (1) Di (2) An-Cc (3) equilibrium in the system $\text{CaO-MgO-K}_2\text{O-Al}_2\text{O}_3\text{-SiO}_2\text{-CO}_2\text{-H}_2\text{O}$ in T-X (CO_2) space at 4kb. pressure. Invariant points are labelled. (After Johannes & Orville, 1972). Source of data from LeAnderson, 1981.

reactions shown on the diagram define limit of XCO_2 which favors their stability.

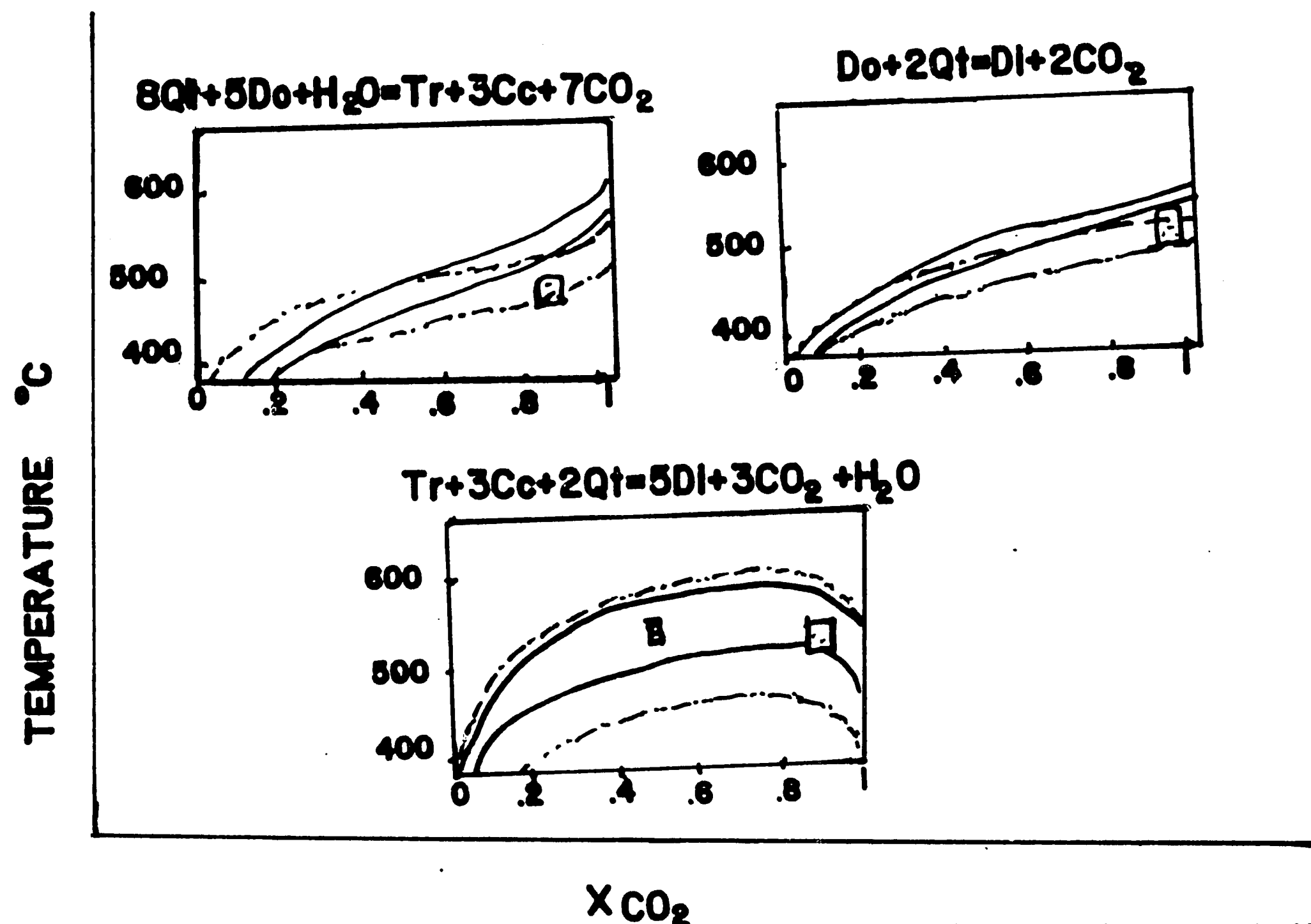
Figure 21 was plotted by Johannes and Orville (1972) and was used by Le-Anderson (1981) for the equilibria in T- XCO_2 space at 4 kb. The data were obtained from Froeses (1976). The calculations listed above it were made starting from the equation

$$\log k = \frac{A}{T} + B + C \frac{(P-P^\circ)}{T}$$

According to the rule of Schreinemakers, (Zen, 1961), the equilibrium curve is stable only on the high XCO_2 side of the intersections. The equilibrium intersection I_3 (on the curve), has been investigated by Johannes and Orville (1972). The curves also assume ideal mixing of H_2O and CO_2 . The invariant points I are labeled. The reactions



were also studied by Slaughter, Kerrick and Wall (1975) at fluid pressure = 2 kb as shown in Figure 22. They illustrated the probable errors encountered in the location of various equilibrium curves. The dashed lines are limits of the positions of equilibrium curves by Skippen (1974) and the solid lines are those of Kerrick and Slaughter (1976). The experimental brackets are at the stippled areas. These illustrations show that because



94

Figure 22. T- X_{CO_2} diagrams at $P_1 = 2 \text{ kb}$ showing total error limits in the location of various equilibria. Dashed lines are limits from Skippen, 1974. Solid lines were calculated at 2 kb, by Slaughter, Kerrick, and Wall, 1975, from the total uncertainty in the location of the invariant point. Stippled areas represent experimental brackets for the reactions shown on the figure.

of errors encountered through making approximations in the thermodynamic data, the positions of most equilibria or the invariant points are not very exact though these uncertainties can be accounted for. Figure 21 also illustrates the uncertainty in the location of the equilibrium curve. This reaction $5\text{Phl} + 6\text{Cc} + 24\text{Qt} = \text{Tr} + 5\text{k-spar} + 2\text{H}_2\text{O} + 6\text{CO}_2$ involves two volatile components in the product assemblage. The stoichiometric molar ratio of the evolved CO_2 and H_2O is 3:1. The isobaric thermal maximum for this equilibrium would occur when the mole fraction of CO_2 in the fluid phase is 0.75. This is compatible with the experimental data by Hoschek (1973) at 4 kb fluid pressure. The association of reactants on the low-temperature side and products on the high-temperature side accentuates the uncertainty in the location of the equilibrium curve. Figure 23 (Zen 1963), illustrates the effect of the "perfect mobility" of CO_2 and H_2O at higher temperatures. Zen studied a granite contact aureole with siliceous Helena dolomite at Lincoln, Lewis and Clark County, Montana. The siliceous dolomite has progressively metamorphosed through the albite-epidote-hornblende and pyroxene-granulite facies, around the granitic rock (Melson, 1966). The progression of the facies is illustrated in Figure 24, which shows the summary of the

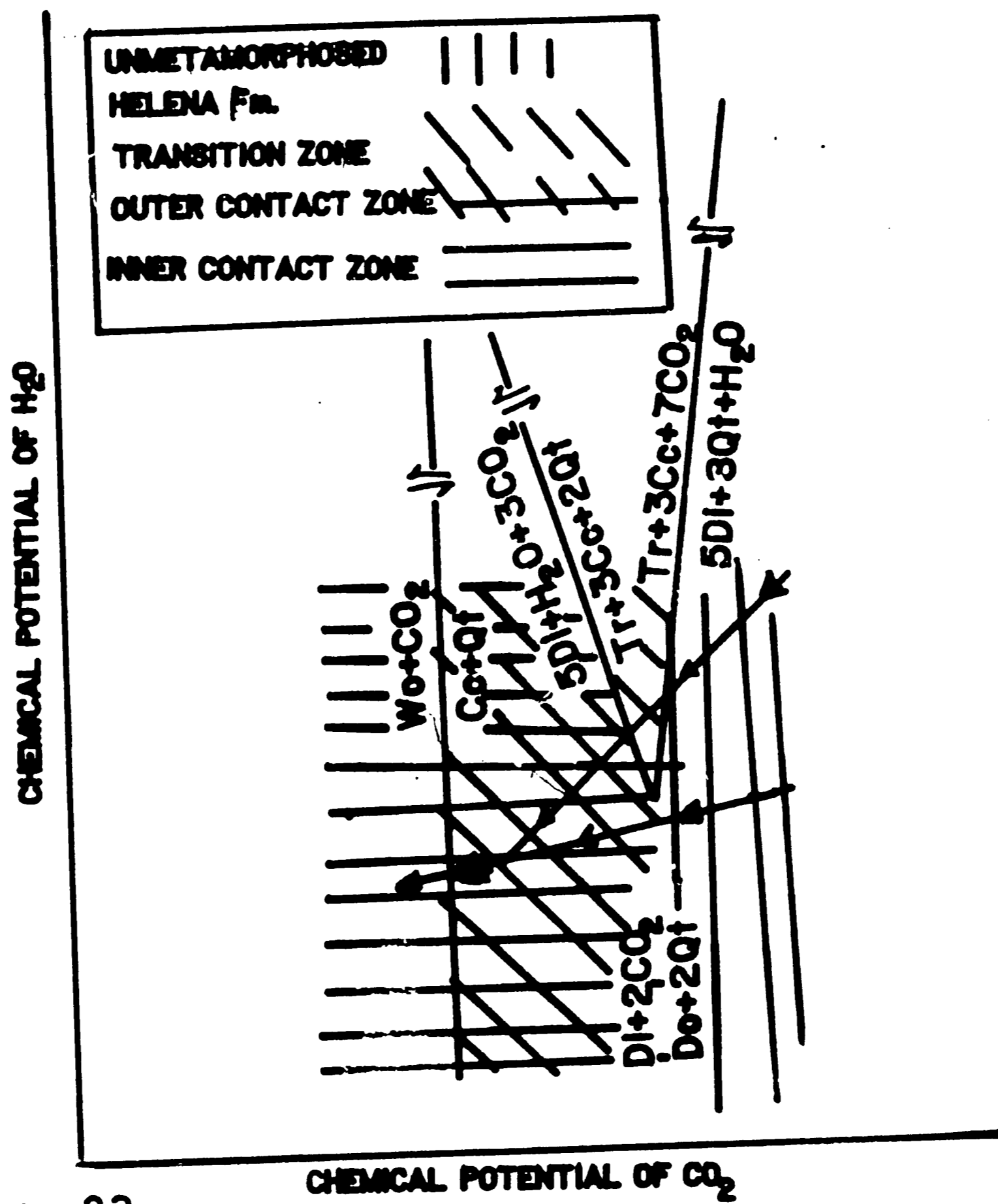


Figure 23. $\text{CO}_2\text{-H}_2\text{O}$ chemical potential diagram for reactions in the carbonate-quartz beds. (After Zen, 1983).

Dolomite progressively metamorphosed through
Ab-Ep-Hbl-Pyx-Granulite facies grade.

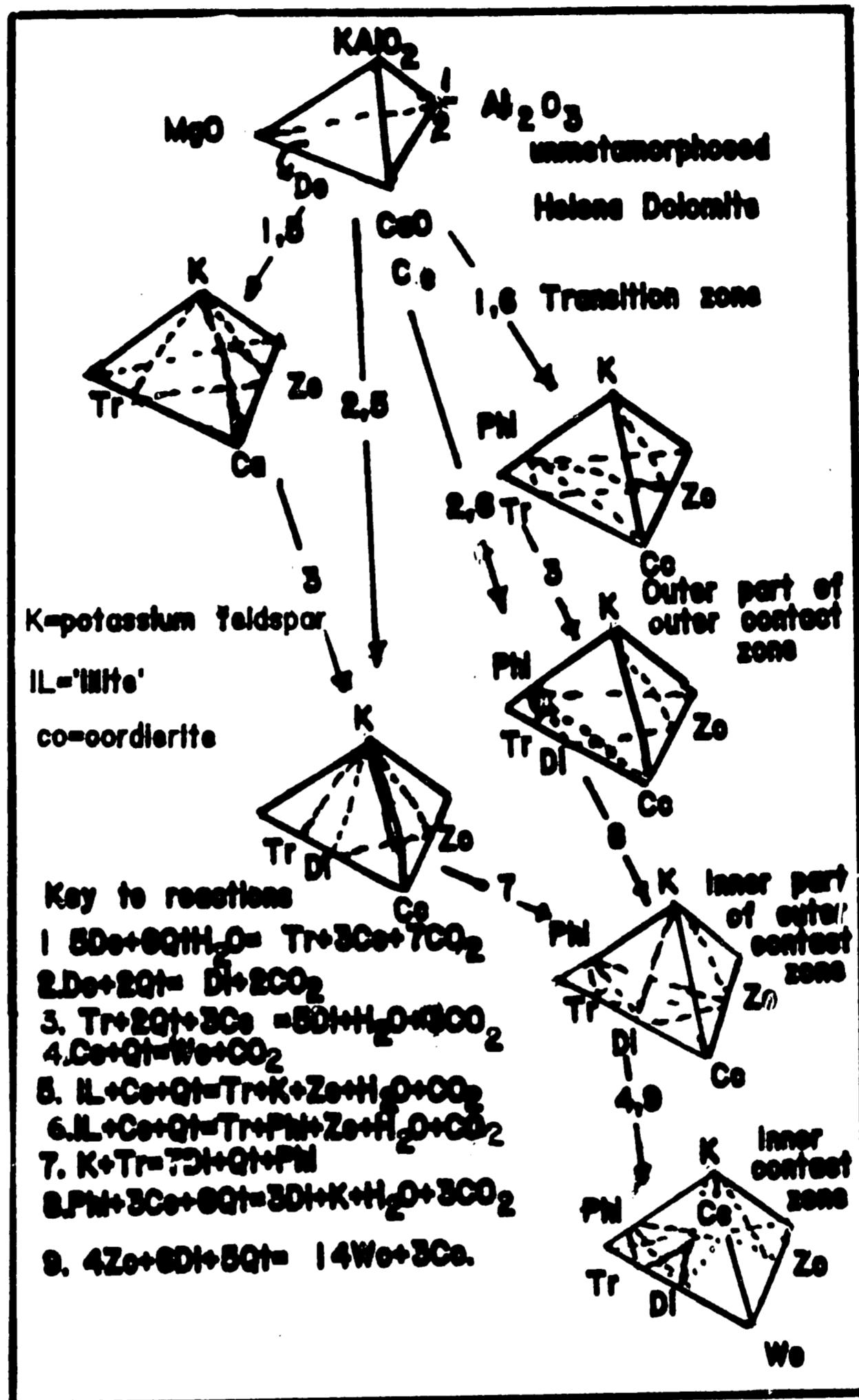


Figure 24. Summary of development of assemblages in the system $CaO-MgO-KAlO_2-Al_2O_3-CO_2-H_2O$ with excess quartz (After Nelson, 1966). (observed in the St. Helens dolomite contact aureole).

development of assemblages in terms of the $\text{CaO-MgO-KAlO}_2 - \text{Al}_2\text{O}_3$
- $\text{CO}_2 - \text{H}_2\text{O}$ system with excess SiO_2 .

The above results and discussions are derived from studies in different environments under varying physical conditions. Table 13 shows the summary of the results of various equilibrium considerations under various temperatures, pressures and fluid compositions. It is noted that different reactions can go to completion under different specified conditions. It is observed that the equilibrium curves are raised with increase in temperature and total rock pressure.

With the above deductions coupled with the equilibrium curves of Ross (1980), at $P_{\text{total}} = P_{\text{CO}_2} + P_{\text{H}_2\text{O}} = 6 \text{ kb}$, a T- XCO_2 space (Figure 25) was drawn. Ross (1980) actually studied the geology and petrogenesis of the marbles in the area of the present study. Table 14 shows some of the reactions, equilibria, and equilibrium constants he used. Other data were taken from Hewitt (1975) for the reaction at 6 kb, and from Skippen, (1974).

Valley and Essene (1980), also used some of these data and prepared Figure 26. The T- XCO_2 plot was made at $6 \text{ kb} = P_{\text{F}} = P_{\text{H}_2\text{O}} + P_{\text{CO}_2}$. The intersections of the equilibrium curves show that the reactions were stable at temperatures of about 600°C to 650°C and XCO_2 between 0.1 to about 0.85. It thus suggests that the

Table 13. Summary of Results of Equilibria Calculations

Total Press	Temperature Range	Reactions and Conditions
1 bar	610°C	Cc + Qt = Wo + CO ₂ (Skippen, 1974)
5 kb	780° - 1200°C	"
1 - 8 kb	450° - 1000°C	" " "
Pf = 2 kb	>500°C	" " , XCO ₂ = 0.05 - 1
Pf = 1 kb	>500°C	" " , " " } Kerrick & Slaughter, 1976
Pf = 1 kb	>450°C	" " + CO ₂ = .01 - 1 Greenwood, 1967a
Pf = 2 kb	>550°C	" " + CO ₂ = .2 - 1 } Harker and Tuttle, 1956
Pf = .5 kb	>500°C	" " + CO ₂ = 0.22 - 1 Greenwood, 1962
Pf = 1 kb	>450°C	" " + XH ₂ O = 1, XCO ₂ = 0.05 - 1 Tr + Cc + Qt = Di + H ₂ O + CO ₂ , XH ₂ O = .8 - 1 XCO ₂ = .2 - .85 5 Do + Qt + H ₂ O = Tr + Cc + CO ₂ , XH ₂ O = .3 , XCO ₂ = .7 Do + Qt = Di + CO ₂ ; XCO ₂ = .95 XH ₂ O = .05 Greenwood, 1962
Pf = 4 kb	>360°C	Zo + CO ₂ = An + Cc + H ₂ O, XCO ₂ = < .1 Storre & Nitsch, 1973 Phl + Cc + Qt = Tr + Ksp, XCO ₂ = 0.1 Tr + 3Cc + Qt = 5Di + H ₂ O + 3CO ₂ = 0.1 LaAnderson, 1981, Johannes & Orville, 1972
Pf = .5- 8 kb	>400°C - 800°C	Tr + Zo = An + Di + Chl Zo + Qt = Gr + An Gr + Chl = Di + Sph Zo + Chl = An + Di + Sph (Rice, 1983)

TABLE 14. STABLE REACTIONS, EQUILIBRIA, AND EQUILIBRIUM CONSTANTS
FOR PHASE RELATIONS IN THE SYSTEM CaO-MgO-SiO₂-H₂O-CO₂

Reaction	Equilibrium	Equilibrium Constants*
Tr + 3Cc + 2Qt = 5Di + 3CO ₂ + H ₂ O	tr + 3cc + 2q = 5di + 3CO ₂ + h ₂ O	-12486 27.950 0.5152
8Qt + 5Do + H ₂ O = Tr + 3Cc + 7CO ₂	8q + 5m + 2cc + H ₂ O tr + 7CO ₂	-28286 61.707 0.6401
Tr + 3Cc = 4Di + Do + CO ₂ + H ₂ O	tr + 2cc = 4di + m + CO ₂ + H ₂ O	- 4332 10.019 0.2842
5Phl + 6Cc + 24Qt =	3Tr + 5Ksp + 6CO ₂ + 2H ₂ O†	
3Do + Kspar + H ₂ O = Phl + 3cc + 3CO ₂	3m + ksp + H ₂ O = phl + 3CO ₂	-13936 24.767 0.2244

Note: Mineral assemblages for invariant points in Figure

Tr + Di + Qt + Cc + Do; Tr + Kspar + Qt + Phl + Do + Cc.

*Constants in an expression of the type log

$$K = \frac{A}{T} + B + \frac{C(P_t - P_r)}{T}$$

†Equilibrium curve was taken directly from curve given by Hewitt (1975) for the reaction at 6 kb. Data for reaction B is from Rice (1977). All other data is from Skippen (1974).

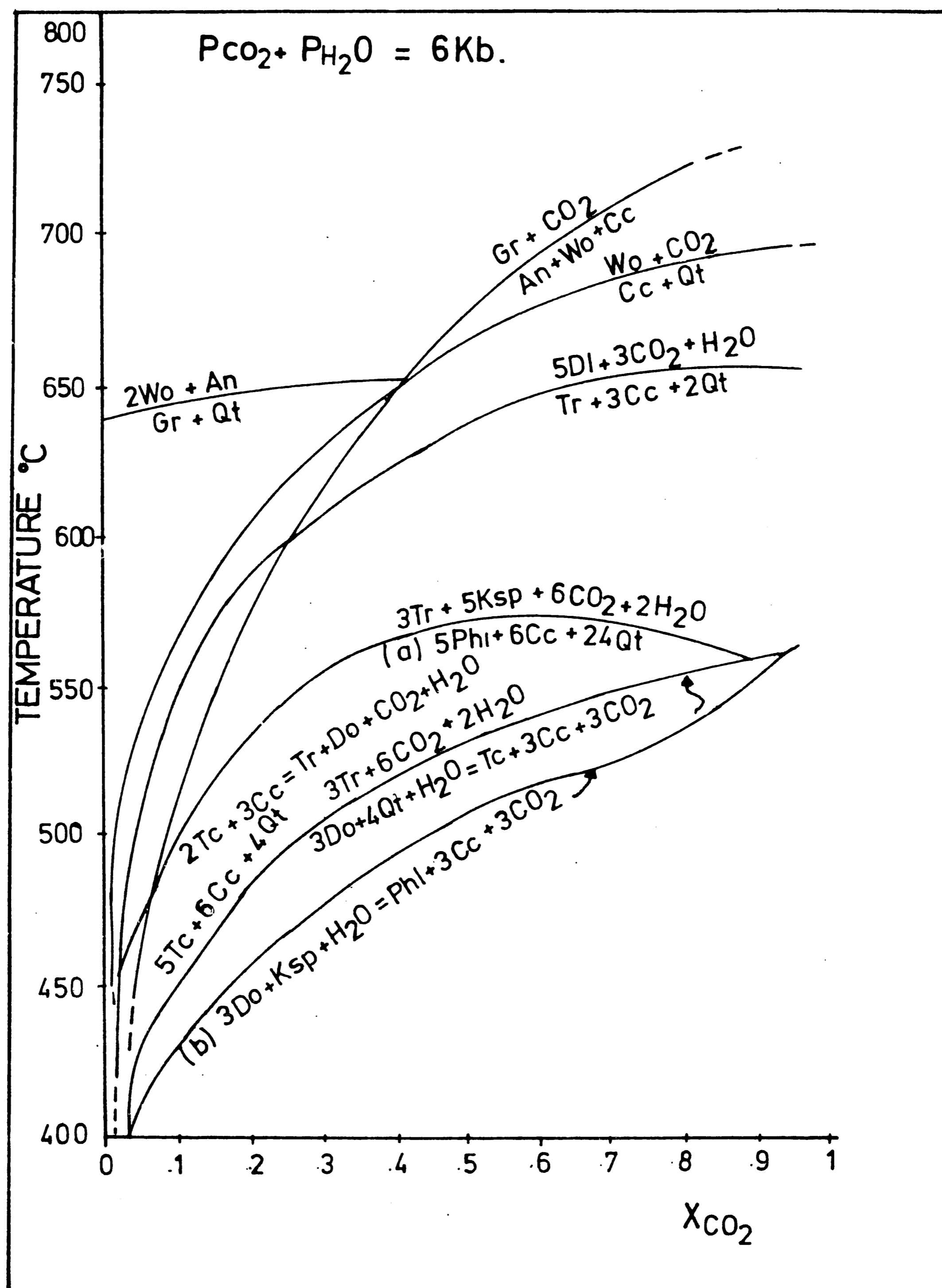


Figure: 25.

Phase relations in the system $\text{CaO} - \text{MgO} - \text{SiO}_2 - \text{H}_2\text{O} - \text{CO}_2 - \text{Al}_2\text{O}_3$ at 6 kb pressure for reactions that affect bulk composition with joint Qt-Do-Cc. Curves (a) and (b) represent upper and lower stability limit of Phi-Cc-Qt, respectively. Model assumes end-member composition of solid phases and ideal mixing of fluid-phase species. (Data from Ross 1980, 1975, Skippen, 1974).

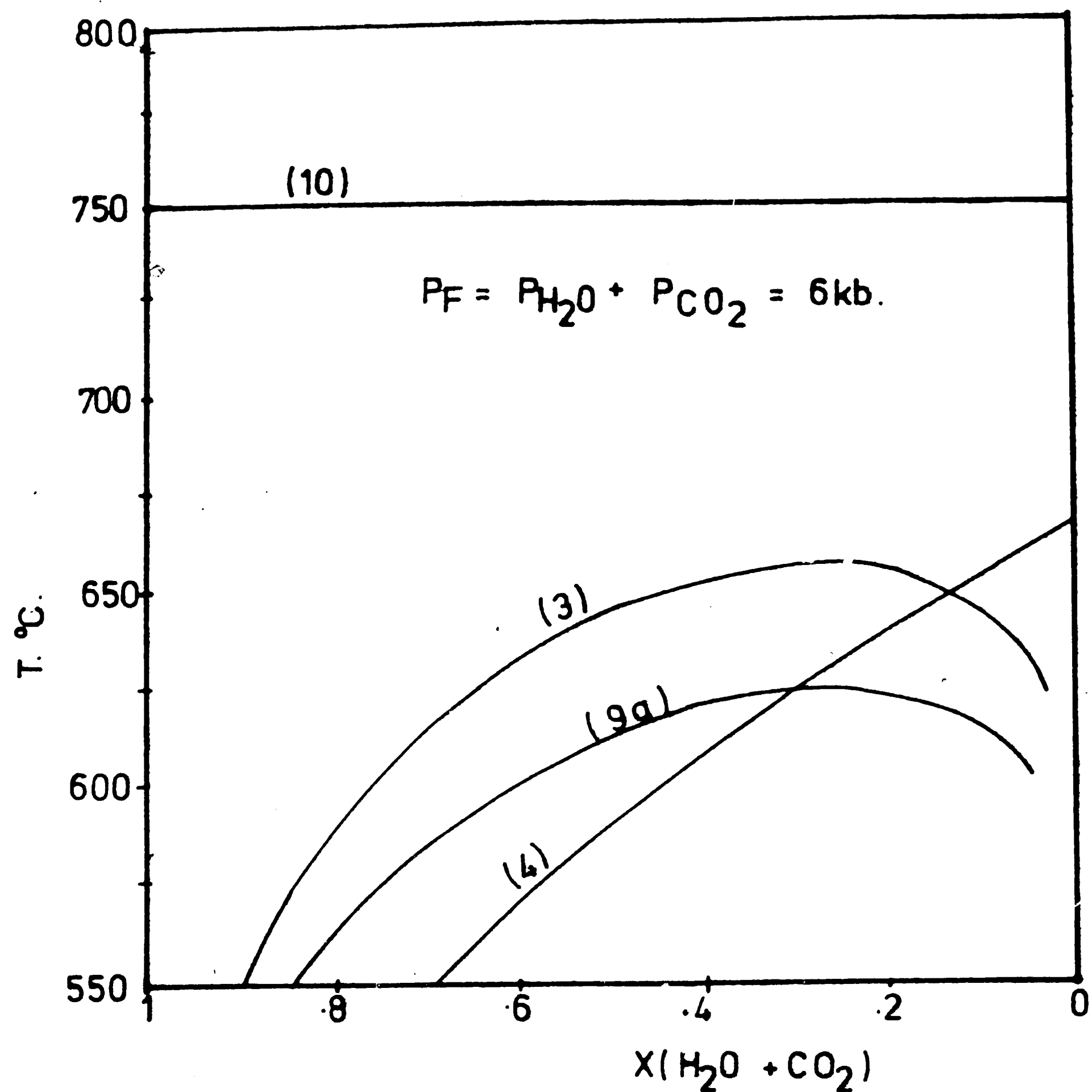
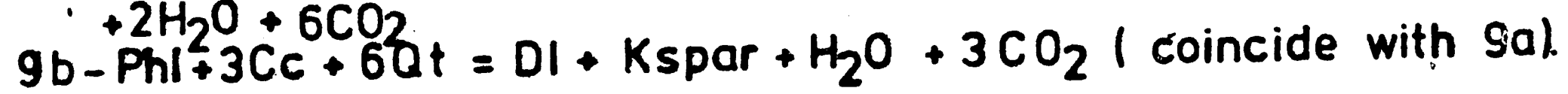
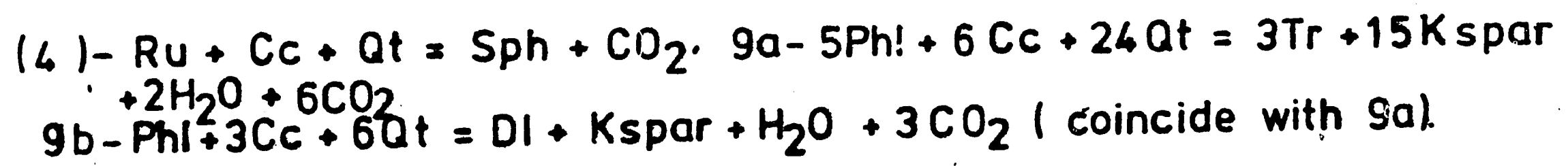
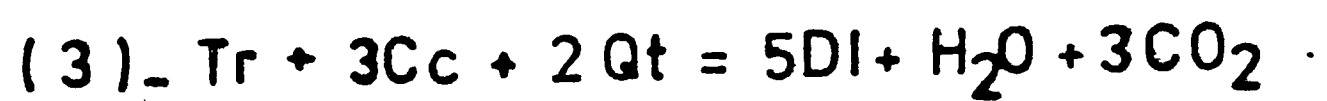


Figure 26.

Temperature plotted versus the mole fraction of H_2O and CO_2 . Reactions were calculated by computer from experimental data by valley and Essene, 1980. Reactions are -:



temperature at about 6 kb was greater than 600°C for the formation of the wollastonite at $X_{CO_2} = 0.1$ to 0.85.

GENERAL DISCUSSION

The mineral assemblages and the reactions that produce them can be a useful guide in setting the limits for the temperature ranges that existed during the contact and the superimposed regional metamorphism. It should be realized that the wollastonite marble that was studied is exposed within a small area of about 125 x 200 square meters. Its geological characterization is thus limited.

Based on mineral assemblages, the wollastonite marble was metamorphosed to a grade corresponding to the first appearance of tremolite, diopside and phlogopite and then to the higher grade of plagioclase, wollastonite and grossularite rank. The irregularly distributed bulk chemical composition in the marble does not allow for distinct differentiation of mineral isograds. The boundary between mineral zones is not well defined because of the occurrence of mixed phases throughout the deposit. The occurrence of hydrous minerals, such as epidote, phlogopite, chlorite and tremolite in the deposit may indicate the presence of a fluid phase whose abundance might have increased with the rising temperature of the reactions (see Figure 27). The different mineral assemblages can be explained in terms of a

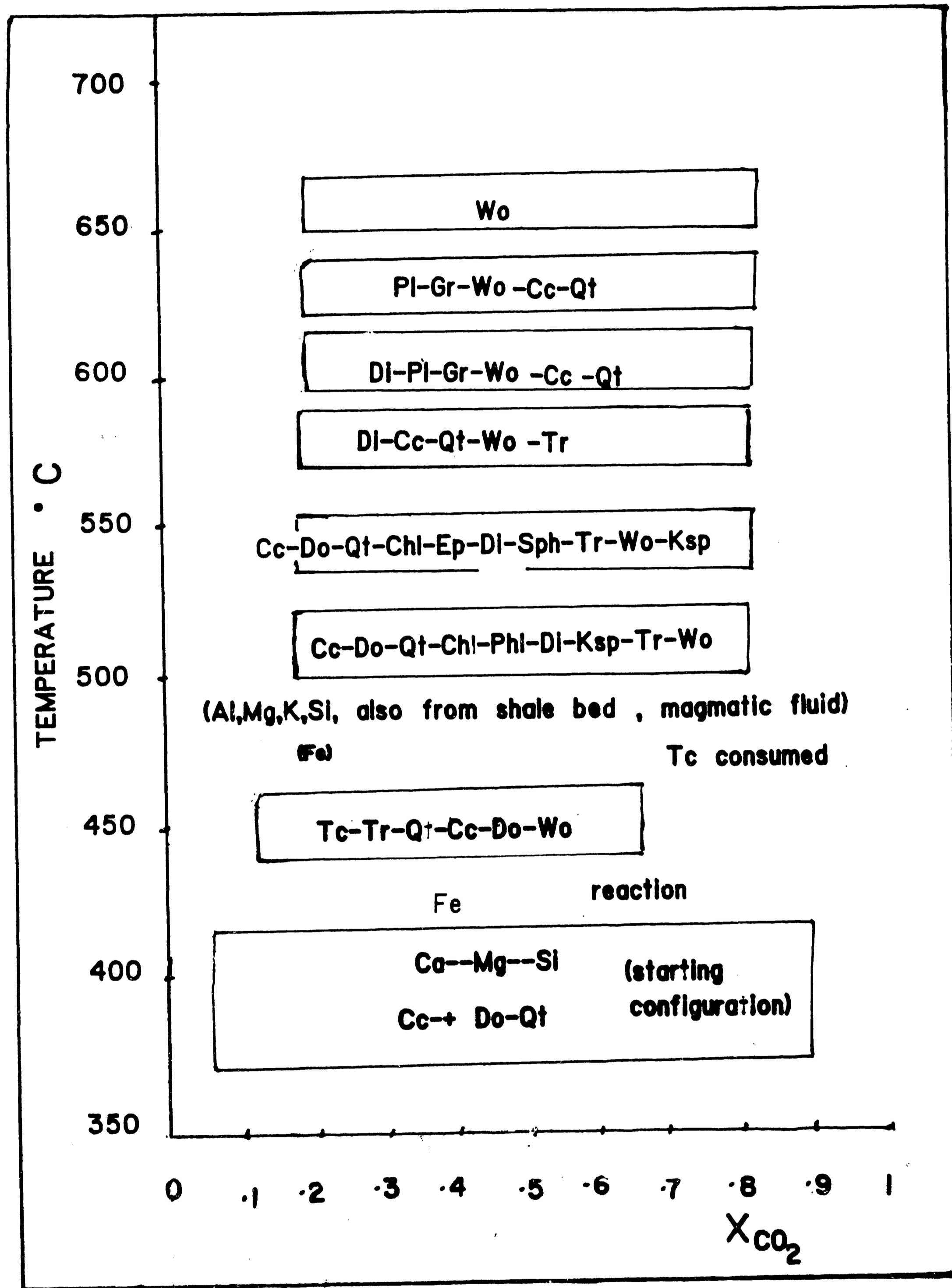
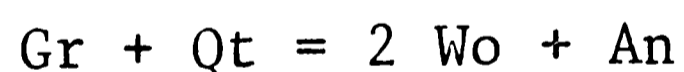
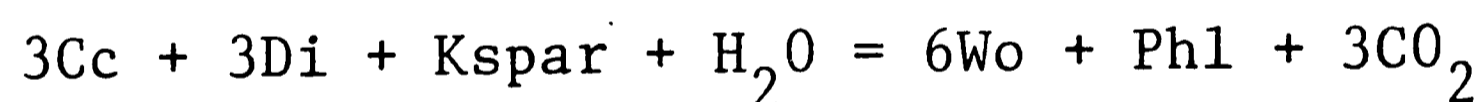
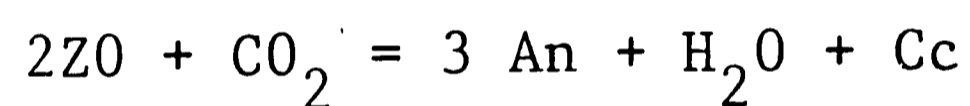
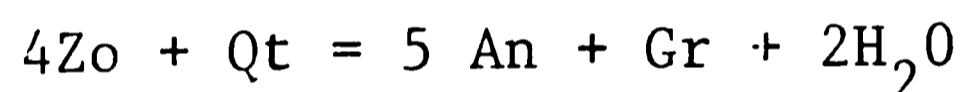


Figure 27. Diagram showing predictable stages of growth of reactions in the wollastonite marble as observed in some selected samples. Widths of reactions are not drawn to scale.

change from closed-system metamorphism with internally buffered fluid composition, as suggested by Greenwood (1973), to an open system with fluid migration. The wollastonite-forming reaction proceeded with the liberation of CO_2 . The CO_2 builds up and becomes diluted such that the fluid pressure (Pf) becomes less than the total rock pressure (Pt), under which condition the reaction would proceed to completion. The X_{CO_2} favorable for this reaction might have ranged from about 0.20 to about 1.0 and under $P_t = P_{\text{H}_2\text{O}} + P_{\text{CO}_2} = 6.0 \text{ kb to } 6.5 \text{ kb}$ and temperatures of about 600°C to 650°C . Under these conditions, the wollastonite would have reacted thus: $\text{Wo} + \text{Cc} + \text{An} = \text{Gr} + \text{CO}_2$. Other high-temperature reactions such as



may have occurred at the higher temperatures. The reaction $2\text{Zo} + \text{CO}_2 = 3 \text{An} + \text{H}_2\text{O} + \text{Cc}$ is favored by lower temperatures and appears to be precluded from this general scheme.

The maximum marble temperature can be used to mark the minimum contact temperature between the syenite and marble during the initiation of the contact metamorphism. By using the thermal relations established by Lovering (1936), Carslaw and Jaeger

(1959), and Jaeger (1961, 1964) as shown in Table 15 of thermal constants, the approximate intrusive temperature can be calculated. The values of 883°C at $T_c = 600^{\circ}\text{C}$ and 956°C , at $T_c = 650^{\circ}\text{C}$, were obtained, which correspond to the maximum temperature estimate in the marble.

Perhaps, the magmatic intrusion stopped into the marble at temperatures between about 883°C and 956°C . Most prograde reactions in the marble might have occurred well below 883°C during the solidification and recrystallization in the syenite intrusive itself. This estimate assumes that the initial temperature attained by the marble was zero which is unlikely since burial effects and/or geothermal gradient may have prevailed to impose some initial temperature in the marble. Under this consideration, the estimated intrusive temperature would be lower than that calculated above.

The mole percent of CaCO_3 and MgCO_3 in calcite of the wollastonite deposit were made using the electron microprobe. The calcite grains were assumed to contain both calcite and dolomite and to have re-equilibrated during peak metamorphism. The MgCO_3 content was very low, and the maximum temperature determined using isobaric curves in the Ca-rich portion of the system $\text{CaCO}_3\text{-MgCO}_3$ and extrapolated to 6 kb, using the method of Goldsmith and Newton (1969), averaged about $400^{\circ}\text{C} \pm 50^{\circ}\text{C}$. This

Table 15. Thermal Constants

Constants	Marble/Limestone	Syenitic Granitic Rocks
K	0.005	0.0081
h_2	0.009	0.0155
h_1	0.095	0.1246
$\frac{K}{h}$	0.053	0.0650

where K = thermal conductivity

h_1 = thermal diffusivity at contact temp. T_c

h_2 = thermal diffusivity at intrusive temp. T_o

δ = specific heat

$$= \frac{K \sqrt{k} \text{ (granite/syenite)}}{K \sqrt{k} \text{ (marble/limestone)}} \quad (1)$$

If magma intruded at T_o , the contact temperature, T_c , is given by the relation

$$T_c = \frac{\delta(T_o)}{(1+\delta)} \quad (2)$$

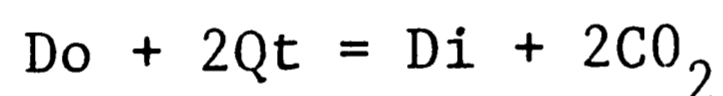
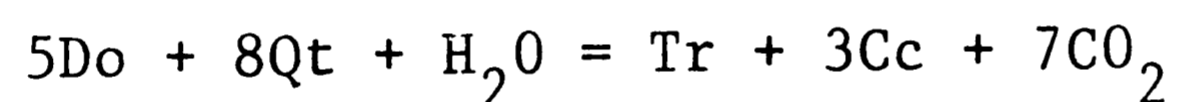
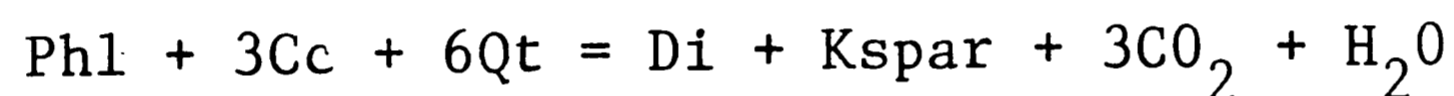
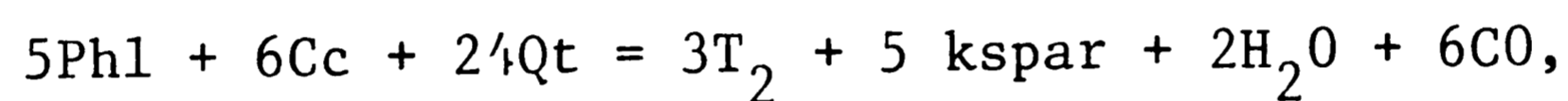
$$T_o > T_c$$

Results of the Calculations

T_c	T_o
600°C	883°C
650°C	956°C

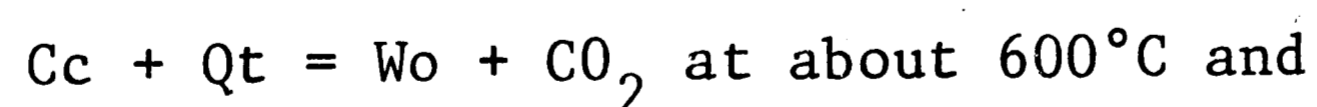
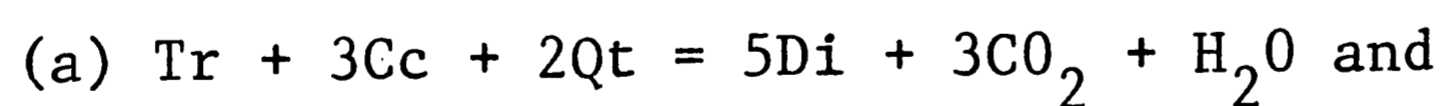
low value compared to 610°C obtained by Bohlen and Essene (1977a) at several kilometers south of Dekalb and north of the wollastonite deposit. It appears that re-equilibration between CaCO_3 and MgCO_3 occurred after peak metamorphism and subsequently erased the temperature of higher grade metamorphism. The contact effects, in addition to the formation of the silicate minerals and the means by which the heat was derived for the various reactions, also contributed to the recrystallization of all the relatively pure limestone to coarse grained crystalline marble.

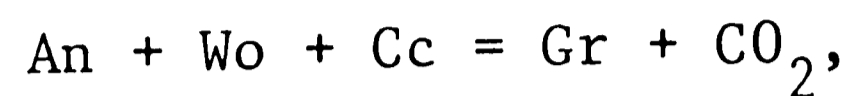
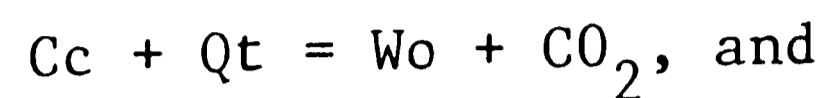
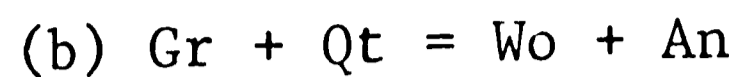
Most assemblages, such as



constitute, more or less, low-temperature reactions, probably within the range 400°C to 550°C or more. The reactions may be favored by either the amount of H_2O (XH_2O) initially present, or XCO_2 liberated, or the stoichiometric molar ratio $\text{CO}_2/\text{H}_2\text{O}$ as discussed above.

The intersections of these reactions





at about 650°C also tend to mark the highest temperature range for the stability of the high-temperature phases such as wollastonite and grossularite at XCO_2 ranging from 0.20 up to about 1.0.

According to the data of Holdaway (1966) the assemblage, $\text{ZnO} + \text{Calcic-plagioclase} + \text{Gr}$ at about 2 kb forms at above 590°C to 600°C in the presence of fluid rich in XH_2O . Above 600°C, the reaction $\text{Gr} + \text{Qt} = \text{Wo} + \text{An}$ (Newton, 1966), occurs destroying grossularite and creating wollastonite. The mineral assemblages observed in this study support the temperature range of 600°C to 650°C.

CONCLUSIONS

The crystalline marble in which the wollastonite and other metamorphic minerals occur is a member of the Grenville Precambrian metasediments. Subsequent to the deposition of the original siliceous limestones about 1.5 - 1.2 b.y. ago, they were invaded by a syenite intrusion about 1.0 to 1.3 b.y. ago. The limestones and the syenite were metamorphosed (about 1.1 to 0.9 b.y. ago) to marble and syenite gneiss though this event was later superimposed by regional metamorphism in the Adirondack Lowlands. Later erosion exposed these rocks as we see them today.

Recrystallization of minerals in the marble occurred because of the heat supplied by the intrusion. Exchange of material substances in aqueous fluids probably took place between the two rock types as shown by the occurrence of calcite in the syenite of the contact. It could not be likely that all the elements, such as Mg, Fe, Mn, Na, and Si found in the mineral phases in the marble would have come from the marble itself. Some might well have come from the syenite fluids. The reaction between the calcite and silica in the marble took place under sufficient fluid phase to form the wollastonite at $PCO_2 < 6\text{kb}$ and $P_{\text{total}} = PH_2O + PCO_2 = 6.0\text{ kb}$ or more. The X_{CO_2} would have varied between 0.1 to about 1.0 under these conditions. The CO_2 liberated

during the wollastonite reaction must have been diluted by H_2O to support the conclusion that PCO_2 was less than 6.0 kb. The presence in the syenite of amphibole and plagioclase, and the presence in the marble of grossularite, plagioclase, and wollastonite suggests that thermal metamorphism produced a higher temperature which transformed the mineralogical assemblages observed.

The occurrence of metamorphic minerals such as wollastonite, grossularite, diopside, tremolite and phlogopite in the marble support the concept that these mineral phases resulted from contact metamorphism.

This study has not successfully established the mechanism for the transfer of heat from the syenite or the transfer of materials. Vidale (1969) showed that differential movement of ions occurred when a calcareous and a pelitic sample were juxtaposed in experimental capsules and held at $600^\circ C$ at 2 kb aqueous solution pressure for 2 - 4 weeks. She concluded that Ca can move from the calcareous samples toward the pelitic one, Mg, Si, and Al could move the other way. The diffusion of the elements may be limited to very small distances of a few millimeters. It is not possible to conclude from this study which way or to what extent or distance cations have moved. The migration of Fe from either the syenite or within the marble and

the shaly portion of the marble is supported by the amount of Fe-bearing epidote or by the amount of Fe present in some bulk chemical analyses.

The temperature range for the formation of grossularite, diopside, wollastonite and plagioclase can be accepted as having been higher than that for the formation of tremolite, epidote, phlogopite, sphene and chlorite. It appears that, under favorable conditions, sufficient amounts of Mg, Fe or Al have moved to form silicate minerals containing these elements. The small amount left would move into the wollastonite and diopside as the analyses can show.

From the mineral assemblages both in the syenite gneiss and the wollastonite-bearing marble, the greenschist to lower-middle amphibolite facies grade can be assigned to the metamorphic rank. The prevalence of the isobarically univariant assemblage Qt-±Do-Tr-Cc, indicates a closed system and internal buffering of the fluid-phase composition. Open-system behavior commenced as CO₂-rich fluids were generated during the growth of tremolite. The CO₂ might have migrated into the surrounding marble through the intergranular pore fluid, cracks, and cleavage fractures. This might have caused local alteration of tremolite to pseudomorphic quartz-calcite-dolomite (Ross, 1980) and buffered the unreacted assemblages.

The isobaric T-XCO₂ model provides support that the fluid composition at the onset of metamorphism could have controlled the distribution of mineral phases.

REFERENCES

- Agar, W. M., 1923. Contact metamorphism in the western Adirondacks. Proc. Amer. Philos. Soc., 62, 95-174.
- Alling, H. L., 1927. Stratigraphy of the eastern Adirondacks. Geol. Soc. Amer. Bull. 38, 795-804.
- Birch, F., 1966. Compressibility, elastic constants: In Handbook of Physical Constants (S. P. Clark, Ed.), Geol. Soc. Amer. Mem. 97, 97-173.
- Bohlen, S. R. and Essene, E. J., 1977a. Feldspar and oxide thermometry of granulites in the Adirondack Highlands: Contr. Mineralogy and Petrology, 62, 153-169.
- _____ and Hoffman, K. S., 1980. Feldspar and oxide thermometry in the Adirondacks: An update. Geol. Soc. Amer. Bull., 91.
- Brown, P. E., Essene, E. J., Kelly, W. C., 1978. Sphalerite geobarometry in the Balmat-Edwards district, New York. Amer. Mineral., 63, 250-257.
- Brown, C. E., 1978. Reconnaissance investigation of high-calcium marble in the Beaver Creek area, St. Lawrence County, New York. U.S. Geol. Surv. Circular No. 774, 10 pp.
- Buddington, A. F. and Smyth, C. H., 1926. Geology of Lake Bonaparte quadrangle, New York. New York State Museum Bull. 269, 106 pp.
- Buddington, A. F., 1939. Adirondack igneous rocks and their metamorphism. Geol. Soc. Amer. Mem. 7, 343 pp.
- _____, 1934. Geology and mineral resources of the Hammond, Antwerp and Lowville quadrangles. N. Y. State Mus. Bull. 296, 51 pp.
- _____, 1963. Isograds and the role of H₂O in metamorphic facies of the orthogneisses of the NW Adirondack area, N. Y. Bull. Geol. Soc. Amer. 74, 1155-1187.

- Burnham, G. W., Holloway, J. P. and Davis, N. F., 1969. The thermodynamic properties of water to 1000°C and 10,000 bars. Geol. Soc. Amer. Spec. Paper, 132, 96 pp.
- Carl, J. D. and Van Diver, B. B., 1975. Precambrian Grenville Alaskite bodies as ash-flow tuffs, NW Adirondack, New York. Geol. Soc. Amer. Bull. 86, 1691-1707.
- Carslaw, H. S. and Jaeger, J. C., 1959. Conduction of heat in solids. 2nd Ed., Oxford University Press, N. Y., 510 pp.
- Cooper, J. R., 1957. Metamorphism and volume losses in carbonate rocks near Johnson Camp, Cochise County, Arizona. Geol. Soc. Amer. Bull. 68, 577-610.
- Cushing, H. P. and Newland, D. H., 1925. Geology of the Gouverneur quadrangle. New York State Mus. Bull. No. 259, 122 pp.
- Daly, R. A., 1917. Metamorphism and its phases. Geol. Soc. Amer. Bull. 28, 375 pp.
- Danielson, A., 1950. Das calcit-wollastonitgleichgewicht. Geochim. Cosmochim. Acta 1, 55-69.
- deLorraine, W., 1979. Geology of the Fowler ore body, Balmat No. 4 Mine, NW Adirondack, N. Y. (Unpublished M.S. thesis, University of Massachusetts, 15 pp.
- Deer, W. A., Howie, R. A. and Zussman, J., 1966. An introduction to the rock-forming minerals. London Longman's, p. 528.
- deWaard, D., 1969. Facies series and P-T conditions of metamorphism in the Adirondack Mountains. Konk. Nederl. Akademie Van Wetenschappen Proceedings Ser. B, 72, 124-131.
- DeWitt, D. B. and Essene, E. J., 1974. Sphalerite geobarometry on Grenville marbles. Geol. Soc. Amer. Abstr. with Programs, 6, p. 709.
- Ellis, A. J. and Fyfe, W. S., 1956. A note on the wollastonite-calcite equilibrium. Amer. Mineral. 41, 805.

- Engel, A. E. J., 1956. Apropos the Grenville, in The Grenville Problem. Royal Society of Canada, Special Publication 1, p. 285, in press. The Precambrian geology and talc deposits of the Balmat-Edwards district, N. Y., U. S. Geol. Surv. Prof. Paper.
- Engel, A. E. J. and Engel, C. G., 1953. Grenville Series in the NW Adirondack Mountains, N. Y. Part 2: Origin and metamorphism of the major paragneiss. Geol. Soc. Amer. Bull. 64, 1049-1097.
- _____, 1958b. Progressive metamorphism and gravitization of the major paragneiss, NW Adirondack, N. Y. Part 1: Total rock. Geol. Soc. Amer. Bull. 69, 1369-1414.
- _____, 1960, Part 2 of 1958b: Mineralogy. Geol. Soc. Amer. Bull. 71, 1-58.
- Essene, E. J., Bohlen, S. R., Valley, J. W., 1978. Determination of regional water fugacities in the Adirondacks. Geol. Assoc. Canada and Mineral. Assoc. Canada Abstr. with programs, 3, 397.
- Eskola, P., 1914. On the Petrology of the Orijärvi Region in SW Finland. Bull. Commiss. Geol. Finland.
- Fisher, D. W., 1977. Correlation of the Hadrynian, Cambrian and Ordovician rocks in New York State. New York State Museum and Science Service, Map and Chart Series, No. 25.
- Fisher, J. R. and Zen, E-an, 1971. Thermochemical calculations from hydrothermal phase equilibrium data and free energy of H₂O. Amer. Jour. Sci. 270, 297-314.
- Foose, M. P., 1974. The structure, stratigraphy and metamorphic history of the Bigelow area, NW Adirondack, N. Y. (Unpublished Ph.D. dissert.) Princeton University, Princeton, N. J., 224 pp.
- Foose, M. P. and Carl, J. D., 1977. Setting of Alaskite bodies in the NW Adirondacks. Geology, 5, 77-81.
- Friedman, G. M., 1959. Identification of carbonate minerals by staining methods. J. Sed. Pet., 29, 87-97.

- Froese, E., 1974. The assemblage Qtz-K-Spar-Biotite-Garnet-Sillimanite, as indicator of P - T conditions. *Canad. Jour. Earth Sci.*, 10, 1575-1579.
- Goldschmidt, V. M., 1912. Die geseetze der gesteinsmetamorphose, Mit beispielen aus der geologic des Sudlichen. *Vidensk. Skrif.*, I, Mat.-Natur. Kl., No. 22.
- Gordon, T. M., 1973. Determination of internally consistent thermodynamic data from phase equilibrium experiments. *J. Geol.*, 81, 199-208.
- Gordon, T. M. and Greenwood, H. J., 1971. The stability of grossularite in the H_2O - CO_2 mixtures. *Amer. Mineral.*, 56, 1676-1688.
- Greenwood, H. J., 1962. Metamorphic reactions involving two volatile components. *Carnegie Inst. Wash. Yearbook*, 61, 82-85.
- _____, 1967a. Mineral equilibria in the system MgO - SiO_2 - H_2O - CO_2 . In Abelson, P. H., ed., *Researches in Geochemistry*, 2, John Wiley and Sons, 542-567.
- _____, 1967b. Wollastonite: Stability in H_2O - CO_2 mixtures and occurrence in a contact metamorphic aureole near Salmo, British Columbia. *Amer. Mineral.* 52, 1669-1680.
- _____, 1973. Thermodynamic properties of gaseous mixtures of H_2O and CO_2 between 450° and $800^\circ C$ and 0 to 500 bars. *Amer. Jour. Sci.*, 273, 561-571.
- Harker, A. and Tuttle, O. F., 1956. Stability of wollastonite. *Amer. J. Sci.* 251, 239.
- Helgeson, H. C., Delany, J. M., Nesbitt, H. W. and Bird, D. K., 1978. Summary and critique of the thermodynamic properties of rock-forming minerals. *Amer. J. Sci.* 278-A, 1-229.
- Hewitt, D. A., 1973. The metamorphism of micaceous limestone from south-central Connecticut. *Amer. Jour. Sci.*, 273-A, 444-467.

- Hoschek, G., 1973. Die reaktion phlogopit + calcit + quarz = tremolit + kalifeldspar + H_2O + CO_2 . Geochim. Cosmochim. Acta 41, 279-288.
- Holdaway, M. J., 1966. Hydrothermal stability of clinozoisite + quartz. Amer. Jour. Sci., 264, 643-667.
- Holloway, J. R., 1977. Fugacity and activity of molecular species in supercritical fluids. In: Fraeser, D. C., ed., Thermodynamics in Geology, p. 161-181.
- Holmes, A., 1937. The age of the earth. Nelson and Sons, Edinburgh, 196 pp.
- Hunt, J. A. and Kerrick, D. M., 1976. The stability of sphene, experimental redetermination and geologic implications. Geochim. Cosmochim. Acte. 41, 279-288.
- Hurley, P. M., 1951. Alpha ionization damage as a cause of low helium ratios. U.S. Office of Naval Research Tech. Rept., 10 pp.
- Jaeger, J. C., 1961. The cooling of irregularly shaped igneous bodies. Amer. Jour. Sci., 259, 721-734.
- _____, 1964. Thermal effects of intrusions. Reviews of Geophysics, 2, 443-446.
- Jaffe, et al., 1978, Orthoferrosilite and other iron-rich pyroxenes in micro-perthite gneiss of the Mt. Marcy Area, Adirondack Mountains. Amer. Mineral. V. 63, No. 11-12, p. 1116-1136.
- Johannes, W. and Orville, P. M., 1972. Zur stabilität der mineral paragenesen-muskovit + calcit + quarz zoisite + muskovit + quarz + anorthit + K-feldspar and anorthit + calcit. Fortschr. Mineral., 50, 46-47.
- Kemp, J. F., 1921. Geology of the Mount Marcy quadrangle, Essex County, New York. N. Y. State Museum Bull. 229-230, 86 pp.
- Kerrick, D. M. and Slaughter, J., 1976. Comparison of methods for calculating and extrapolating equilibria in P-T- XCO_2 -space. Amer. Jour. Sci. 276, 883-916.

- Korzhinskii, D. S., 1959. Physicochemical basis of analysis of the paragenesis of minerals, New York. Consultants Bur., 142 p.
- Le Anderson, P. J., 1981. Calculation of temperature and $X(\text{CO}_2)$ values for tremolite-k-feldspar-diopside-epidote-assemblages. *Canad. Mineral.*, 19, 619-630.
- Leake, B. E., 1968. A catalog of analysed calciferous and subcalciferous amphiboles together with their nomenclature and associated minerals. *Geol. Soc. Amer. Spec. Papers* 98, 210 p.
- Lewis, J. R., 1969. Structure and stratigraphy of the Rossie Complex, NW Adirondack, N. Y. (Unpublished Ph.D. dissert.) Syracuse, N. Y., Syracuse Univ., 141 p.
- Lovering, T. S., 1936. Heat conduction in dissimilar rocks and the use of thermal models. *Bull. Geol. Soc. Amer.* 47, 87-100.
- Marble, J. P., 1943. Possible age of allanite from Whiteface Mountains, Essex County, N. Y. *Amer. Jour. Sci.* 241, 32-42.
- McLelland, J. and Isachsen, Y. W., 1980. Synthesis of the southern and central Adirondacks, a model for the Adirondacks as a whole, and plate tectonic interpretations in geology of the Adirondack Mountains. *Geol. Soc. Amer. Bull.* 91, 168-172.
- McLelland, J. and Whitney, P. R., 1980. A generalized garnet-forming reaction for meta-igneous rocks in the Adirondacks. (Abstr.) *Geol. Soc. Amer., Abs. with Progr.*, 12, 73.
- Melson, W. G., 1966. Phase equilibria in calc-silicate hornfels, Lewis and Clark County, Montana. *Amer. Mineral.* 51, 402-421.
- Newton, R. C., 1966. Some calc-silicate equilibrium relations. *Amer. Jour. Sci.* 264, 204-222.
- Nitsch, K., 1972. Das P-T- XCO_2 stabilitätsfeld von lawsonit. *Contrib. Miner. Petr.*, 34, 116-134.

- Ohmoto, H. and Kerrick, D. M., 1977. Devolatilization equilibria in graphite systems. *Amer. Jour. Sci.*, 277, 1013-1044.
- Osborne, F. F., 1936a. Lachute map area: Quebec Bur. Mines Ann. Rept. Part C, 1-40.
- Perkins, D. P., et al., 1980. The thermodynamic properties and phase relations of some minerals in the system $\text{CaB-Al}_2\text{O}_3\text{-SiO}_2\text{-H}_2\text{O}$. *Geochim. Cosmochim. Acta.* 44, 61-84.
- Pistorius, C. W. F. T. and Kennedy, G. C., 1960. Stability of grossularite and hydrogrossularite at higher temperatures and pressures. *Amer. Jour. Sci.*, 258, 247-257.
- Rice, J. M., 1977. Progressive metamorphism of impure dolomitic limestone in the Marysville aureole, Montana. *Amer. Jour. Sci.*, 277, 1-24.
- Rice, J. M., 1983. Metamorphism of rodingites. Part I. Phase relations in a portion of the system $\text{CaO-MgO-Al}_2\text{O}_3\text{-SiO}_2\text{-CO}_2\text{-H}_2\text{O}$. *Amer. Jour. Sci.*, 283 A, 121-150.
- Robie, R. A., Hemingway, B. S., and Fisher, J. R., 1978. Thermodynamic properties of mineral and related substances at 298.15°K and 1 bar (10^5 pascals) pressure and at higher temperatures. *U. S. Geol. Surv. Bull.* 1452, p. 100.
- Robie, R. A., Bethke, P. M. and Beardsley, K. M., 1967. Selected X-ray crystallographic data, molar volume and densities of minerals and related substances. *U. S. Geol. Surv. Bull.* 1248.
- Robie, R. A. and Waldbaum, D. R., 1968. Thermodynamic properties of minerals and related substances at 298.15°K (25.0°C) and one atmosphere (1.013 bars) pressure and at higher temperatures. *U. S. Geol. Survey Bull.* 1259.
- Ross, G. M., 1980. Geology and petrogenesis of marbles in the DeKalb area of northern New York. *Geol. Soc. Amer. Bull.* 91, 617-658.

- Shaub, B. M., 1940. Age of the uraninite from the McLear pegmatite near Michville Station, St. Lawrence County, New York. *Amer. Mineral.* 25, 480-487.
- Silver, L. T., 1969. A geochronologic investigation of the anorthosite complex, Adirondack Mountains, New York. IN: Isachsen, Y., ed., *Origin of Anorthosites and related rocks*. New York State Museum and Science Service Mem. 18, p. 233-251.
- Skinner, B. J., 1966. Thermal expansion. IN: *Handbook of Physical Constants*, (S. P. Clark, Jr., ed.), 75-96. *Geol. Soc. Amer. Mem.* 97, 587 pp.
- Skippen, G. B., 1974. An experimental model for low pressure metamorphism of siliceous dolomitic marble. *Amer. Jour. Sci.* 274, 487-509.
- _____ and Carmichael, D. M., 1977. Mixed volatile equilibria. IN: Greenwood, H. J., ed. *Application of thermodynamics to petrology and ore deposits*. Mineral. Assoc. Canada, 109-125.
- Slaughter, J., Kerrick, D. M. and Wall, V. J., 1975. Experimental and thermodynamic study of equilibria in the system $\text{CaO-MgO-SiO}_2\text{-H}_2\text{O-CO}_2$. *Amer. Jour. Sci.*, 275, 143-162.
- Smyth, C. H., 1895. Crystalline limestones and associated rocks of the NW Adirondack region. *Bull. Geol. Soc. Amer.*, 6, 263-284.
- Stormer, J. C., 1975. A practical two-feldspar geothermometer. *Amer. Mineralogist* 60, 667-674.
- Storre, B. and Nitsch, K. H., 1972. Die reaction $2\text{Zo} + 1\text{CO}_2 = 3\text{AntlCc} + 1\text{H}_2\text{O}$. *Contr. Mineral. Petrol.*, 35, 1-10.
- _____, 1973. The upper stability of margarite in the presence of quartz. *Natur. Wissen.* 60, 152.
- Thompson, A. B., 1971b. PCO_2 in low grade metamorphism: zeolite carbonate, clay mineral, prehnite relation in the system $\text{CaO-Al}_2\text{O}_3\text{-SiO}_2\text{-CO}_2\text{-H}_2\text{O}$. *Contr. Miner. Petrol.* 33, 145-161.

- _____, 1975. Mineral reaction in calc-silicate-mica-schist from Gassetts, Vermont, U. S. A., *Contr. Miner. Petrol.* 53, 105-127.
- Trommsdorff, V. and Evans, B. W., 1972. Progressive metamorphism of antigorite schist in the Bergell tonalite aureole (Italy). *Amer. Jour. Sci.*, 272, 423-437.
- Valley, J. W. and Essene, E. J., 1977. Regional metamorphic wollastonite in the Adirondacks. *Geol. Soc. Amer. Abstr. with Progr.* 9, 326-327.
- _____, 1980. Calc-silicate reactions in Adirondack marbles: The role of fluids and solid solutions. *Geol. Soc. Amer. Bull.* 91, 720-815.
- Vidale, R., 1969. Metasomatism in a chemical gradient and the formation of the calc-silicate bands. *Amer. Jour. Sci.*, 267, 857-874.
- Wall, V. J. and Essene, E. J., 1972. Subsolidus equilibrium in $\text{CaO-Al}_2\text{O}_3\text{-SiO}_2\text{-H}_2\text{O}$. *Geol. Soc. Amer. Abstr. with Programs*, 4, 700 pp.
- Wiener, R. W., 1977. Timing of emplacement and deformation of the Diener complex along the Adirondack Highlands-NW Lowlands boundary. *Geol. Soc. Amer. Abstracts with Programs*, 9, 329-330.
- Wiener, R. W., 1981. Stratigraphy, structural geology and petrology of bedrock along the Adirondack Highlands, NW Lowlands boundary, near Harrisville, N. Y. Unpublished doctoral dissertation, University of Mass. Amherst, MA.
- Wynne-Edwards, H. R., 1972. The Grenville province (in Price, R. A. and Douglas, R. J. W., eds.), Variations in tectonic style in Canada. *Geol. Assoc. Canada, Spec. Paper*, 11, p. 262-334.
- Yoder, H. S., Jr., 1950. Stability relations of grossularite. *Jour. Geol.* 58, 221-253.

Zen, E-an, 1961. The zeolite facies: an interpretation. Amer. Jour. Sci. 259, 401-409.

_____, 1963. Components, phases and criteria of chemical equilibrium in rocks. Ibid: 261, 929-942.

VITA

Collins T. Awak received the B.S. degree in geology with Third Class Honors in 1978 from Ahmadu Bello University of Nigeria. He then spent one year in the National Youth Service Corps during which period he was posted to the Exploration and Mining Division of the National Steel Council. Subsequently he was employed as a Grade One Geologist in this organization. Between November 4 and December 14, 1981, he successfully completed a course on methods and techniques in exploration geophysics organized by the National Geophysical Research Institute, Hyderabad, India and sponsored by UNESCO and the government of India. In 1982 he was awarded a scholarship by the Federal Ministry of Education for post-graduate study abroad, and in September, 1982, he entered the M.S. program in the Department of Geological Sciences at Lehigh University. His current address is National Steel Council, Exploration and Mining Division, Kaduna, Nigeria.